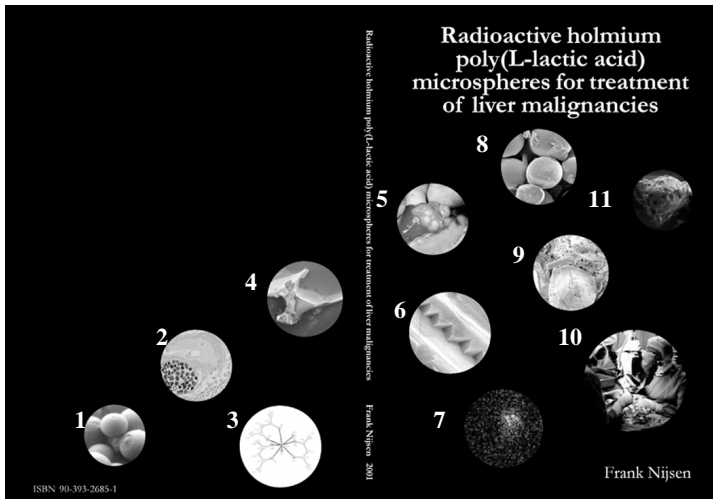


**Radioactive holmium  
poly(L-lactic acid) microspheres for  
treatment of liver malignancies**

**Frank Nijssen**

## CONTENTS

<b>Chapter 1</b>	General introduction: Advances in Nuclear Oncology, microspheres for internal radionuclide therapy of liver tumours <i>invited paper (Current Medicinal Chemistry)</i>	7
<b>Chapter 2</b>	Holmium-166 poly lactic acid microspheres applicable for intra-arterial radionuclide therapy of hepatic malignancies: effects of prepration and neutron activation techniques <i>European Journal of Nuclear Medicine</i> 1999;26:699-704	31
<b>Chapter 3</b>	Diaquattris(pentane-2,4-dionato-O,O')holmium(III) monohydrate and diaquattris(pentane-2,4-dionato-O,O')-holmium(III) 4-hydroxypentan-2-one solvate dihydrate <i>Acta Crystallographica Section C</i> 2000;C56:156-158	45
<b>Chapter 4</b>	Characterization of poly(L-lactic acid) microspheres loaded with holmium acetylacetonate <i>in press (Biomaterials)</i>	57
<b>Chapter 5</b>	Influence of neutron irradiation on holmium acetylacetonate loaded poly(L-lactic acid) microspheres <i>submitted (Biomaterials)</i>	77
<b>Chapter 6</b>	Targeting of liver tumour in rats by selective delivery of holmium-166 loaded microspheres: a biodistribution study <i>in press (European Journal of Nuclear Medicine)</i>	95
<b>Chapter 7</b>	Radioactive holmium loaded poly(L-lactic acid) microspheres for treatment of hepatic malignancies: efficacy in rabbits	109
<b>Chapter 8</b>	Summary and concluding remarks	123
	Samenvatting	135
	Dankwoord	141
	Curriculum vitae	145
	List of Publications	147



- 1)  $^{165}\text{Ho}$  loaded PLLA microspheres.
- 2) Micrograph of a cluster of microspheres in a tumour bloodvessel.
- 3) Unit cell of HoAcAc.
- 4) Microspheres irradiated for 2h ( $2 \times 10^{14} \text{ cm}^{-2} \cdot \text{s}^{-1}$ ).
- 5) VX2 tumour in rabbit liver.
- 6) HoAcAc crystal ( $\times 20,000$ ).
- 7) Scintigraphic image of the rat liver
- 8)  $^{166}\text{Ho}$  loaded PLLA microspheres.
- 9) PLLA film with 20% Ho (w/w) loading.
- 10) Operation theatre (Nico, Frank and Mrs Rabbit).
- 11)  $^{166}\text{Ho}$  microspheres after incubation in human plasma.

## Radioactive holmium poly(L-lactic acid) microspheres for treatment of liver malignancies

J.F.W. Nijzen

Ph.D. Thesis, with summary in Dutch

Utrecht University, The Netherlands

April 2001

ISBN 90-393-2685-1

Copyright © 2001 by J.F.W. Nijzen. All rights reserved. No part of this thesis may be reproduced or transmitted in any form or by any means, without written permission from the author.

# **Radioactive holmium poly(L-lactic acid) microspheres for treatment of liver malignancies**

Polymelkzuur microsferen met  
radioactief holmium voor de behandeling van  
lever maligniteiten

(met een samenvatting in het Nederlands)

## **Proefschrift**

ter verkrijging van de graad van doctor  
aan de Universiteit Utrecht  
op gezag van Rector Magnificus,  
Prof. Dr. W.H. Gispen ingevolge het besluit  
van het College voor Promoties in het openbaar te verdedigen  
op donderdag 26 april 2001 des middags te 12.45 uur.

door

Johannes Franciscus Wilhelmus Nijsen

Geboren 22 november 1970 te Hilversum



Promotores: Prof. Dr. Ir. W.E. Hennink  
Prof. Dr. Ir. M.A. Viergever

Co-promotores: Dr. A.D. van het Schip  
Dr. P.P. van Rijk

Publication of this thesis was financially supported by:

NRG

Mallinckrodt Medical BV

Acros Organics NV

ATL Nederland. A Philips Medical Systems Company

# Chapter 1

---

## **General introduction:**

### **Advances in nuclear oncology, microspheres for internal radionuclide therapy of liver tumours**

*invited paper (Current Medicinal Chemistry)*



**J.F.W. Nijsen<sup>1</sup>, A.D. van het Schip<sup>1</sup>, W.E. Hennink<sup>2</sup>, D.W. Rook<sup>1</sup>,  
P.P. van Rijk<sup>1</sup> and J.M.H. de Klerk<sup>1</sup>**

<sup>1</sup>*Department of Nuclear Medicine, University Medical Center, Utrecht, The Netherlands*

<sup>2</sup>*Department of Pharmaceutics, Utrecht Institute for Pharmaceutical Sciences, Utrecht University, Utrecht, The Netherlands*

**Abstract:** Liver metastases cause the majority of deaths from colorectal cancer, and response to chemotherapy and external radiotherapy is poor. An alternative is internal radionuclide therapy using  $^{90}\text{Y}$  labeled microspheres. These microspheres are very stable and have a proven efficacy in the field of treatment of primary or metastatic hepatic cancer. Whilst these spheres showed encouraging results in patients, their high density is a serious drawback. Currently, other materials with lower densities and other radioisotopes are being investigated in order to optimize this promising new therapy. Three major radiolabeled microsphere materials, viz. glass, resin-based and polymer-based, are now available for therapy or are being tested in animals. In this review the preparation, stability and degradation of these spheres are highlighted.

## 1.1 Introduction

In western countries malignant tumours originating from colorectal carcinoma are frequently seen in the liver. Surgical resection is presently the treatment of choice in patients with liver metastases. After this procedure the 5-year survival is around 35% [1]. However, most tumours are inoperable by the time of diagnosis. Other treatment options for these tumours include conventional chemotherapy and external radiotherapy [2,3]. Unfortunately, neither of the latter regimens have shown an obvious improvement in patient survival. The regional administration of therapeutic agents [4] via the hepatic artery is one strategy that has been developed to improve tumour response, since both primary and metastatic liver tumours are well vascularized and receive the bulk of their blood supply from the hepatic artery [5]. These therapies must satisfy two requirements in order to be successful: (a) the relevant agent must be effective in the in-vivo orthotopic microenvironment of tumours, and (b) this agent must reach the target cells in-vivo in optimal quantities [6]. All conventional and novel therapeutic agents for regional administration may be divided into three categories: molecules, particles and cells. In this review we focus on the injection of particles into the hepatic artery in order to obtain selective delivery of radioisotopes to the tumour, thus maximizing the irradiation effect while sparing toxicity to the surrounding healthy liver [2]. Among the more promising of these radiotherapeutics are beta-emitting microspheres. These microspheres can be based on polymers, polymeric resins, albumin or inorganic materials e.g. glass. Radioisotopes used for labeling are yttrium-90 ( $^{90}\text{Y}$ ), rhenium-186/rhenium-188 ( $^{186}\text{Re}/^{188}\text{Re}$ ) and holmium-166 ( $^{166}\text{Ho}$ ).

This chapter reviews the current literature on radioactive microspheres used for the treatment of liver malignancies and concludes with the aims and outline of the thesis.

## 1.2 Microspheres: materials and preparation

The ideal properties for radiolabeled microspheres or particles for intra-arterial therapy are summarised in Table 1. Müller and Rossier [8] first described the use of particles radiolabeled with gold-198 ( $^{198}\text{Au}$ ), which were used in the treatment of lung cancer. Early studies used angular fragments that were made by crushing the bulk material and sieving the particles to grade in the desired diameter [9]. The first plastic microspheres were labeled with  $^{90}\text{Y}$  and showed an unpredictable and catastrophic leaching of yttrium, which brought them into question [10]. This problem was solved later by the use of glass beads. As well as these glass beads, resin-based and other polymeric microspheres are currently being used. An overview is given in Table 2.

**Table 1.** Ideal properties of radiolabeled microspheres for intra-arterial therapy [7]

- 
1. High mechanical stability to resist breakdown and passage through the capillary network
  2. High chemical stability to resist elution of radioactive label, macrophage removal, or radiolysis
  3. Uniform size
  4. Unit density to prevent settling or streaming
  5. Relative ease of label
  6. Radionuclide label with high-energy beta particle, low photofraction, and intermediate (days) half-life
- 

**Table 2.** Radiolabeled microspheres currently in use

Radionuclide	Microsphere	Labeling	Ref.
$^{166}\text{Ho}$	PLLA	N	[13,29]
	Resin (Aminex A-5)	Lr	[14]
$^{90}\text{Y}$	Glass (TheraSpheres <sup>®</sup> )	N	[10]
	Resin (Bio-Rex-70)	Lr	[19]
	Resin	Lr	[22]
	PLLA	Lr/Lp	[33]
	Albumin	Lr	[27]
$^{186}\text{Re}/^{188}\text{Re}$	Glass	N	[16]
	Resin (Aminex A-27)	Lr	[21]
	PLLA	Lr/Lp	[2]
	Albumin	Lr	[25]
$^{32}\text{P}$	Glass	N	[18]

---

N= activated by neutron bombardment; Lr= labeled with radioactive compound, retrospectively; Lp= labeled with radioactive compound, preceding production of microspheres.

### 1.2.1.1 Glass

Glass is relatively resistant to radiation-damage, highly insoluble, and non-toxic. Glass can be easily spheridized in uniform sizes and has minimal radionuclidic impurities. The manufacturing process is described comprehensively by Ehrhardt and Day [10]. The yield of microspheres with the desired diameter, 20-30  $\mu\text{m}$  (see below), is around 15%. Advances in this technology have led to the production of glass microspheres with practically no leaching [11]. Although the glass spheres have several advantages, their high density (3.29 g/ml [12]) and their non-biodegradability are major drawbacks [13,14]. The relatively high density increases the chance of intravascular settling [15]. These glass microspheres produced under the name TheraSpheres<sup>®</sup> are the first registered microsphere product for internal radionuclide therapy, and are used in patients with primary or metastatic tumours. Because of the lack of  $\gamma$ -emission of  $^{90}\text{Y}$ , radioactive rhenium ( $^{186}\text{Re}/^{188}\text{Re}$ ) microspheres were also produced. The general method of manufacture of these spheres was the same as for the  $^{90}\text{Y}$  spheres [2,16].

Brown et al. [17] prepared  $^{166}\text{Ho}$ -loaded glass particles (2-5  $\mu\text{m}$ ) for direct injection into tumours of mice, which resulted in an effective modality for deposition of intense  $\gamma$ -radiation for use in localised internal radionuclide therapy. However, no further studies were done.

Kawashita et al. [18] suggested the use of phosphorus-rich  $\text{Y}_2\text{O}_3\text{-Al}_2\text{O}_3\text{-SiO}_2$ -glass microspheres containing phosphorus ions, which were produced by thermoelectron bombardment of red phosphorus vapour and implanted into glass, thus resulting in a high phosphorus content and high chemical durability. After activation by neutron bombardment the glass contains phosphorus-32 ( $^{32}\text{P}$ ).

### 1.2.1.2 Resins

Resin-based microspheres are much favoured for radio-embolization. Chloride salts of holmium and yttrium were added to cation exchange resins. Different resins were investigated by Schubiger et al. [19], amongst which were Bio-Rex 70, Cellex-P, Chelex 100, Sephadex SP and AG 50W-X8. The resins with  $^{90}\text{Y}$  bound to the carboxylic acid exchange groups of the acrylic polymer were sterilised and used for renal embolization of pigs. Only the pre-treated Bio-Rex 70 resulted in applicable particles, with a retention of beta activity in the target organ of >95% of injected dose, and no histologically detectable particles in lung tissue samples [20].

As well as Bio-Rex 70, Aminex resins (Bio-Rad Inc. Hercules CA, USA) loaded with  $^{166}\text{Ho}$  or  $^{188}\text{Re}$ , also resulted in applicable preparations. Turner et al. [14] prepared microspheres by addition of  $^{166}\text{Ho}$ -chloride to the cation exchange resin Aminex A-5, which has sulphonic acid functional groups attached to styrene divinylbenzene copolymer lattices. Reproducible, non-uniform distributions of the

$^{166}\text{Ho}$ -microspheres throughout the liver were observed on scintigraphic images, following intrahepatic arterial administration in pigs. This predictable distribution allowed these investigators to determine the radiation absorbed dose from a tracer activity of  $^{166}\text{Ho}$ -microspheres, and to define the administered activity required to provide a therapeutic dose.

Aminex A-27 was labelled with  $^{188}\text{Re}$  by adding  $^{188}\text{Re}$ -perrhenate and  $\text{SnCl}_2$  to vacuum-dried resin particles [21]. The mixture was boiled and centrifuged and microspheres were separated and resuspended in saline. Spheres were tested by direct intratumoural injection into rats with hepatoma. Survival over 60 days was significantly better in the treated vs. the control group (80% vs. 27%).

Investigators from Australia and Hong Kong have used unspecified resin-based particles labeled with  $^{90}\text{Y}$  for treatment of patients with primary or secondary liver cancer [22,23]. The spheres had a diameter of 29-35  $\mu\text{m}$ , a density of 1.6 g/ml and a specific activity of approximately 30-50 Bq per sphere. Treatment was well tolerated with no bone-marrow or pulmonary toxicity. The median survival was 9.4 months (range 1.8-46.4) in 71 patients, and the objective response rate in terms of drop in tumour marker levels was higher than that based on reduction in tumour volume shown by computed tomography [15,24].

### 1.2.1.3 Albumin

Technetium-99m-microspheres ( $^{99\text{m}}\text{Tc}$ -microspheres) of human serum albumin (HSA) have been widely used for clinical nuclear medicine, particularly for lung scanning, since 1969 (25,26).  $^{188}\text{Re}$  labeled HSA microspheres used by Wunderlich et al. [25] are uniform in size, with a mean diameter of 25  $\mu\text{m}$ , and are biocompatible and biodegradable. However, the labeling process is time-consuming and depends on  $\text{SnCl}_2 \cdot 2\text{H}_2\text{O}$  and gentisic acid concentration. On the surface of the microspheres a shell of about 1  $\mu\text{m}$  thickness was seen, probably consisting of precipitated tin hydroxide. The particle labeling (coating) may be achieved by a combination of the reduction reaction of  $\text{Re(VII)}$  with  $\text{Sn(II)}$  and a particle surface-related coprecipitation effect of tin hydroxide colloid with high adsorption capacity and reduced, hydrolysed rhenium. The labeling yield under optimal reaction conditions is more than 70%. Biodistribution experiments in rats, using the lungs as a model for a well-perfused tumour, resulted in excellent in vivo stability.

As well as rhenium, yttrium was bound to HSA for internal radiotherapy [27].  $^{90}\text{Y}$ -acetate and macroaggregates of HSA (MAA) (Macrokit<sup>®</sup>, Dainabot, Tokyo, Japan) were suspended in sodium acetate buffer and incubated at room temperature. Experiments in mice were carried out in order to investigate the possibility of using  $^{90}\text{Y}$ -MAA as an internal radiotherapeutic agent for whole-lung irradiation. Yttrium-activity in the lung was cleared within 72h post injection and activity was

redistributed in other organs, especially in the bone, but this could be prevented by the combined use of  $\text{CaNa}_3\text{DTPA}$ . Based on its rapid clearance  $^{90}\text{Y}$ -MAA was suggested as being useful for fractionated internal radiotherapy of the lung.

#### *1.2.1.4 Polymers*

Polymer-based microspheres have many advantages over other materials, in particular their near-plasma density, biodegradability and biocompatibility. However, their major disadvantage is their inability to withstand high thermal neutron fluxes [16]. Additives [13,28] and adjustment of irradiation-parameters [29] can overcome this problem.

Polymer-based microspheres used for internal radionuclide therapy are mainly prepared by a solvent evaporation technique. In the solvent evaporation process, the polymer is dissolved in a suitable water immiscible volatile solvent, and the medicament is dispersed or dissolved in this polymeric solution. The resulting solution or dispersion is then emulsified by stirring in an aqueous continuous phase, thereby forming discrete droplets. In order that the microspheres should form, the organic solvent must first diffuse into the aqueous phase and then evaporate at the water/air interface. As solvent evaporation occurs the microspheres harden, and free flowing microspheres can be obtained after suitable filtration and drying [30]. The solvent evaporation method has been used for preparation of poly(L-lactic acid) (PLLA) microspheres containing  $^{166}\text{Ho}$ ,  $^{90}\text{Y}$  and  $^{186}\text{Re}/^{188}\text{Re}$ .

Mumper et al. [13,28,31] and also our group [29] prepared PLLA microspheres with holmium-165-acetylacetonate (HoAcAc) [32]. HoAcAc complex and PLLA were dissolved in chloroform and the solution was added to a polyvinyl alcohol (PVA) solution and stirred until the solvent had evaporated. Microspheres were graded and collected according to size, on stainless steel sieves of 20-50  $\mu\text{m}$ . These microspheres can be dispensed in patient-ready doses, that only need to be activated by neutron bombardment to a therapeutic amount of radioactivity in a nuclear reactor [29]. These holmium loaded microspheres are currently being tested by intrahepatic arterial administration to rat liver tumours (Fig. 1a). A seven-fold increase of the  $^{166}\text{Ho}$ -microspheres in and around the tumour compared with normal liver is found (Fig. 1b), based on distribution of radioactivity.



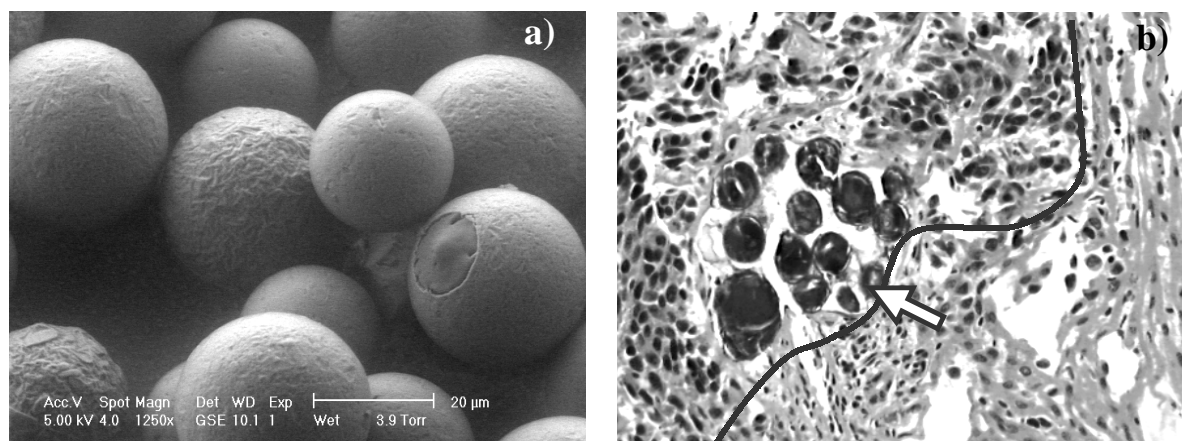


**Fig. 1.** Scanning electron micrograph of holmium loaded PLLA microspheres (a). Radioactive holmium loaded microspheres in an artery of tumour-tissue in rat liver (white arrow). Artificial black line shows the border between tumour tissue (left) and liver tissue (right) (b).

Magnetic PLLA microspheres loaded with yttrium were made by Häfeli et al. [33,34], in order to direct them to the tumour. Their method resulted in stably loaded spheres, with the possibility of pre- or afterloading. To produce preloaded microspheres PLLA was dissolved with L- $\alpha$ -phosphatidylcholine in methylene chloride. Commercially available  $^{90}\text{YCl}_3$  and magnetite  $\text{Fe}_3\text{O}_4$  were added to the solution, vortexed, and sonicated. The suspension was injected into PBS with PVA, and microspheres were prepared following a solvent evaporation technique. Afterloaded spheres were prepared by suspending dried microspheres in a solution of PBS, after which  $^{90}\text{YCl}_3$  in HCl was added. Spheres were subsequently vortexed, incubated, and washed, resulting in labeled microspheres. Leaching of  $^{90}\text{Y}$  was around 4% after 1 day in PBS at 37°C. Specific activity was 1.85 MBq/mg in both methods.  $^{90}\text{Y}$  was bound to the carboxylic endgroups of the PLLA. Experiments in mice showed a 12-fold increase in activity in the tumour with a directional magnet fixed above it [34]. Rhenium loaded PLLA microspheres were also developed, but these microspheres were unable to withstand the high neutron fluxes in a nuclear reactor which are necessary to achieve the high specific activity required in the treatment of liver tumours [2].

#### 1.2.2.1 Size of microspheres for treatment of hepatic malignancies

The size of the microsphere is an important factor for the distribution in the liver and tumour. The production parameters of microspheres can be modified to result in high yields of spheres with the desired diameter. For example, lowering the stirring rate during production and a higher viscosity of the aqueous phase, result in increasing diameters of the polymeric microspheres. Although the size of the microspheres can

be regulated by production methods, a sifting step is necessary after production of cold or radioactive spheres.

A range of sizes has been reported in the literature with microsphere diameters varying from 13 to 75  $\mu\text{m}$  [14,22,23,35,36]. The widely used  $^{90}\text{Y}$  glass microspheres have a mean diameter of 22  $\mu\text{m}$  with a range of 15 to 30  $\mu\text{m}$  [10,12,37].

Larger microspheres, 40-50  $\mu\text{m}$ , are distributed more homogeneously in the liver and with fewer spills to other organs such as lungs and spleen than smaller particles. However, with larger particles the tumour/liver ratio decreases. Microspheres of around 30  $\mu\text{m}$  are the optimum size for hepatic radionuclide therapy, as they are most evenly distributed within the normal liver tissue, yet still provide a concentrated dose of radiation to tumour tissue [8,38,39]. Distribution of intra-arterial microspheres with a diameter of 32  $\mu\text{m}$  was extensively investigated in the microvasculature of tumour in human liver by Campbell et al. [40]. Microspheres were found to deposit preferentially in the richly vascularized periphery of the tumour.

#### *1.2.2.2 Choice of radionuclide*

The ultimate radionuclide suitable for internal radionuclide therapy of primary and metastatic malignancies requires the following properties: 1) The radioisotope must have an appropriate radiation spectrum for treating small to large multiple tumours. Large tumours with a vascular periphery but a necrotic centre take up less microspheres per volume, therefore a high energy  $\beta$ -emitter with a subsequently high tissue range is needed to reach the interior of the tumour. 2) A high dose rate is advantageous for the radiobiological effect [41,42]. Consequently, a short half-life is preferable. 3) For external imaging of the biodistribution of the radioisotope with a gamma camera, a  $\gamma$ -emitter is necessary. However, the energy should be low to prevent unnecessary radiation burden to the patient and environment [13]. 4) The labeling of particles has to be simple without any leakage of the isotope. 5) A large thermal neutron cross section is needed to enable high specific activities to be achieved within short neutron activation times [16].

Only a few radioisotopes have characteristics, which make them potentially suitable for the treatment of tumours (see Table 3). Taking into account the aforementioned properties three radioisotopes are the most likely candidates, yttrium-90, rhenium-188 and holmium-166. Yttrium-90 has two major disadvantages as a radioisotope for therapy. First, long neutron activation times (>2 weeks) are needed to achieve therapeutic activities of yttrium because  $^{90}\text{Y}$ 's precursor has a small thermal neutron cross section of 1.28 barn. Secondly, the biodistribution of microspheres loaded with  $^{90}\text{Y}$  cannot be directly determined in clinical trials, since  $^{90}\text{Y}$  is a pure  $\beta$ -emitter and does not produce imageable  $\gamma$ -rays.

**Table 3.** Characteristics of radionuclides suitable for therapeutical application [43-46]

Radio-nuclide	Production	Half-life (h)	$\beta_{\max}$ (MeV)	$\gamma$ (MeV)	Max. tissue range (mm)	Cross section (barn)
$^{32}\text{P}$	$^{31}\text{P}(\text{n}, \gamma)$ $^{34}\text{S}(\text{d}, \alpha)$ $^{32}\text{S}(\text{n}, \text{p})$	343.2	1.71		7.9	0.19
$^{90}\text{Y}$	$^{89}\text{Y}(\text{n}, \gamma)$ $^{90}\text{Sr}/^{90}\text{Y}$	64.1	2.27		11	1.3
$^{109}\text{Pd}$	$^{108}\text{Pd}(\text{n}, \gamma)$	13.4	1.03	0.088	4.2	8.8
$^{140}\text{La}$	$^{139}\text{La}(\text{n}, \gamma)$ $^{140}\text{Ba}/^{140}\text{La}$	40	1.31 (79%) 2.18 (6%)	0.487 0.329 0.815	10	8.9
$^{153}\text{Sm}$	$^{152}\text{Sm}(\text{n}, \gamma)$ $^{150}\text{Nd}(\alpha, \text{n})$	46.8	0.80	0.070 0.103	3.0	220
$^{165}\text{Dy}$	$^{164}\text{Dy}(\text{n}, \gamma)$	2.4	1.29	0.095	5.7	800
$^{166}\text{Ho}$	$^{165}\text{Ho}(\text{n}, \gamma)$	26.8	1.84 (51%) 1.78 (48%)	0.081	8.6	64
$^{169}\text{Er}$	$^{168}\text{Er}(\text{n}, \gamma)$	230.4	0.34	0.008	0.9	2
$^{186}\text{Re}$	$^{185}\text{Re}(\text{n}, \gamma)$	90.6	1.07	0.137	4.5	110
$^{188}\text{Re}$	$^{187}\text{Re}(\text{n}, \gamma)$ $^{188}\text{W}/^{188}\text{Re}$	17	2.11	0.155	10	70
$^{198}\text{Au}$	$^{197}\text{Au}(\text{n}, \gamma)$ $^{198}\text{Pt}(\text{p}, \text{n})$	64.8	0.96	0.412	3.9	99

Natural rhenium is composed of two isotopes ( $^{185}\text{Re}$  and  $^{187}\text{Re}$ ) that form  $\beta$ -emitting  $^{186}\text{Re}$  and  $^{188}\text{Re}$  radioisotopes respectively, upon neutron activation. The nuclear and dosimetric properties of the rhenium radioisotopes are comparable to those of  $^{90}\text{Y}$ , but they have imageable  $\gamma$ -photons and  $^{188}\text{Re}$  is easily available from a  $^{188}\text{W}/^{188}\text{Re}$ -generator system.

Like the rhenium radioisotopes,  $^{166}\text{Ho}$  emits  $\beta$ -particles and photons. It has a physical half-life of 26.8h resulting in a high dose rate. Its cross section is comparable with rhenium, but  $^{165}\text{Ho}$  has a natural abundance of 100% and thus only one radioisotope,  $^{166}\text{Ho}$ , is formed by neutron bombardment. Taking these characteristics into consideration,  $^{166}\text{Ho}$  is therefore an attractive candidate for use in future treatments.

### 1.3 Characteristics in-vitro and in-vivo

#### 1.3.1 Irradiation damage of neutron activated microspheres

Glass is relatively resistant to irradiation damage, as is shown by the long irradiations that are necessary to produce rhenium loaded glass microspheres [16]. The  $\gamma$ -heating, neutrons and other radiation conditions in a nuclear reactor result in considerable irradiation damage to polymers. Literature concerning  $\gamma$ -irradiations for sterilisation of the product can be found to gain an impression of the damage caused by irradiation of polymeric microspheres, which must be irradiated in a nuclear reactor to produce radioactive pharmaceuticals. We investigated the changes in morphology of the surface of holmium loaded microspheres after irradiation [29]. Non-irradiated  $^{165}\text{Ho}$ -PLLA-microspheres show a smooth, spherical appearance, whilst irradiated spheres show minor surface changes of small free PLLA fragments. These fragments represent, under the irradiation conditions used, a negligible part of total particle volume. However, changes in molecular weight of PLLA were substantial [29] and this was also confirmed in other studies using  $\gamma$ -sterilisation [47,48]. Two major mechanisms of degradation (Fig. 2) take place in a polymer as it is subjected to radiation: (1) chain scission occurs as a random rupturing of bonds, resulting in reduction of the molecular weight or, (2) cross-linking which results in the formation of three-dimensional networks. These mechanisms usually occur simultaneously. The cause of the decrease in molecular weight of polymers is mainly radiation chain scission owing to radical formation [49]. In  $\gamma$ -irradiation of PLLA chain scission occurs predominantly in the amorphous phase of the polymer [31,47]. High crystalline polymers are more radiation resistant. The reduction in molecular weight is also dependent on the environment. Oxygen, water, additives and device dimensions are major factors influencing the degradation [29,49,50]. In most polymers such as PLLA, dl-PLA [51], poly(lactic-co-glycolic acid) (PLGA) [52,53,54] or polyglycolic acid (PGA) [55] the mechanisms of degradation are comparable.

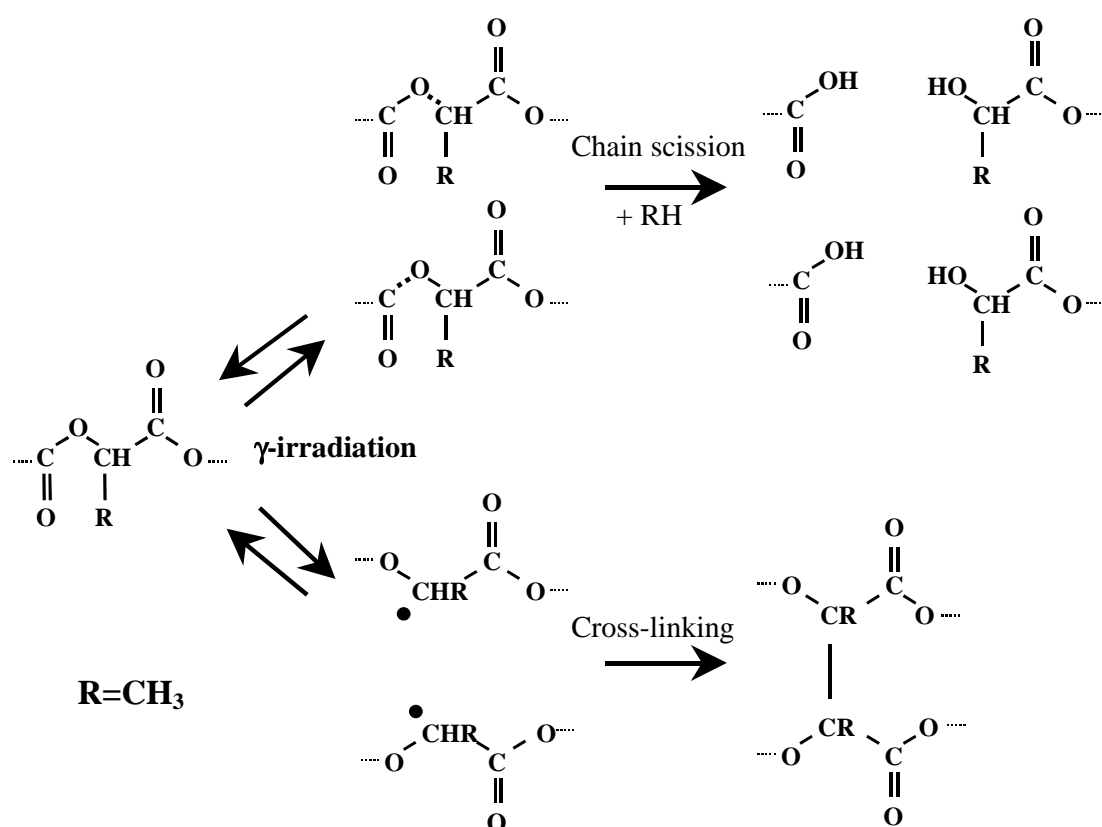


**Fig. 2.** Hypothetical degradation mechanisms of PLLA upon  $\gamma$ -irradiation [49].

### 1.3.2 Degradation, biodegradability, biocompatibility

Glass and resin particles do not undergo degradation *in vivo*. Unlike resin or glass microspheres, polymers such as PLLA and PLGA do degrade [10,56]. Polymeric microspheres  $<300 \mu\text{m}$  in diameter undergo a homogeneous hydrolytic degradation, the extent of degradation of the core being equivalent to the degradation at the surface [57]. Factors affecting the hydrolytic degradation of biodegradable polyesters are indicated in Table 4. The porosity of microspheres may play a major role in enhancing the rate of biodegradation. Micropores in the spheres permit the release of low molecular weight degradation products, whose carboxylic end groups may facilitate the autocatalytic degradation of the polymer. During the degradation process, the crystallinity of the polymer gradually increases, resulting in a relatively stable product [57].

**Table 4.** Factors affecting the hydrolytic degradation behaviour of biodegradable polyesters [57]

- 
- Water permeability and solubility (hydrophilicity/hydrophobicity)
  - Chemical composition
  - Mechanism of hydrolysis (noncatalytic, autocatalytic, enzymatic)
  - Additives (acidic, basic, monomers, solvents, drug)
  - Morphology (crystalline, amorphous)
  - Device dimensions (size, shape, surface to volume ratio)
  - Porosity
  - Glass transition temperature (glassy, rubbery)
  - Molecular weight and molecular weight distribution
  - Physico-chemical factors (ion exchange, ionic strength, pH)
  - Sterilization
  - Site of implantation
- 

Anderson and Shive reported in detail the biocompatibility and tissue/material interactions of biodegradable microspheres [57]. Injection of microspheres, either subcutaneously or intramuscularly, results in the implantation of a high surface area/low volume of material into a given tissue volume. Depending upon the packing and volume of microspheres within an implant site, days to weeks may be required for cellular infiltration from the surface of the microsphere volume, to its centre. The infiltration of inflammatory cells and in particular, monocytes, macrophages and fibroblasts, results in each microsphere having its attendant tissue/material interaction. The volume of microspheres also elicits a response, which is generally seen early as a granulation tissue response leading to a fibrous site. Given biocompatible biodegradable microspheres, the response during the first two weeks is generally similar, regardless of the degradation rate of the biodegradable polymer. A minimal inflammatory reaction is observed. The second phase of the tissue response is initiated by the predominance of monocytes and macrophages. This response occurs after 50-60 days with poly(DL-lactide-co-glycolide) particles, and after more than 350 days with PLLA [58]. The last phase is the breakdown of spheres in particles smaller than 5  $\mu\text{m}$ , small enough to initiate a tissue response which is predominated by macrophages.

### 1.3.3 Release

Improvements in radiolabelling techniques have resulted in increasingly stable  $^{90}\text{Y}$  microspheres. A new generation of glass (TheraSpheres<sup>®</sup>, Theragenics, Atlanta, GA, USA) and resin microspheres (supplied by the Australian Nuclear Science and

Technology Organisation) have overcome the problem of leaching. Routine tests on resin and glass microspheres showed that less than 0.1% of the activity leaches from the microspheres. Clinical studies on metastatic liver cancer, using these newer glass [59] and resin microspheres, have produced good results with very little toxicity [23].

Polymeric microspheres loaded with  $^{166}\text{Ho}$  showed a high stability. Mumper et al. and also our group showed that more than 98% of  $^{166}\text{Ho}$  activity was retained in the microspheres after 192h incubation at  $37^\circ\text{C}$ , in several physiological media [13,29]. On the one hand, this is a favourable characteristic of these microspheres for the attempted application, but on the other hand this is surprising, since generally low molecular weight compounds are released to a high extent and relatively rapidly from PLLA microspheres [57,60-62]. We found that HoAcAc can be dispersed in the amorphous PLLA phase up to 17% (w/w) indicating the presence of favourable PLLA/HoAcAc interactions in the microspheres. Carbonyl groups of PLLA are likely to interact with the holmium ion in the HoAcAc complex, by which this complex is immobilized in the PLLA matrix. This interaction thus accounts for the high stability (= low holmium release) found in HoAcAc loaded microspheres.

#### *1.3.4 Radiotoxicity*

Radiotoxic effects are reported from the old generation of glass and resin microspheres, by leaching of the radioisotope from the particles, which can result in pancytopenia [63]. The new generation of spheres showed no such leaching. These spheres were used for the first time in the well-known dog experiments by Wollner et al. [64], showing that the animals survived a liver dose of up to 350 Gy. However, at such exceedingly high (and clinically unrealistic) doses, sequelae related to cirrhosis would be likely to become a significant problem. Even 800 Gy to the whole liver of rabbits was tolerated [65]. These experiments showed that internal radiotherapy using non-leaking microspheres can be performed safely with high doses. In patients in which doses up to 100 Gy were directed to the liver, the hepatic toxicity of the treatment appears to be low, as is shown by the liver enzyme levels [2]. Gastroduodenal ulceration has been reported as a complication of intra-hepatic arterial glass microsphere therapy, and this may be related to migration of microspheres to organs outside the liver, caused by the high density of the spheres [15,29,66,67]. Radiation pneumonitis was documented in a patient in which the lung dose was greater than 30 Gy, whereas most patients received a lung dose of less than 20 Gy [11,68].

## **1.4 Application in oncology**

Since recent developments, especially the increased skills of interventional radiologists, there is an awakened interest in unique selective radionuclide therapy. Many kinds of radiolabeled particles and radionuclides have been tested for local treatment of a variety of tumours in organs, including liver, lung, tongue, spleen and soft tissue of extremities. The purpose of this treatment is the superselective application of suitable radioactive (high energetic  $\beta$ -emitters) particles to deliver high doses to the tumour, with as little surrounding tissue damage as possible. These new embolization methods are extremely important particularly for cancers with an extremely poor prognosis and without other adequate therapies, such as primary and metastatic malignancies of the liver.

### *1.4.1 Liver cancer*

Patients with primary or metastatic tumours were treated by radio-embolization via a catheter [59,69] or direct injection of beads into the tumour, with a needle [21,70]. Most studies describe administration of microspheres to patients via a catheter, whereby the tip was placed in the hepatic artery. The spheres eventually lodge in the microvasculature of the liver and tumour, remaining until the complete decay of the radioisotope. Lung shunting and tumour-to-normal liver ratio was determined after infusion of  $^{99m}\text{Tc}$ -labeled macroaggregated albumin, and microspheres were subsequently administered to patients [71,72]. Tumour-to-normal liver ratio was approximately 3-5 [12,22,56,73]. In some studies the blood flow within the liver was temporarily redirected in favour of the tumour by a bolus infusion of a vasoconstrictor, and the spheres were then embolized into the arterial circulation [69]. While external beam radiation causes radiation hepatitis at doses above 30-35 Gy [74] the liver can tolerate up to 80-150 Gy, using internal radionuclide therapy [12,69,72]. Increased longevity, pain relief, tumour response and total clinical improvement are frequently reported [12,24,37,70].

### *1.4.2 Head-and-neck cancer*

Chemo-embolization with ethylcellulose microspheres of 100-450  $\mu\text{m}$  has been used in the treatment of maxillary tumours. The role of intra-arterial radioisotope therapy in the treatment of head-and-neck cancer is just beginning in rabbits, in the work of van Es et al. [75]. The optimal size of microspheres for treatment of unresectable head-and-neck cancer is still to be established. Van Es et al. suggest that large microspheres of 40-65  $\mu\text{m}$  should be used for the embolization of these tumours. Other embolizations in the treatment of head-and-neck cancer have been carried out with particles of 100-450  $\mu\text{m}$  [76].



### 1.4.3 Ovarian cancer

The overall 5-year survival in patients with epithelial ovarian cancer is as low as 35-38%. Initially, intraperitoneal  $^{198}\text{Au}$ -colloid was used as an adjunct in the treatment of ovarian cancer, but this resulted in a significant number of major complications and associated deaths [77]. Subsequently  $^{32}\text{P}$  became the radioisotope of choice because of a higher  $\beta$  energy compared with  $^{198}\text{Au}$ . Vergote et al. [45] used  $^{211}\text{At}$ -microspheres for the treatment of mice with ovarian cancer. This was prepared by copolymerization of glycidyl methacrylate and ethylene glycol dimethacrylate with a diameter of 1.8  $\mu\text{m}$ . The  $\alpha$ -emitters such as  $^{211}\text{At}$ ,  $^{212}\text{Bi}$  and  $^{212}\text{Pb}$  may be a useful addition to future treatment of small clusters of cancer cells.

### 1.4.4 Other cancers

Intra-arterial administration of  $^{90}\text{Y}$ -microspheres has been carried out in the spleen [78]. Of nine patients with lymphosarcoma, five manifested no clinical response after splenic irradiation. One patient who complained of weakness, rapid fatigue and anorexia, had relief of all symptoms after splenic irradiation.

## 1.5 Perspectives

Improvements in radiolabelling techniques have resulted in increasingly stable microspheres with a leakage of less than 0.1% of the activity. Three major radiolabeled microsphere materials, glass, resin-based and polymer-based are now available for therapy or are being tested in animals. The only commercially available glass-type  $^{90}\text{Y}$  microspheres are very stable and have a proven reputation in the treatment of primary or metastatic hepatic cancer, but their high density is a serious drawback. Consequently, less dense particles have been developed in the form of resin and polymeric spheres. Resin-based spheres also have a high chemical stability and, with half the density of glass, they provide good prospects for the treatment of liver cancer. Resin particles are currently being investigated in patients, and these particles show results comparable to glass. Polymeric microspheres like poly(L-lactic acid) spheres have a near plasma density and additional advantages such as biocompatibility and biodegradability. A polymeric sphere appears to be the best particle for this kind of therapy, although with the drawback of low resistance to irradiation in a nuclear reactor. Recent studies have demonstrated that polymeric microspheres can be prepared with sufficient amounts of activity for therapeutic application. These microspheres are therefore one of the future materials for use in the battle with liver cancer. Other oncological applications such as the treatment of head-and-neck cancer, bone metastases and ovarian cancer are in the pipeline. Internal radionuclide therapy is likely to play a substantial role in the control of hepatic and other types of cancer in the future.

## 1.6 Aims and scope of the thesis

In this thesis the feasibility of poly(L-lactic acid) microspheres loaded with  $^{166}\text{Ho}$  for internal radiation therapy of liver malignancies is investigated. Aspects of preparation, characterization, biodistribution and therapeutical effect in animals were addressed in order to answer the following questions:

- 1 Is it possible to prepare holmium containing microspheres in a reproducible way to enable routine production and facilitate therapeutic application?
- 2 What are the physical characteristics of these microspheres before and after neutron activation?
- 3 Can selective targeting of liver tumours be accomplished in vivo?
- 4 Is there a therapeutic effect of these microspheres on liver tumours?

## 1.7 Outline of the subsequent chapters

In **Chapter 2** the preparation and neutron activation of holmium containing poly(L-lactic acid) microspheres is presented. The microspheres were prepared using a solvent evaporation technique and the effect of the formulation and processing parameters on the holmium loading were evaluated. Further, the effects of neutron irradiation conditions were examined and defined in detail. In **Chapter 3** the crystal structures of two holmium acetylacetonate complexes were elucidated using X-ray diffraction. **Chapter 4** describes an in depth characterization of PLLA microspheres loaded with HoAcAc. PLLA microspheres, and as a control PLLA films, with and without HoAcAc were investigated using a variety of advanced techniques. **Chapter 5** deals with the influence of neutron irradiation on the HoAcAc loaded PLLA microspheres. Possible radiation damage of both the PLLA matrix and the Ho-complex was investigated. In **Chapter 6** the biodistribution of PLLA microspheres loaded with  $^{166}\text{Ho}$  is studied in rats with liver tumours. The distribution of the activity, especially the tumour-to-normal liver-tissue ratio, after administration of  $^{166}\text{Ho}$ -PLLA microspheres with sizes between 20 and 50  $\mu\text{m}$  was determined. Also, an extensive histological evaluation was performed. **Chapter 7** reports on the therapeutic effect of  $^{166}\text{Ho}$ -PLLA microspheres in a rabbit model. Liver function was examined by histology and analysis of liver enzyme activity. **Chapter 8** summarises this thesis and gives suggestions for further research to enable clinical application of Ho-loaded PLLA microspheres for the internal radionuclide therapy of tumours.

**References**

1. Scheele J and Altendorf-Hofmann A. Resection of colorectal liver metastases. *Langenbeck's Arch. Surg.* **1999**;313-327.
2. Häfeli UO, Casillas S, Dietz DW, Pauer GJ, Rybicki LA, Conzone SD and Day DE. Hepatic tumor radioembolization in a rat model using radioactive rhenium (<sup>186</sup>Re/<sup>188</sup>Re) glass microspheres. *Int. J. Radiation Oncology Biol. Phys.* **1999**;44:189-199.
3. Link KH, Kornman M., Formentini A, Leder G, Sunelaitis E, Schatz M, Preßmar J and Beger HG. Regional chemotherapy of non-resectable liver metastases from colorectal cancer – literature and institutional review. *Langenbeck's Arch. Surg.* **1999**;384:344-353.
4. Bastian P, Bartkowski R, Köhler H and Kissel T. Chemo-embolization of experimental liver metastases. Part I: distribution of biodegradable microspheres of different sizes in an animal model for the locoregional therapy. *Eur. J. Pharm. Biopharm.* **1998**;46:243-254.
5. Ackerman NB, Lien WM, Kondi ES and Silverman NA. The blood supply of experimental liver metastases. The distribution of hepatic artery and portal vein blood to “small” and “large” tumors. *Surgery* **1969**;66:1067-1072.
6. Jain RK. Delivery of molecular and cellular medicine to solid tumors. *J. Cont. Release* **1998**;53:49-67.
7. Harbert JC. *In Nuclear Medicine: Diagnosis and Therapy*; Harbert JC, Eckelman WC and Neumann RD. *Thieme Medical Publishers, Inc.*, New York, **1996**;1141-1155.
8. Müller JH and Rossier PH. A new method for treatment of cancer of the lungs by means of artificial radioactivity (<sup>63</sup>Zn and <sup>198</sup>Au). *Acta Radiol.* **1951**;35:449.
9. Grady ED, Sale W, Nicolson WP and Rollins CR. Intra-arterial radioisotopes to treat cancer. *Am. Surg.* **1960**;26:678-684.
10. Ehrhardt GJ and Day DE. Therapeutic use of <sup>90</sup>Y Microspheres. *Nucl. Med. Biol.* **1987**;14:233-242.
11. Ho S, Lau WY, Leung TWT, Chan M, Ngar YK, Johnson PJ and Li AKC. Clinical evaluation of the partition model for estimating radiation doses from yttrium-90 microspheres in the treatment of hepatic cancer. *Eur. J. Nucl. Med.* **1997**;24:293-298.
12. Andrews JC, Walker SC, Ackermann RJ, Cotton LA, Ensminger WD and Shapiro B. Hepatic radioembolization with yttrium-90 containing glass microspheres. Preliminary results and clinical follow-up. *Eur. J. Nucl. Med.* **1994**;35:1637-1644.
13. Mumper RJ, Ryo UY and Jay M. Neutron activated holmium-166-Poly(L-lactic acid) microspheres: A potential agent for the internal radiation therapy of hepatic tumours. *J. Nucl. Med.* **1991**;32:2139-2143.

14. Turner JH, Claringbold PG, Klemp PFB, Cameron PJ, Martindale AA, Glancy RJ, Norman PE, Hetherington EL, Najdovski L and Lambrecht RM.  $^{166}\text{Ho}$ -microsphere liver radiotherapy: a preclinical SPECT dosimetry study in the pig. *Nucl. Med. Comm.* **1994**;15:545-553.
15. Ho S, Lau WY, Leung TWT and Johnson PJ. Internal radiation therapy for patients with primary or metastatic hepatic cancer. *Cancer* **1998**;83:1894-1907.
16. Conzone SD, Häfeli UO, Day DE and Ehrhardt GJ. Preparation and properties of radioactive rhenium glass microspheres intended for in vivo radioembolization therapy. *J. Biomed. Mater. Res.* **1998**;42:617-625.
17. Brown RF, Lindesmith LC and Day DE.  $^{166}\text{Ho}$ -containing glass for internal radiotherapy of tumors. *Int. J. Rad. Appl. Instrum. B* **1991**;18:783-790.
18. Kawashita M, Miyaji F, Kokubo T, Takaoka GH, Yamada I, Suzuki Y and Inoue M. Surface structure and chemical durability of  $\text{P}^+$ -implanted  $\text{Y}_2\text{O}_3\text{-Al}_2\text{O}_3\text{-SiO}_2$  glass for radiotherapy of cancer. *J. Non-Cryst. Solids* **1999**;255:140-148.
19. Schubiger PA, Beer H-F, Geiger L, Rösler H, Zimmerman A, Triller J, Mettler D and Schilt, W.  $^{90}\text{Y}$ -resin particles-animal experiments on pigs with regard to the introduction of superselective embolization therapy. *Nucl. Med. Biol.* **1991**;18:305-311.
20. Zimmerman A, Schubiger PA, Mettler D, Geiger L, Triller J and Rösler H. Renal pathology after arterial yttrium-90 microsphere administration in pigs. A model for superselective radioembolization therapy. *Invest. Rad.* **1995**;30:716-723.
21. Wang S-J, Lin W-Y, Chen M.-N, Chi C-S, Chen J-T, Ho W-L, Hsieh B-T, Shen L-H, Tsai Z-T, Ting G, Mirzadeh S and Knapp FF. Intratumoral injection of rhenium-188 microspheres into an animal model of hepatoma. *J. Nucl. Med.* **1998**;39:1752-1757.
22. Burton MA, Gray BN, Klemp PF, Kelleher DK and Hardy N. Selective internal radiation therapy: distribution of radiation in the liver. *Eur. J. Cancer Clin. Oncol.* **1989**;25:1487-91.
23. Lau WY, Leung WT, Ho S, Leung NWY, Chan M, Lin J, Metreweli C, Johnson P and Li AKC. Treatment of inoperable hepatocellular carcinoma with intrahepatic arterial yttrium-90 microspheres: a phase I and II study. *Br. J. Cancer* **1994**;70:994-999.
24. Lau WY, Ho S, Leung TWT, Chan M, Ho R, Johnson PJ and Li AKC. Selective internal radiation therapy for nonresectable hepatocellular carcinoma with intraarterial infusion of  $^{90}\text{Y}$  microspheres. *Int. J. Radiation Oncology Biol. Phys.* **1998**;40:583-592.
25. Wunderlich G, Pinkert J, Andreeff M, Stintz M, Knapp FF, Kropp J and Franke WG. Preparation and biodistribution of rhenium-188 labeled albumin microspheres B 20: a promising new agent for radiotherapy. *Appl. Radiat. Isotopes* **2000**;52:63-68.
26. Rhodes BA, Zölle I, Buchanan JW and Wagner HN. Radioactive albumin microspheres for studies of the pulmonary circulation. *Radiology* **1969**;92:1453-1460.

27. Watanabe N, Oriuchi N, Endo K, Inoue T, Tanada S, Murata H and Sasaki Y. Yttrium-90-labeled human macroaggregated albumin for internal radiotherapy: combined use with DTPA. *Nucl. Med. Biol.* **1999**;26:847-851.
28. Jay M, Khare SS, Mumper RS and Ryo UY. Microencapsulation of activable radiotherapeutic agents. *Biological and Synthetic Membranes* **1989**;292:293-300.
29. Nijsen JFW, Zonnenberg BA, Woittiez JRW, Rook DW, Swildens-van Woudenberg IA, van Rijk PP and van het Schip AD. Holmium-166 poly lactic acid microspheres applicable for intra-arterial radionuclide therapy of hepatic malignancies: effects of preparation and neutron activation techniques. *Eur. J. Nucl. Med.* **1999**;26:699-704.
30. O' Donnell PB and McGinity JW. Preparation of microspheres by solvent evaporation technique. *Adv. Drug Del. Rev.* **1997**;28:25-42.
31. Mumper RJ and Jay M. Poly(L-lactic acid) microspheres containing neutron-activatable holmium-165: A study of the physical characteristics of microspheres before and after irradiation in a nuclear reactor. *Pharm. Res.* **1992**;9:149-154.
32. Kooijman H, Nijsen JFW, Spek AL and van het Schip AD. Diaquatrakis(pentane-2,4-dionato-O,O')holmium(III) monohydrate and diaquatrakis(pentane-2,4-dionato-O,O')holmium(III) 4-hydroxypentan-2-one solvate dihydrate. *Acta. Cryst.* **2000**;C56:156-158.
33. Häfeli UO, Sweeney SM, Beresford BA, Sim EH and Macklis RM. Magnetically directed poly(lactic acid) <sup>90</sup>Y-microspheres: Novel agents for targeted intracavitary radiotherapy. *J. Biomed. Res.* **1994**;28:901-908.
34. Häfeli UO, Sweeney SM, Beresford BA, Humm JL and Macklis RM. Effective targeting of magnetic radioactive <sup>90</sup>Y-microspheres to tumor cells by an externally applied magnetic field. Preliminary in vitro and in vivo results. *Nucl. Med. Biol.* **1995**;22:147-155.
35. Mantravedi RVP, Spigos DG, Tan WS and Felix EL. Intraarterial yttrium-90 in the treatment of hepatic malignancy. *Radiology* **1982**;142:783-786.
36. Rösler H, Triller J, Baer HU, Geiger L, Beer HF, Becker C and Blumgart LH. Superselective radioembolization of hepatocellular carcinoma: 5-year results of a prospective study. *Nucl. Med.* **1994**;33:206-214.
37. Herba MJ, Illescas FF, Thirlwell MP, Boos GJ, Rosenthal L, Atri M and Bret PM. Hepatic malignancies: improved treatment with intraarterial Y-90. *Radiology* **1988**;169:311-314.
38. Meade VM, Burton MA, Gray BN and Self GW. Distribution of different sized microspheres in experimental hepatic tumours. *Eur. J. Clin. Oncol.* **1987**;23:37-41.
39. Bastian P, Bartkowski R, Köhler H and Kissel T. Chemo-embolization of experimental liver metastases. Part I: distribution of biodegradable microspheres of different sizes in an animal model for the locoregional therapy. *Eur. J. Pharm. Biopharm.* **1998**;46:243-254.

40. Campbell AM, Bailey IH and Burton MA. Analysis of the distribution of intra-arterial microspheres in human liver following hepatic yttrium-90 microsphere therapy. *Phys. Med. Biol.* **2000**;45:1023-1033.
41. Spencer RP. Applied principles of radiopharmaceutical use in therapy. *Nucl. Med. Biol.* **1986**;13:461-463.
42. Spencer RP. Short-lived radionuclides in therapy. *Nucl. Med. Biol.* **1987**;14:537-538.
43. ICRP Publication 38. *Radionuclide transformations energy and intensity of emissions*, Pergamon Press: Oxford, **1983**.
44. Neves M, Waerenborgh F and Patricio L. Palladium-109 and holmium-166 potential radionuclides for synoviotherapy-radiation absorbed dose calculations. *Appl. Radiat. Isot.* **1987**;38:745-749.
45. Vergote I, Larsen R H, de Vos L, Nesland JM, Bruland Ø, Bjørgum J, Alstad J, Tropé C and Nustad K. Therapeutic efficacy of the  $\alpha$ -emitter  $^{211}\text{At}$  bound on microspheres compared with  $^{90}\text{Y}$  and  $^{32}\text{P}$  colloids in a murine intraperitoneal tumor model. *Gynecol. Oncol.* **1992**;47:366-372.
46. Wang SJ, Lin WY, Chen MN, Hsieh BT, Shen LH, Tsai ZT, Ting G, Chen JT, Ho WL, Mirzadeh S and Knapp FF. Rhenium-188 microspheres: A new radiation synovectomy agent. *Nucl. Med. Biol.* **1998**;19:427-433.
47. Collet JH, Lim LY and Gould PL. Gamma-irradiation of biodegradable polyesters in controlled physical environments. *Polymer reprints* **1989**;30:468-469.
48. Schakenraad JM, Oosterbaan JA, Nieuwenhuis P, Molenaar I, Olijslager J, Potman W, Eenink MJD and Feijen J. Biodegradable hollow fibres for the controlled release of drugs. *Biomaterials* **1988**;9:116-120.
49. Sintzel MB, Merkli A, Tabatabay C and Gurny R. Influence of irradiation sterilization on polymers used as drug carriers-A review. *Drug Develop. Ind. Pharm.* **1997**;23:857-878.
50. Esselbrugge H, Grootoink J and Feijen J.  *$\gamma$ -irradiation of poly(L-lactide) hollow fibers*. Thesis, University of Twente, The Netherlands: Biodegradable hollow fibres for controlled drug delivery, Appendix A, **1992**;245-258.
51. Henn GG, Birkinshaw C, Buggy M and Jones EA. comparison of the effects of  $\gamma$ -irradiation and ethylene oxide sterilization on the properties of compression moulded poly-d, l-lactide. *J. Mater. Sci. Mat. Med.* **1996**;7:591-595.
52. Montanari L, Costantini M, Signoretti EC, Valvo L, Santucci M, Bartolomei M, Fattibene P, Onori S, Faucitano A, Conti B and Genta I. Gamma irradiation effects on poly(DL-lactide-co-glycolide) microspheres. *J. Control. Release* **1998**;56:219-229.
53. Mohr D, Wolff M and Kissel T. Gamma irradiation for terminal sterilization of  $17\beta$ -estradiol loaded poly(DL-lactide-co-glycolide) microparticles. *J. Control. Release* **1999**;61:203-217.

54. Bittner B, Mäder K, Kroll C, Borchert H-H and Kissel T. Tetracycline-HCl-loaded poly(DL-lactide-co-glycolide) microspheres prepared by a spray drying technique: influence of  $\gamma$ -irradiation on radical formation and polymer degradation. *J. Control. Release* **1999**;59:23-32.
55. Chu CC and Campbell ND. Scanning electron microscopic study of the hydrolytic degradation of poly(glycolic acid) suture. *J. Biomed. Mater. Res.* **1982**;16:417-430.
56. Ho S, Lau WY, Leung TWT, Chan M, Ngar YK, Johnson PJ and Li AKC. Partition model for estimating radiation doses from yttrium-90 microspheres in treating hepatic tumours. *Eur. J. Nucl. Med.* **1996**;23:947-952.
57. Anderson JM and Shive MS. Biodegradation and biocompatibility of PLA and PLGA microspheres. *Adv. Drug Del. Rev.* **1997**;28:5-24.
58. Visscher GE, Robison RL, Maulding JW, Fong JW, Pearson JE and Argentieri GJ. Note: Biodegradation of and tissue reaction to poly(DL-lactide) microcapsules. *J. Biomed. Mater. Res.* **1986**;20:667-676.
59. Houle SH, Yip TK, Shepherd FA, Rotstein LE, Sniderman KW, Theis E, Cawthorn RH and Richmond-Cox K. Hepatocellular carcinoma: Pilot trial of treatment with Y-90 microspheres. *Radiology* **1989**;172:857-860.
60. Jalil R and Nixon JR. Microencapsulation using poly(L-lactic acid) IV: Release properties of microcapsules containing phenobarbitone. *J. Microencapsul.* **1990**;7:53-66.
61. Miyajima M, Koshika A, Okada J, Ikeda M and Nishimura K. Effect of polymer crystallinity on papaverine release from poly(L-lactide acid) matrix. *J. Control. Release* **1997**;49:207-215.
62. Miyajima M, Koshika A, Okada J and Ikeda M. Mechanism of drug release from poly(L-lactic acid) matrix containing acidic or neutral drugs. *J. Control. Release* **1999**;60:199-209.
63. Mantravedi RVP, Spigos DG, Tan WS and Felix EL. Intraarterial yttrium 90 in the treatment of hepatic malignancy. *Radiology* **1982**;142:783-786.
64. Wollner I, Knutsen C, Smith P, Prieskorn D, Chrisp C, Andrews J, Juni J, Warber S, Klevering J, Crudup J and Ensminger W. Effects of hepatic arterial yttrium 90 glass microspheres in dogs. *Cancer* **1988**;61:1336-1344.
65. Yan Z-P, Lin G, Zhao H-Y and Dong Y-H. An experimental study and clinical pilot trials on yttrium-90 glass microspheres through the hepatic artery for treatment of primary liver cancer. *Cancer* **1993**;72:3210-3215.
66. Shepherd FA, Rotstein LE, Houle S, Yip T-CK, Paul K and Sniderman KW. A phase I dose escalation trial of yttrium-90 microspheres in the treatment of primary hepatocellular carcinoma. *Cancer* **1992**;70:2250-2254.

67. Anderson JH, Goldberg JA, Bessent RG, Kerr DJ, McKillop JH, Stewart I, Cooke TG and McArdle CS. Glass yttrium-90 microspheres for patients with colorectal liver metastases. *Radiotherapy and Oncology* **1992**;25:137-139.
68. Lin M. Radiation pneumonitis caused by yttrium-90 microspheres: radiologic findings. *Am. J. Rad.* **1994**;162:1300-1302.
69. Gray BN, Burton MA, Kelleher D, Klemp P and Matz L. Tolerance of the liver to the effects of yttrium-90 radiation. *Int. J. Radiation Oncology Biol. Phys.* **1990**;18:619-623.
70. Tian J-H, Xu B-X, Zhang J-M, Dong B-W, Liang P and Wang X-D. Ultrasound-guided internal radiotherapy using yttrium-90-glass microspheres for liver malignancies. *J. Nucl. Med.* **1996**;37:958-963.
71. Leung W, Lau W, Ho SKW, Chan M, Leung NWY, Lin J, Metraweli C, Johnson PJ and Li AKC. Measuring lung shunting in hepatocellular carcinoma with intrahepatic-arterial technetium-99m macroaggregated albumin. *J. Nucl. Med.* **1994**;35:70-73.
72. Ho S, Lau WY, Leung TWT, Chan M, Chan KW, Lee WY, Johnson PJ and Li AKC. Tumour-to-normal ratio of <sup>90</sup>Y microspheres in hepatic cancer assessed with <sup>99m</sup>Tc macroaggregated albumin. *Brit. J. Rad.* **1997**;70:823-828.
73. Yorke ED, Jackson A, Fox RA, Wessels BW and Gray N. Can current models explain the lack of liver complications in Y-90 microsphere therapy? *Clin. Cancer Res.* **1999**;5:3024s-3030s.
74. Ingold J, Reed G, Kaplan H and Bagshaw M. Radiation hepatitis. *Am. J. Roentgenol. Radium Ther. Nucl. Med.* **1965**;93:200-208.
75. Van Es RJJ, Franssen O, Dullens HFJ, Bernsen MR, Bosman F, Hennink WE and Slootweg PJ. The VX2 carcinoma in the rabbit auricle as an experimental model for intra-arterial embolization of head neck squamous cell carcinoma with hydrogel dextran microspheres. *Lab. Anim.* **1999**;33:175-184.
76. Tomura N, Kato K, Hirano H, Hirano Y and Watarai J. Chemoembolization of maxillary tumors via the superficial temporal artery using a coaxial catheter system. *Radiation Med.* **1998**;16:157.
77. Vergote I, Larsen RH, de Vos L, Winderen M, Ellingsen T, Bjørgum J, Hoff P, Aas M, Tropé C and Nustad K. Distribution of intraperitoneally injected microspheres labeled with the  $\alpha$ -emitter astatine (<sup>211</sup>At) compared with phosphorus (<sup>32</sup>P) and yttrium (<sup>90</sup>Y) colloids in mice. *Gynecol. Oncol.* **1992**;47:358-365.
78. Ariel IM and Padula G. Irradiation of the spleen by the intra-arterial administration of <sup>90</sup>yttrium microspheres in patients with malignant lymphoma. *Cancer* **1972**;31:90-96.

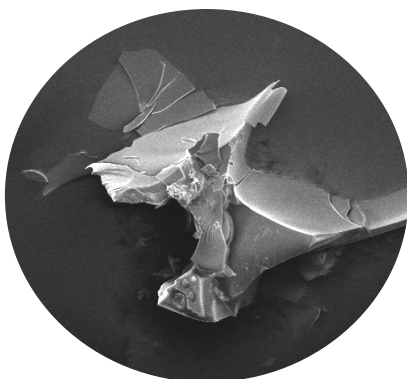


## Chapter 2

---

# **Holmium-166 poly (L-lactic acid) microspheres applicable for intra-arterial radionuclide therapy of hepatic malignancies: effects of preparation and neutron activation techniques**

*European Journal of Nuclear Medicine 1999;26:699-704*



**J.F.W. Nijsen<sup>1</sup>, B.A. Zonnenberg<sup>2</sup>, J.R.W. Woittiez<sup>3</sup>, D.W. Rook<sup>1</sup>,  
I.A. Swildens-van Woudenberg<sup>1</sup>, P.P. van Rijk<sup>1</sup> and  
A.D. van het Schip<sup>1</sup>**

<sup>1</sup>*Department of Nuclear Medicine, University Medical Center, Utrecht, The Netherlands*

<sup>2</sup>*Oncology Section, Department of Internal Medicine, University Medical Center,  
Utrecht, The Netherlands*

<sup>3</sup>*Netherlands Energy Research Foundation, Petten, The Netherlands*

### **Abstract**

Since one of the most frequent sites of human metastatic cancer is the liver, particularly in colon and rectum carcinoma, there is a special need for the development of an effective therapy. This study describes the parameters for reproducible production of poly(L-lactic acid) (PLLA) microspheres with an average diameter of 37  $\mu\text{m}$  and labelled with neutron-activated  $^{166}\text{Ho}$  ( $E_{\text{max}} = 1.84 \text{ MeV}$ ,  $t_{1/2} = 26.8\text{h}$ ), suitable for use in internal radionuclide therapy of liver metastases. It is demonstrated that holmium loaded PLLA microspheres can be prepared by a relatively simple method, with incorporation of  $17.0 \pm 0.6\%$  holmium ( $n=5$ ), and that 20 GBq can be obtained from 400 mg neutron activatable microspheres. In order to produce this high amount of activity, the microspheres must be free of water and irradiation must be performed in a polyethylene vial, with a relatively low neutron flux ( $5 \times 10^{13} \text{ cm}^{-2} \cdot \text{s}^{-1}$ ) within 1h. Under these well-defined conditions minor surface changes were seen which barely affected total volume and consequently total radioactivity of the microspheres with a diameter of 20–50  $\mu\text{m}$ . Overall structural integrity was maintained in terms of form and size. In vitro analyses showed that  $>99.3\%$  of  $^{166}\text{Ho}$  activity was retained in the microspheres after 192h incubation in PBS, plasma and leucocytes, while in liver homogenate retention was still 98.4%.

## 2.1 Introduction

Liver metastases frequently occur during the progression of various solid tumours, especially colorectal cancers, and are the cause of 25–50% of all cancer deaths [1–3]. The median survival of patients with liver metastases ranges from 2–12 months depending on volume of the metastases and histology of the original tumour [1,4]. External beam radiotherapy in the treatment of hepatic malignancies is limited by the tolerance of the hepatic parenchyma, which can tolerate doses of only up to 30 Gy for whole liver irradiation; this treatment modality is therefore ineffective [3,5,6].

A particularly useful alternative mode of therapy is the use of intra-arterially injected radioactive particles of a size sufficient to lodge in endarterioles. The basis for such therapy is that tumours are usually rich in vasculature and that liver metastases are almost exclusively dependent on arterial blood supply. This contrasts with normal liver, which receives most of its flow from the portal vein [7–9]. This selectivity can also be increased by the use of vasoactive drugs, which cause vasoconstriction of the normal liver arterioles, but to which tumour vessels, lacking smooth muscle, are insensitive [10–14].

Treatment with radioactive microspheres is based on this principle. Microspheres with a diameter between 20 and 50  $\mu\text{m}$  will lodge in the vascular bed of the liver [3, 15–17]. The spheres are administered via a catheter through the hepatic artery, after administration of a vasoactive drug. Owing to the high selectivity of this technique, the radiation is mainly restricted to the tumour, with absorbed radiation doses to the tumour varying between 50 and 150 Gy [2,18].

Studies on selective internal radiation therapy of colorectal liver metastases using <sup>90</sup>Y glass microspheres have shown encouraging results [5]. In this technique the microspheres are injected into the hepatic artery and are preferentially directed into the vascular network of liver metastases by enhancing the proportion of blood flow to the tumour, as opposed to normal liver parenchyma, using vasoactive agents [14]. Although the glass spheres have several advantages, their high density (3.29 g/ml), their apparent non-biodegradability and the lack of  $\gamma$ -emission of <sup>90</sup>Y ( $E_{\text{max}} = 2.28$  MeV,  $t_{1/2} = 64.1\text{h}$ ) for imaging may be considered disadvantages [19,20]. The high density is a particularly serious drawback since this accounts for the considerable toxicity caused by backflow to surrounding tissues such as the stomach.

Neutron-activated <sup>166</sup>Ho is a  $\beta$ -emitter ( $E_{\text{max}} = 1.84$  MeV) with radiotherapeutic properties appropriate for therapy, that also emits photons (81 keV, 6.2%) suitable for imaging. The use of <sup>166</sup>Ho embedded in microspheres of poly(L-lactic acid) (PLLA-MS) combines the advantages of microspheres with the additional advantages of biocompatibility, biodegradability, short physical half-life of 26.8h, natural abundance of <sup>165</sup>Ho (100%) and near plasma density.

PLLA-MS containing  $^{166}\text{Ho}$  were first described by Mumper et al. [19]. A sample consisting of 50 mg microspheres and 150 mg inositol was irradiated in a reactor for up to 3h, in a thermal neutron flux of  $8.88 \times 10^{12} \text{ cm}^{-2} \cdot \text{s}^{-1}$ , resulting in 1295 MBq of activity. Inositol was added to disperse the internal heat produced during neutron irradiation.

This study describes the production of PLLA-MS with an average diameter of 37  $\mu\text{m}$  and labelled with  $^{166}\text{Ho}$ , for the treatment of liver metastases. Effects of production together with irradiation parameters were examined. Optimisation of these parameters resulted in a reproducible and straightforward method for the production of holmium loaded PLLA-MS, of uniform size and high chemical stability, which gave therapeutic amounts of activity within 1h irradiation time and precluded the need for any additives.

## 2.2 Materials and methods

### 2.2.1 Chemicals

All chemicals were commercially available. Acetylacetone, 2,4-pentanedione (AcAc; MW 100.12; >99%) was obtained from Sigma Aldrich (Steinheim, Germany). Holmium(III) chloride hexahydrate ( $\text{HoCl}_3 \cdot 6\text{H}_2\text{O}$ ; MW 379.38; 99.9%) was obtained from Phase Separations BV (Waddinxveen, The Netherlands). Ammonium hydroxide ( $\text{NH}_4\text{OH}$ ; MW 35.05; 29.3%) and polyvinyl alcohol (PVA, average MW 30,000–70,000) were obtained from Sigma Chemical Co. (St. Louis, Mo.). Poly(L-lactic acid) (PLLA; MW 26,000, intrinsic viscosity 0.09 l/g in chloroform 25°C) was supplied by Purac Biochem BV (Gorinchem, The Netherlands). Hydrochloric acid (HCl; MW 36.46; 37%) and chloroform (MW 119.39; Lichrosolv) were supplied by Merck (Darmstadt, Germany).

### 2.2.2 Methods

#### 2.2.2.1 Preparation of Ho-acetylacetonate (Ho-AcAc)

Acetylacetone (180 g) was dissolved in 1080 g water. The pH of this solution ranged between 3.5 and 4.0. Ammonium hydroxide was added to the stirring colourless acetylacetone solution until pH 8.5 was reached and the solution became yellow from the formation of acetylacetonate. Holmium chloride (10 g in 30 ml water) was then stirred into this solution and HoAcAc crystals were allowed to form at room temperature for at least 1 day. The crystals were collected by filtration over a 5.0  $\mu\text{m}$  Millipore filter, washed 3 times with water and dried under nitrogen.

The HoAcAc crystals were examined by infrared spectroscopy, nuclear magnetic resonance (NMR), elemental analysis, X-ray crystallography and scanning electron microscopy (SEM).

#### *2.2.2.2 Synthesis of holmium loaded microspheres*

Biodegradable poly(L-lactic acid) microspheres were manufactured in a glass beaker with four baffles. HoAcAc complex (10 g) and PLLA (6 g) were added to continuously stirred 186 g chloroform. PVA was dissolved in continuously stirred water of 40°C and poured into the glass beaker after cooling. The solutions and the beaker were kept at 25°C. The chloroform solution was added to the PVA solution and continuously stirred (500 rpm) until the chloroform was completely evaporated [19,21]. To remove residual PVA and unincorporated HoAcAc, the formed microspheres were washed sequentially with water, 0.1 N HCl and water.

The microspheres were graded and collected according to size on stainless steel sieves of 20 and 50 µm (20 µm sieve, S/Steel, NEN 2560, Endecotts, London; 50 µm sieve, S/Steel, ASIM E 11 87; B.V. Metaalgaasweverij, Twente, The Netherlands) under sprinkled water, and dried under nitrogen.

Characterisation of non-irradiated and irradiated microspheres was carried out by SEM, laser particle size analysis and  $\gamma$ -spectrometry of <sup>166</sup>Ho, after neutron activation of the <sup>165</sup>Ho incorporated in the PLLA-MS. For determination of PLLA molecular weight, microspheres were dissolved in chloroform and analysed by high performance liquid chromatography (HPLC) using a gel permeation chromatography column (Shodex KD 800) from Showa Benco, Japan.

#### *2.2.2.3 Low and high neutron flux irradiations of <sup>165</sup>Ho-PLLA-MS*

All irradiations were performed twice in the reactor facilities in Petten, The Netherlands. Two high neutron flux facilities were used, the pneumatic rabbit system (PRS) and the reloadable isotope production system (HIP). Irradiation in the PRS facility (neutron flux  $5 \times 10^{13} \text{ cm}^{-2} \cdot \text{s}^{-1}$ ) was carried out in a polyethylene or quartz vial packed in a polyethylene “rabbit”. Irradiation in the HIP facility (neutron flux  $2 \times 10^{14} \text{ cm}^{-2} \cdot \text{s}^{-1}$ ) was performed in a quartz vial in a sealed aluminium cylinder, which was itself then enclosed in a polyethylene cylinder. Amounts of 10, 200 or 400 mg of dried <sup>165</sup>Ho-PLLA-MS were irradiated for 0.5, 1, 2 or 4h. The effect of the presence of water during irradiation was studied by spiking some samples of microspheres with 50 µl of water. The holmium content of the <sup>165</sup>Ho-PLLA-MS was determined by neutron activation in the low neutron flux facility (neutron flux  $3.1 \times 10^{11} \text{ cm}^{-2} \cdot \text{s}^{-1}$ ).

#### *2.2.2.4 In vitro biodegradability and release studies.*

Irradiated microspheres (100 mg in 0.5 ml saline) were incubated in 2 ml 10 mM phosphate-buffered saline pH 7.4 (PBS), a suspension of human leucocytes in saline and homogenised pig liver (1.0 g) suspended in PBS. Release of <sup>166</sup>Ho was determined by incubation at 37°C in a dialysis cassette (Slide-A-Lyzer, Pierce, Rockford, Ill.). After incubation for 1, 3, 24, 96, 192 and 288h, release of free <sup>166</sup>Ho

was assayed in a gamma counter. Samples incubated for 288h were investigated for their biodegradability by SEM.

## 2.3 Results

### 2.3.1 Preparation and analysis of HoAcAc

After the addition of holmium chloride to the solution of acetylacetonate, pink crystals of HoAcAc appeared within 4h. Infrared spectroscopy and NMR analysis of the HoAcAc crystals established the presence of three acetylacetonate molecules and two to three molecules of water. Results of elemental analysis indicated the complexation of one holmium atom together with three acetylacetonate molecules and the presence of three water molecules (Table 1).

**Table 1.** Elemental analysis of holmium-trisacetylacetonate: measured versus theoretical values.

Element	Mass content (%)	Theoretical Ho-complex 3×H <sub>2</sub> O
C	36.55	34.90
H	4.98	5.27
O	27.12	27.89
Cl	0.00	0.00
Ho	31.19	31.94

This was definitively confirmed by X-ray crystallography, which revealed a monohydrated crystal structure in which one holmium atom was complexed by three acetylacetonate molecules and two water molecules (Fig. 1). From the X-ray crystallography and SEM data the HoAcAc crystals appeared to have a flat morphological structure with a length of 2–3 mm and a width of 0.1–0.3 mm. The density of the crystals appeared to be 1.74 g/ml and the molecular mass 516.30 including the non-coordinating water molecule.

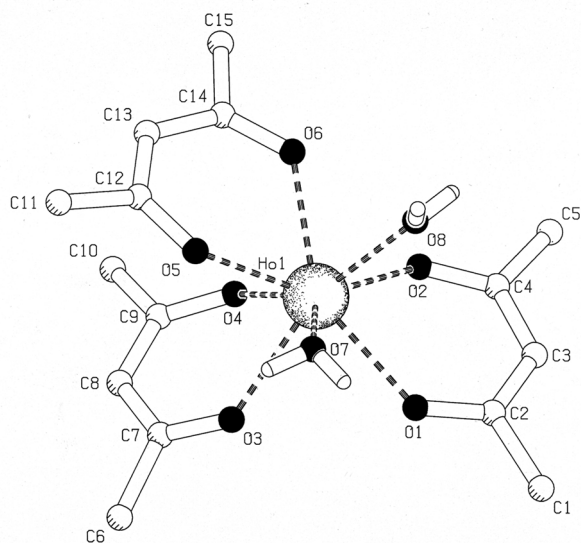


**Fig. 1.** Unit cell of holmiumtrisacetylacetonate with two coordinated water molecules as shown by X-ray crystallography (C, carbon atom; O, oxygen atom; Ho, holmium atom; hydrogen atoms not shown).

### 2.3.2 Synthesis and analysis of holmium loaded microspheres

Microsphere size and form depend on several parameters. Parameters investigated in this study were: PVA concentration, stirring rate, temperature and Ho-acetylacetonate concentration. Low concentrations of PVA (<0.2%) gave small and mostly non-spherical particles. Concentrations of 2%–3% PVA gave smooth microspheres while higher concentrations (>4%) resulted in non-spherical particles. Increased stirring rate resulted in decreased particle size; 750 rpm gave particles with an average diameter of 32  $\mu\text{m}$  while 500 rpm resulted in an average diameter of 37  $\mu\text{m}$ . Effects of temperature and HoAcAc concentration were minor. Increasing the temperature, from 18°C to 25°C to 37°C, resulted in a slightly larger particle size. High concentrations of HoAcAc, >12 g in 186 g chloroform, resulted in a mixture of microspheres HoAcAc crystals; the latter were hard to remove and required washing at least 4 times with 20 ml 1 N HCl. The parameters examined resulted in a standard method under the following conditions: 2% PVA, 10 g HoAcAc in 186 g chloroform, 25°C and 500 rpm, yielding 3–4.5 g of microspheres with a diameter of 20–50  $\mu\text{m}$  and incorporation of 17.0% $\pm$ 0.6% holmium (w/w) according to neutron activation (n=5).

### 2.3.3 Characterisation of microspheres after reactor irradiation

Samples were irradiated individually and within 1 day, in order to create reactor conditions as closely comparable as possible. It appeared that well-defined irradiation conditions were necessary to produce therapeutic dosages of <sup>166</sup>Ho-PLLA-MS while maintaining their integrity and suitability for therapy. Irradiation parameters affecting the integrity to a greater or lesser extent were (1) irradiation time, (2) the facility, (3) the amount of microspheres per vial, (4) water content of the microspheres and (5) material of the vial. Irradiation conditions and extent of loss of structural integrity after irradiation are summarised in Table 2. Non-irradiated <sup>165</sup>Ho-PLLA-MS show a

smooth, spherical appearance (Fig. 2A). After irradiation in the PRS facility (neutron flux  $5 \times 10^{13} \text{ cm}^{-2} \cdot \text{s}^{-1}$ ) for 1h in polyethylene vials, minor surface changes were seen with SEM (Fig. 2B), giving rise to small PLLA fragments. These led to a larger number of particles  $<20 \mu\text{m}$  (Fig. 3A). Nevertheless, the total volume of these small particles (Fig. 3B) and hence their total radioactivity hardly increased (the latter is likely to be related to the size and thus the volume of the particles). While overall structural integrity was maintained in terms of form and size, the microspheres showed a minimal tendency towards aggregation; they could, however, be easily suspended in PBS and should be suitable for intra-arterial therapy. Similar results were obtained when quartz instead of polyethylene vials were used, although some aggregation of the microspheres was observed. The presence of water had a more destructive effect. The microspheres appeared to have melted and were stacked (Fig. 2C). Irradiation in the PRS facility of 200 or 400 mg microspheres for 2h instead of 1h had a disastrous effect on the integrity of the microspheres in both polyethylene and quartz vials. A mixture of small and very large sharply edged particles of  $50\text{--}400 \mu\text{m}$  was obtained (Fig. 2D). Irradiation of only 10 mg under the same conditions resulted in intact microspheres.

**Table 2.** Summary of irradiation conditions and structural integrity after irradiation of microspheres

Time (h)	PRS ( $5 \cdot 10^{13}$ )			HIP ( $2 \cdot 10^{14}$ )	
	Polyethylene			Quartz	Quartz
	10 mg	200 mg	400 mg	200 mg	200 mg
0.5					–
1.0	++	++/+ <sup>a</sup>	++	++	–
2.0	++	–	–	–	–

Irradiations were done twice in the pneumatic rabbit system (PRS) or reloadable isotope production (HIP) facility. ++, Integrity maintained, suitable for radionuclide therapy: spherical particles, uniform size, minimal aggregation, easy to suspend; +, integrity affected: recognisable but aggregated spheres, no uniform size; –, integrity completely destroyed: large aggregated structures, no recognisable spheres. <sup>a</sup>Spiked with water (50  $\mu\text{l}$ ).



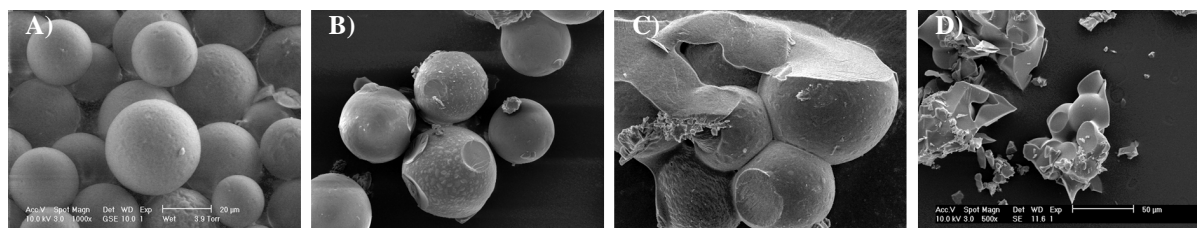


**Fig. 2A–D.** Electron micrographs illustrating effect of neutron irradiation. **A** <sup>165</sup>Ho-PLLA-MS before irradiation (×1000). **B** Microspheres irradiated for 1h (×1000). **C** Microspheres spiked with 50 µl water irradiated for 1h (×1500). **D** Microspheres irradiated for 2h (×500). Irradiations were performed with 200 mg microspheres in polyethylene vials and neutron flux  $5 \times 10^{13} \text{ cm}^{-2} \cdot \text{s}^{-1}$ .

The HIP facility (neutron flux  $2 \times 10^{14} \text{ cm}^{-2} \cdot \text{s}^{-1}$ ) in which only quartz vials are used appeared to be impracticable for our purpose. Irradiation of 200 mg microspheres for 0.5h gave similar results to those shown in Fig. 2C, while longer irradiation times resulted in crispy, yellow material.

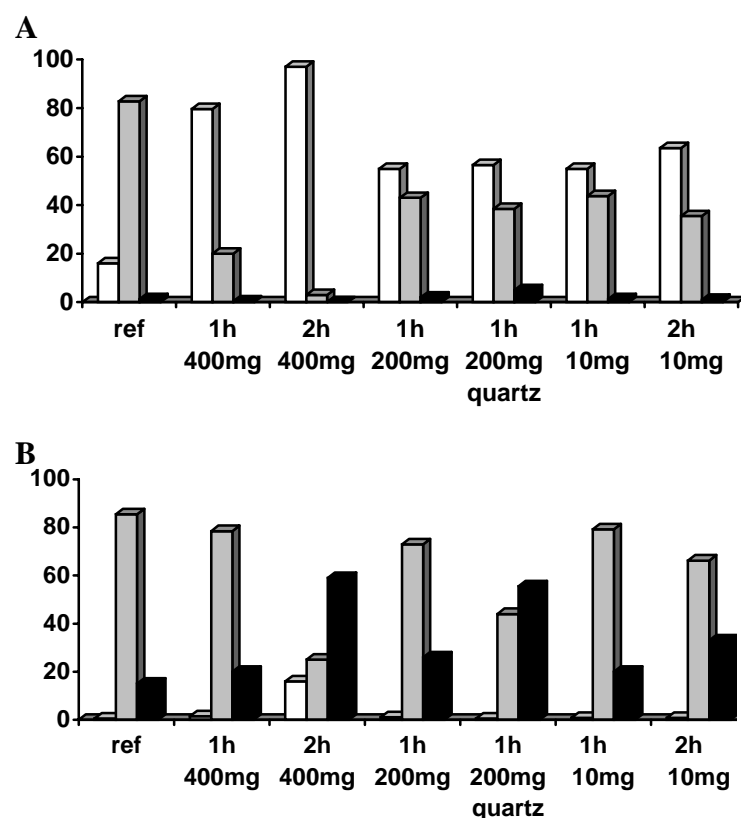


**Fig. 3A-B.** Population distribution of irradiated (1–2h and 10–400 mg) and non-irradiated (*ref*) microspheres (A). *Bars* represent percentage of total number of particles per group: ○ <20 µm; ● 20–50 µm; ● >50 µm. Volume weight distribution of irradiated (1-2h and 10–400 mg) and non-irradiated (*ref*) microspheres (B). *Bars* represent percentage of total volume of particles per group: ○ <20 µm, ● 20–50 µm; ● >50 µm.

### 2.3.4 *In vitro* biodegradability and release studies

Analysis of the molecular weight of PLLA of microspheres before and after irradiation (1h, neutron flux  $5 \times 10^{13} \text{ cm}^{-2} \cdot \text{s}^{-1}$ ) revealed a reduction in polymer molecular weight of 93% by gel permeation chromatography. Visible changes were also observed following incubation for 288h, 37°C, in PBS and pig liver homogenate (Fig. 4A,B). Despite these physical and morphological changes, >99.3% of  $^{166}\text{Ho}$  activity was retained in the microspheres after 192h (>7 half-lives) incubation in PBS, plasma and leucocytes, while in liver homogenate retention was still 98.4% (Fig. 4C).

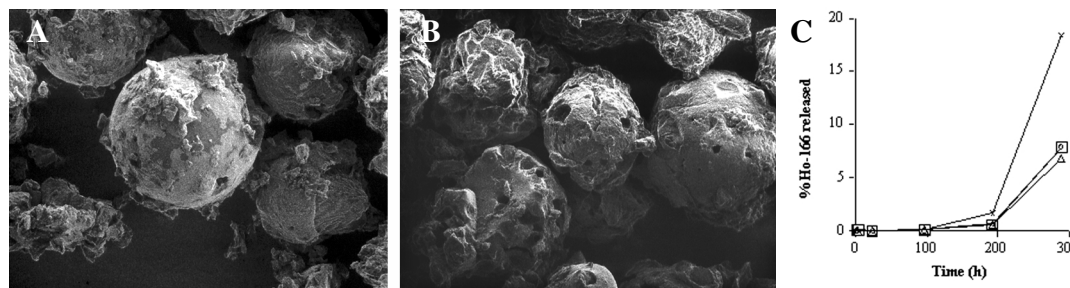


**Fig. 4A–C.** Biodegradability and  $^{166}\text{Ho}$  release of  $^{166}\text{Ho}$ -PLLA-MS. Microspheres were irradiated for 1h, neutron flux  $5 \times 10^{13} \text{ cm}^{-2} \cdot \text{s}^{-1}$  and incubated for 288h at 37°C in PBS (A) or pig liver homogenate (B) ( $\times 1500$ ). C In vitro release of  $^{166}\text{Ho}$  after incubation in: PBS ( $\Delta$ ), human plasma ( $\square$ ), human white blood cells ( $\bullet$ ) and pig liver homogenate ( $\times$ ).

## 2.4 Discussion

The use of radioactive microspheres administered arterially as radionuclide therapy for liver metastases has the potential to overcome the disadvantages of external beam radiation, which is limited by the radiosensitivity of the healthy tissue. As yet this application is restricted to the use of  $^{90}\text{Y}$  glass microspheres, which have suboptimal properties.

The potential use of PLLA-MS containing  $^{166}\text{Ho}$ , as first suggested by Mumper et al. [19], combines the best of two worlds: low density, biocompatible microspheres for embolization of tumour and immobilisation of  $^{166}\text{Ho}$ , which has favourable physical characteristics for image guided radionuclide therapy.  $^{166}\text{Ho}$  emits negatrons ( $E_{\text{max}} = 1.84 \text{ MeV}$ ) for therapy as well as photons (81 keV, 6.2%). This allows for dosimetric calculations and interaction during administration, and contributes only 1.1% to the overall absorbed radiation dose [20] that will be delivered at a relatively high dose rate, due to the 26.8h half-life as compared to the 64h half-life of  $^{90}\text{Y}$ . Moreover,  $^{165}\text{Ho}$  has a natural abundancy of 100% and a cross-section of 64 barn, allowing for short neutron activation times.

The aim of this study was to develop a well-characterised method for reproducible preparation of  $^{165}\text{Ho}$ -PLLA-MS, to be dispensed in patient-ready doses, that only

needs to be activated by neutron bombardment to a therapeutic amount of radioactivity and is ready for patient administration without any additional handling. To attain this goal, the holmium content of the microspheres must be sufficiently high, and neutron activation in a high flux reactor is necessary to obtain appropriate amounts of activity in workable time. At the same time, activation conditions must be such as to maintain the structural integrity of the microspheres and their stability with respect to <sup>166</sup>Ho release.

Holmium was complexed with acetylacetonate to enable incorporation into PLLA. Under the conditions we used, pH=8.5 and a 70-fold molar excess of AcAc, 80% of holmium is complexed as HoAcAc, of which standard 31.2% (w/w) is holmium. Subsequently, HoAcAc was embedded in PLLA microspheres prepared by the solvent evaporation technique. The form, diameter and stability of the microspheres appeared to be affected by several parameters, of which the concentration of PVA, used as an emulsifier, was the most prominent. An optimum concentration of 2% PVA resulted in spherical particles with a smooth surface and an average diameter of 37 μm (range 5–100 μm); 74% of the microspheres were between 20 and 50 μm, with a density of 1.4 g/ml and a reproducible <sup>165</sup>Ho content of 17.0±0.6% (w/w). After sieving out and drying of the 20 to 50 μm fraction of the microspheres, less than 1% of its total volume was <20 μm. The drying phase after sieving proved to be particularly important. Residual water caused aggregation of microspheres and rendered them useless for therapy, especially after neutron irradiation (Fig. 2C).

The conditions during neutron activation of the <sup>165</sup>Ho-PLLA-MS needed to be strictly defined. This study demonstrated that microspheres must be free of water and that high neutron flux (>5×10<sup>13</sup> cm<sup>-2</sup>.s<sup>-1</sup>) and irradiation time of more than 1h must be avoided. It should be stressed that the reactor facilities we used differ by a factor of 4 in neutron flux. However, distance from the core, geometry and neutron flux together determine the radiation environment of the microspheres and their condition after neutron activation. Therefore, our findings cannot be interpreted solely in terms of neutron flux, and they should be extrapolated to other reactors only with prudence.

Aggregation of microspheres was slightly greater after neutron bombardment in quartz vials than in polyethylene vials; this can be explained by neutron activation of the vial material, giving a higher radiation burden to the microspheres in the case of the quartz. The amount of microspheres per vial had a more pronounced effect in that small amounts (10 mg) were intact after irradiation in the PRS facility for 2h, while larger amounts (>200 mg) were completely destroyed under identical conditions; this may be explained by the higher total water content of the latter.

Using the optimised reactor conditions, reduction in the molecular weight of PLLA was the only change in microspheres observed after irradiation. However, this apparently did not affect stability in terms of <sup>166</sup>Ho release even after more than 7 half-

lives incubation under physiological conditions, thus making  $^{166}\text{Ho}$ -PLLA-MS applicable for therapy.

The present study has demonstrated that holmium loaded PLLA-MS can be prepared straightforwardly with reproducible incorporation of  $17.0\pm 0.6\%$  (w/w)  $^{165}\text{Ho}$ , which is high enough to produce sufficient amounts of therapeutic  $^{166}\text{Ho}$  activity provided that the proper irradiation conditions are adhered to. This study explicitly shows that production of the desired amount of activity entails more than a simple adjustment of irradiation parameters. The effect of changing irradiation parameters appeared to be unpredictable and had to be determined experimentally in each case. Adjustment of the parameters used by Mumper et al. [19] to produce substantially more activity in a shorter time was therefore impracticable. Mumper et al. were able to produce up to 1295 MBq of  $^{166}\text{Ho}$  within 3h by irradiation (neutron flux  $8.88\times 10^{12}\text{ cm}^{-2}\cdot\text{s}^{-1}$ ) of 50 mg microspheres with 150 mg inositol as an additive. In contrast, from the present work irradiation conditions could be defined such that 20 GBq of  $^{166}\text{Ho}$  is obtained within 1h by neutron activation (neutron flux  $5\times 10^{13}\text{ cm}^{-2}\cdot\text{s}^{-1}$ ) of 400 mg microspheres without any additives (n=10 irradiations). This would strongly facilitate routine production and transport to the therapy site. Efficacy studies in animals with liver tumours are now being undertaken. Other therapeutic applications, such as radionuclide synovectomy, are conceivable, by simply adapting the size of the microspheres.

### **Acknowledgements**

The authors gratefully acknowledge the dedicated assistance of W.A.M. van Maurik in SEM acquisition and Dr. D. Grove for his enthusiastic help with NMR and infrared spectroscopy analysis. The authors thank Prof. Dr. Ir. W.E. Hennink and M.J. van Steenbergen for their stimulating comments and help with HPLC and laser particle size analysis. We are indebted to P. Snip for performing the reactor experiments and to Dr. H. Kooijman for X-ray crystallography analysis. We also thank Dr. J.W. van Isselt and Dr J.M.H. de Klerk for critically reading this manuscript.

## References

1. Cady B. Natural history of primary and secondary tumours of the liver. *Semin. Oncol.* **1983**;10:127–135.
2. Ehrhardt GJ and Day DE. Therapeutic use of <sup>90</sup>Y microspheres. *Nucl. Med. Biol.* **1987**;14:233–242.
3. Stribley KV, Gray BN, Chmiel RL, Heggie JCP and Bennett RC. Internal radiotherapy for hepatic metastases. I. The homogeneity of hepatic arterial blood flow. *J. Surg. Res.* **1983**;34:17–24.
4. Jaffe BM, Donegan WL, Watson F and Spratt JS. Factors influencing survival in patients with untreated hepatic metastases. *Surg. Gynecol. Obst.* **1968**;127:1–11.
5. Ho S, Lau WY, Leung TWT, Chan M, Ngar YK, Johnson PJ and Li AKC. Clinical evaluation of the partition model for estimating radiation doses from yttrium-90 microspheres in the treatment of hepatic cancer. *Eur. J. Nucl. Med.* **1997**;24:293–298.
6. Gray BN, Burton MA, Kelleher D, Klemp P and Matz L. Tolerance of the effects of yttrium-90 radiation. *Int. J. Radiat. Oncol. Biol. Phys.* **1990**;18:619–623.
7. Burton MA. Selective internal radiation therapy: distribution of radiation in the liver. *Eur. J. Cancer Clin. Oncol.* **1989**;25:1487–1491.
8. Ackerman NB, Lien WM, Kondi ES and Silverman NA. The blood supply of experimental liver metastases. I. The distribution of hepatic artery and portal vein blood to “small” and “large” tumours. *Surgery* **1969**;66:1067–1072.
9. Hoefnagel CA. Radionuclide therapy revisited. *Eur. J. Nucl. Med.* **1991**;18:408–431.
10. Ackerman NB and Hechmer PA. The blood supply of experimental liver metastases. V. Increased tumour perfusion with epinephrine. *Am. J. Surg.* **1980**;140:625–631.
11. Ackerman NB, Lien WM and Silverman NA. The blood supply of experimental liver metastases. III. The effects of acute ligation of the hepatic artery or portal vein. *Surgery* **1972**;71:636–641.
12. Folkman J. Tumour angiogenesis. *Cancer Med.* **1993**;153–170.
13. Sasaki Y, Imaoka S, Hasegawa Y, Nakano S, Ishikawa O, Ohigashi H, Taniguchi K, Koyama H, Iwanaga T and Terasawa T. Changes in distribution of hepatic blood flow induced by intra arterial infusion of angiotensin II in human hepatic cancer. *Cancer* **1985**;55:311–316.
14. Andrews JC, Walker Andrews SC, Juni JA, Warber S and Ensminger WD. Modulation of liver tumour blood flow with hepatic epinephrine: a SPECT study. *Radiology* **1989**;173:645–647.
15. Meade VM, Burton MA, Gray BN and Self GW. Distribution of different sized microspheres in experimental hepatic tumours. *Eur. J. Cancer Clin. Oncol.* **1987**;23:37–41.

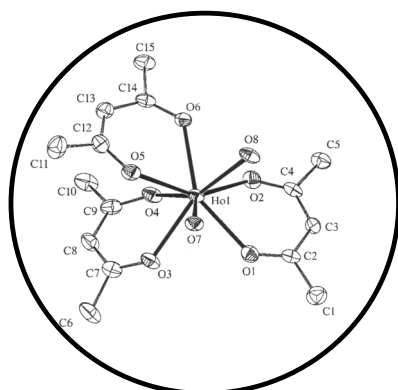
16. Anderson JH, Angerson WJ, Willmott N, Kerr DJ, McArdle CS and Cooke TG. Regional delivery of microspheres to liver metastases: the effects of particle size and concentration on intrahepatic distribution *Br. J. Cancer* **1991**;64:1031–1034.
17. Haesegawa T and Song CW. Effect of hydralazine on the blood flow in tumours and normal tissues in rats. *Int J Radiat Oncol Biol Phys* **1991**;20:1001–1007.
18. Andrews JC. Hepatic radioembolization with yttrium-90 containing glass microspheres: preliminary results and clinical follow up. *J. Nucl. Med.* **1994**;35:1637–1644.
19. Mumper RJ, Ryo UY and Jay M. Neutron activated holmium-166 poly (L-lactic acid) microspheres: a potential agent for the internal radiation therapy of hepatic tumours. *J. Nucl. Med.* **1991**;32:2139–2143.
20. Turner JH, Claringbold PG, Klemp PFB, Cameron PJ, Martindale AA, Glancy RJ, Norman PE, Hetherington EL, Najdovski L and Lambrecht RM. 166 Ho-microsphere liver radiotherapy: a preclinical SPECT dosimetry study in the pig. *Nucl. Med. Commun.* **1994**;15:545–553.

## Chapter 3

---

# Diaquatrakis(pentane-2,4-dionato-O,O')-holmium(III) monohydrate and diaquatrakis(pentane-2,4-dionato-O,O')-holmium(III) 4-hydroxypentan-2-one solvate dihydrate

*Acta Crystallographica Section C* 2000;C56:156-158



**H. Kooijman<sup>1</sup>, J.F.W. Nijssen<sup>2</sup>, A.L. Spek<sup>1</sup> and A.D. van het Schip<sup>2</sup>**

<sup>1</sup>*Bijvoet Center for Biomolecular Research, Department of Crystal and Structural Chemistry, Utrecht University, Utrecht, The Netherlands*

<sup>2</sup>*Department of Nuclear Medicine, University Medical Center, Utrecht, The Netherlands*

**Abstract**

The structures of the title compounds,  $[\text{Ho}(\text{C}_5\text{H}_7\text{O}_2)_3(\text{H}_2\text{O})_2]\cdot\text{H}_2\text{O}$  and  $[\text{Ho}(\text{C}_5\text{H}_7\text{O}_2)_3(\text{H}_2\text{O})_2]\cdot\text{C}_5\text{H}_8\text{O}_2\cdot 2\text{H}_2\text{O}$ , both show an eight-coordinate holmium(III) ion in a square antiprismatic configuration. The packing of these structures consists of an infinite two-dimensional network of hydrogen-bonded molecules. In both structures, the same hydrogen-bonded chain of  $\text{Ho}^{\text{III}}$  complexes is found.

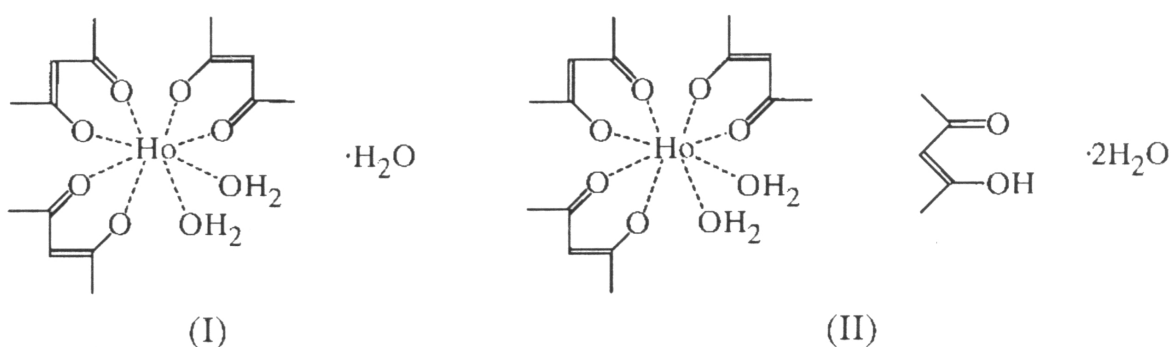


### 3.1 Comment

Holmium in the trivalent state, like other rare earths, reacts with acetylacetonate (pentane-2,4-dione) to form a complex coordinated with three acetylacetonate ligands and one or two water molecules [1,2]. The crystal structure of diaquatris(pentane-2,4-dionato-O,O')-holmium(III) monohydrate was reported by Aslanov et al. [3] with  $R = 0.13$ , but no further data are available from the Cambridge Structural Database (Version of April 1999; [4]). The pentanedione-Ho complex is essential for the development of a new intra-arterial radionuclide therapy for the treatment of liver metastases [5]. For the preparation of microspheres embedded with holmium we needed a stable hydrophobic holmium complex which can be incorporated easily and in high concentration into poly(L-lactic acid) (PLLA) microspheres. This study reports structural data on the holmium acetylacetonate (HoAcAc) complex, which was chosen for further investigation because it has the above-mentioned properties.

The HoAcAc complex showed a high chemical stability in PLLA microspheres before and after irradiation in a nuclear reactor. Release of neutron-activated holmium from the microspheres is  $<1.6\%$  after 192h incubation in liver homogenate. As the incorporation of holmium in PLLA microspheres can be as high as 17% w/w, holmium-loaded microspheres are therefore suitable for selective internal radionuclide therapy. Neutron-activated  $^{166}\text{Ho}$  is a  $\beta$ -emitter which can be used for treatment of liver metastases. It also emits  $\gamma$ -photons which can be used for imaging the distribution of activity in the patient. Owing to the high selectivity of the technique by which it is administered, the radiation is mainly restricted to the tumour.

Crystals of diaquatris(pentane-2,4-dionato-O,O')holmium(III) were obtained under different experimental conditions, such as pH (see Experimental). The crystal structures were determined to identify unambiguously the composition of the materials obtained. Two of these structures are presented here, namely, diaquatris(pentane-2,4-dionato-O,O')holmium(III) monohydrate, (I), and diaquatris(pentane-2,4-dionato-O,O')holmium(III) 4-hydroxypentan-2-one solvate dihydrate, (II), obtained at pH 8.5 and 9.0, respectively.



In both structures, Ho<sup>III</sup> displays square antiprismatic coordination by eight O atoms. There are no significant differences between the geometric parameters of these complexes.

In structure (II), hydrogen bonds between the complexes join them into a chain running in the [010] direction. A link between two Ho atoms is formed either by a hydrogen-bonded motif with graph set  $R_2^2(8)$  or by two symmetry-related motifs, each with graph set  $R_2^2(6)$  [6]. Two non-coordinating water molecules and a free 4-hydroxypentan-2-one molecule also form a hydrogen-bonded chain in the [010] direction. This solvent chain donates three hydrogen bonds to the O atoms coordinated to Ho and accepts one hydrogen bond from a coordinated water molecule, thus forming a two-dimensional network in the (010) plane (see Fig. 3). The hydroxyl atom of the 4-hydroxypentan-2-one is disordered over two positions. The minor position forms a bifurcated intra/intermolecular hydrogen bond, whereas the major component forms only an intermolecular hydrogen bond.

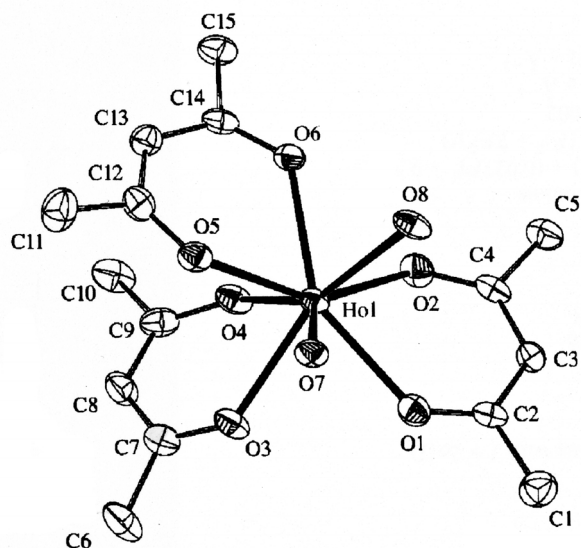


**Fig. 1.** Displacement ellipsoid plot [7] of (I) showing the atomic labelling scheme and 50% probability displacement ellipsoids. H atoms and the non-coordinating water molecule have been omitted for clarity.

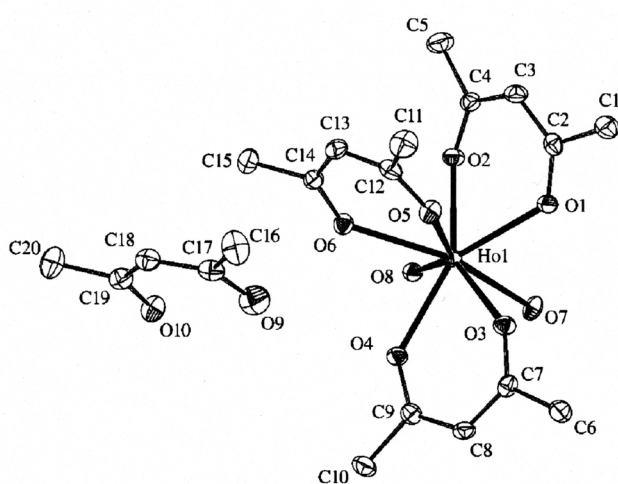


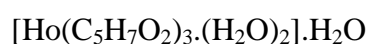
**Fig. 2.** Displacement ellipsoid plot [7] of (II) showing the atomic labelling scheme and 50% probability displacement ellipsoids. H atoms and the non-coordinating water molecule have been omitted for clarity.

**Fig. 3.** Crystal packing diagram for (II). The hydrogen-bonded chain of solvent molecules has been accentuated using solid bonds. Methyl groups and H atoms not involved in hydrogen bonding have been omitted for clarity.

In structure (I), the complexes are joined by hydrogen bonds into an infinite one-dimensional chain running in the [101] direction. This chain is identical to that found in structure (II). The non-coordinating water molecule links these chains in a two-dimensional network in the (010) plane. One of the H atoms of this water molecule is disordered over two positions, in both of which it forms hydrogen bonds.

### **3.2 Experimental**

Pentane-2,4-dione (180 g, 1.80 mol) was dissolved in water (1080 g, 59.34 mol), followed by addition of ammonium hydroxide (28% w/w) until a solution of pH 8.5 was obtained. Holmium chloride hexahydrate (10 g, 26.4 mmol) in water (30 g, 1.64 mol) was then added to the solution, yielding yellow crystals (pink under fluorescent lighting) of (I) after 24h at room temperature. Satisfactory spectroscopic data ( $^1\text{H}$  NMR,  $^{13}\text{C}$  NMR and IR) were obtained. At pH 9.0, crystals of (II) were obtained, which were also yellow in daylight and pink under fluorescent lighting.

**Compound (I)***Crystal data*

$M_r = 516.30$

Monoclinic,  $P2_1/c$ 

$a = 8.242 (2) \text{ \AA}$

$b = 21.782 (6) \text{ \AA}$

$c = 12.557 (3) \text{ \AA}$

$\beta = 119.292 (14)^\circ$

$V = 1966.1 (9) \text{ \AA}^3$

$Z = 4$

$D_x = 1.744 \text{ Mg m}^{-3}$

Mo  $K\alpha$  radiation

Cell parameters from 447

reflections

$\theta = 2-25^\circ$

$\mu = 4.07 \text{ mm}^{-1}$

$T = 150 \text{ K}$

Needle, yellow-pink

$0.35 \times 0.08 \times 0.03 \text{ mm}$

*Data collection*

Nonius KappaCCD diffractometer

Area-detector  $\varphi$  and  $\omega$  scans

Absorption correction: multi-scan

(Spek, 1990)

$T_{\min} = 0.614, T_{\max} = 0.855$

15 088 measured reflections

3548 independent reflections

2947 reflections with  $I > 2\sigma(I)$ 

$R_{\text{int}} = 0.086$

$\theta_{\text{max}} = 25.24^\circ$

$h = -9 \rightarrow 9$

$k = -25 \rightarrow 26$

$l = -15 \rightarrow 13$

*Refinement*Refinement on  $F^2$ 

$R(F) = 0.042$

$wR(F^2) = 0.099$

$S = 1.151$

3548 reflections

254 parameters

H atoms: see below

$w = 1/[\sigma^2(F_o^2) + (0.027P)^2 + 9.5P]$

where  $P = (F_o^2 + 2F_c^2)/3$

$(\Delta/\sigma)_{\text{max}} = 0.002$

$\Delta\rho_{\text{max}} = 1.19 \text{ e \AA}^{-3}$

$\Delta\rho_{\text{min}} = -1.51 \text{ e \AA}^{-3}$

**Table 1.**

Selected geometric parameters (Å, °) for (I).

Ho1 - O1	2.360 (4)	Ho1 - O5	2.306 (5)
Ho1 - O2	2.321 (5)	Ho1 - O6	2.401 (4)
Ho1 - O3	2.374 (5)	Ho1 - O7	2.420 (5)
Ho1 - O4	2.327 (5)	Ho1 - O8	2.364 (5)
O1 - Ho1 - O2	73.15 (16)	O5 - Ho1 - O6	72.84 (16)
O3 - Ho1 - O4	71.05 (17)	O7 - Ho1 - O8	71.49 (16)

**Table 2.**

Hydrogen-bonding geometry (Å, °) for (I).

<i>D</i> -H... <i>A</i>	<i>D</i> -H	H... <i>A</i>	<i>D</i> ... <i>A</i>	<i>D</i> -H... <i>A</i>
O7-H74...O3 <sup>i</sup>	0.78 (6)	2.00 (6)	2.771 (7)	168 (6)
O7-H75...O1 <sup>i</sup>	0.79 (5)	2.29 (6)	2.940 (6)	140 (5)
O8-H84...O9	0.78 (7)	1.98 (7)	2.759 (9)	177 (7)
O8-H85...O6 <sup>ii</sup>	0.79 (6)	2.06 (6)	2.841 (6)	174 (8)
O9-H94...O4 <sup>iii</sup>	0.79 (9)	2.01 (9)	2.760 (8)	159 (9)
O9-H95...O2 <sup>iii</sup>	0.79 (16)	2.39 (16)	2.994 (8)	134 (14)
O9-H95...O9 <sup>iv</sup>	0.79 (16)	2.35 (15)	2.785 (8)	115 (13)
O9-H96...O2 <sup>iii</sup>	0.78 (10)	2.42 (15)	2.994 (8)	131 (12)

Symmetry codes: (i) 1 - *x*, -*y*, 2 - *z*; (ii) -*x*, -*y*, 1 - *z*; (iii) 1 + *x*, *y*, *z*; (iv) 1 - *x*, -*y*, 1 - *z*.

**Compound (II)***Crystal data*[Ho(C<sub>5</sub>H<sub>7</sub>O<sub>2</sub>)<sub>3</sub>(H<sub>2</sub>O)<sub>2</sub>].C<sub>5</sub>H<sub>8</sub>O<sub>2</sub>.H<sub>2</sub>OM<sub>r</sub> = 634.43Monoclinic, *P*2<sub>1</sub>/*c**a* = 11.4903 (11) Å*b* = 11.0242 (6) Å*c* = 20.5442 (15) Å

β = 93.440 (7)°

*V* = 2597.7 (3) Å<sup>3</sup>*Z* = 4D<sub>x</sub> = 1.622 Mg m<sup>-3</sup>Mo *K*α radiationCell parameters from 25  
reflections

θ = 11.49-18.35°

μ = 3.10 mm<sup>-1</sup>*T* = 293 K

Needle, yellow-pink

0.70 x 0.20 x 0.05 mm

*Data collection*

Enraf-Nonius CAD-4T diffractometer

ω scans

Absorption correction: Gaussian  
(Spek, 1990)*T*<sub>min</sub> = 0.517, *T*<sub>max</sub> = 0.857

9388 measured reflections

4697 independent reflections

3764 reflections with *I* > 2σ(*I*)*R*<sub>int</sub> = 0.041θ<sub>max</sub> = 25.25°*h* = -13 → 13*k* = 0 → 13*l* = -24 → 24

3 standard reflections

frequency: 60 min

intensity decay: 1%

*Refinement*Refinement on *F*<sup>2</sup>*R*(*F*) = 0.032*wR*(*F*<sup>2</sup>) = 0.069*S* = 1.173

4697 reflections

338 parameters

H atoms: see below

 $w = 1/[\sigma^2(F_o^2) + (0.02P)^2 + 5P]$ where  $P = (F_o^2 + 2F_c^2)/3$ (Δ/σ)<sub>max</sub> = 0.002Δρ<sub>max</sub> = 1.66 e Å<sup>-3</sup>Δρ<sub>min</sub> = -1.96 e Å<sup>-3</sup>

**Table 3.**

Selected geometric parameters (Å, °) for (II).

Ho1 - O1	2.387 (3)	Ho1 - O5	2.302 (3)
Ho1 - O2	2.334 (3)	Ho1 - O6	2.383 (3)
Ho1 - O3	2.305 (3)	Ho1 - O7	2.356 (3)
Ho1 - O4	2.342 (3)	Ho1 - O8	2.416 (3)
O1 - Ho1 - O2	71.77 (11)	O5 - Ho1 - O6	71.59 (11)
O3 - Ho1 - O4	73.59 (11)	O7 - Ho1 - O8	71.29 (11)

**Table 4.**

Hydrogen-bonding geometry (Å, °) for (II).

<i>D-H...A</i>	<i>D-H</i>	<i>H...A</i>	<i>D...A</i>	<i>D-H...A</i>
O7-H74...O10 <sup>i</sup>	0.82 (4)	1.92 (4)	2.721 (5)	165 (5)
O7-H75...O1 <sup>ii</sup>	0.81 (4)	2.09 (5)	2.854 (5)	159 (5)
O8-H84...O4 <sup>i</sup>	0.84 (4)	1.99 (3)	2.788 (5)	157 (4)
O8-H85...O6 <sup>i</sup>	0.82 (4)	1.99 (5)	2.765 (5)	157 (5)
O9-H94...O12	0.89 (5)	2.01 (5)	2.887 (7)	173 (12)
O11-H114...O2 <sup>iii</sup>	0.84 (4)	2.07 (4)	2.906 (4)	171 (6)
O11-H115...O10 <sup>iv</sup>	0.83 (4)	2.13 (4)	2.918 (5)	159 (6)
O12-H124...O5	0.84 (5)	2.21 (5)	2.879 (5)	136 (5)
O12-H125...O11	0.85 (6)	1.92 (6)	2.756 (5)	170 (6)
C10-H101...O11 <sup>v</sup>	0.96	2.58	3.375 (7)	141

Symmetry codes: (i)  $-x, 1 - y, -z$ ; (ii)  $-x, -y, -z$ ; (iii)  $x, \frac{1}{2} - y, \frac{1}{2} + z$ ; (iv)  $-x, y - \frac{1}{2}, \frac{1}{2} - z$ ; (v)  $-x, \frac{1}{2} + y, \frac{1}{2} - z$ .

For both structures, H atoms bonded to O were located on difference Fourier maps and their coordinates were included as parameters in the refinement. Distance restraints were applied to ensure reasonable intramolecular geometries. Methyl-H atoms were located from difference Fourier syntheses and refined as part of a rigid group allowed to rotate around the C-C bond but not tip or distort. All other H atoms were introduced at calculated positions, riding on their carrier atoms. The high uncertainties shown by some of the data given in Tables 2 and 4 are due to H95 and H96 being disordered components. The occupation ratio of the disordered H atom of (I) was fixed; the occupation ratio of the disordered H atom of (II) was refined. Displacement parameters of all H atoms were related to their carrier atom by a fixed constant. For (I), the highest peak of  $1.66 \text{ \AA}^{-3}$  in the difference Fourier synthesis was located  $1.07 \text{ \AA}$  from Ho1; the deepest trough of  $-1.96 \text{ \AA}^{-3}$  was  $0.92 \text{ \AA}$  from the same position.

Data collection: *COLLECT* [8] for (I), locally modified *CAD-4 Software* [9] for (II); cell refinement: *DENZO-SMN* [10] for (I), *SET4* [11] for (II); data reduction: *DENZO-SMN* for (I), *HELENA* [12] or (II); for both compounds, program(s) used to solve structure: *SHELXS86* [13]; program(s) used to refine structure: *SHELXL97* [14]; molecular graphics: *PLATON* [7]; software used to prepare material for publication: *PLATON*.

### **Acknowledgement**

This work was supported in part (ALS) by the Council for Chemical Sciences of the Netherlands Organization for Scientific Research (CW-NWO).



## References

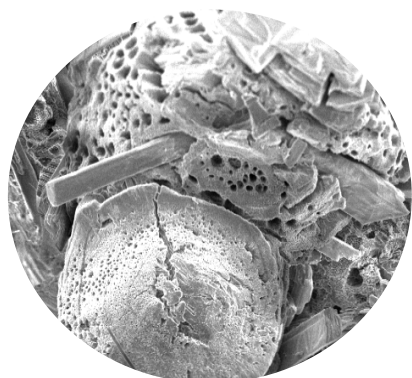
1. Stites JG, McCarty CN and Quill LL. The rare earth metals and their compounds VIII. An improved method for the syntheses of some rare earth acetylacetonates. *J. Am. Chem. Soc.* **1948**;70:3142-143.
2. Brown WB, Steinbach JF and Wagner WF. Extraction of the lanthanides with acetylacetone. *J. Inorg. Nucl. Chem.* **1960**;13:119-124.
3. Aslanov LA, Korytnii EF. and Porai-Koshits, M. A. *Zh. Strukt. Khim.* **1971**;12:661-662.
4. Allen FH and Kennard O. *Chem. Des. Autom. News* **1993**;8:31-37.
5. Nijssen JFW, Zonnenberg BA, Woittiez JRW, Rook DW, Swildens-van Woudenberg IA, van Rijk PP and van het Schip AD. Holmium-166 poly lactic acid microspheres applicable for intra-arterial radionuclide therapy of hepatic malignancies: effects of preparation and neutron activation techniques. *Eur. J. Nucl. Med.* **1999**;26:699-704
6. Bernstein J, Davis RE, Shimoni L and Chang N-L. *Angew. Chem. Int. Ed. Engl.* **1995**;34:1555-1573.
7. Spek AL. *Acta Cryst.* **1990**:A46:C-34.
8. Nonius. COLLECT. Nonius BV, Delft, The Netherlands **1997**.
9. Enraf-Nonius. CAD-4 Software. Version 5.0. Enraf-Nonius, Delft, The Netherlands **1989**.
10. Otwinowski Z. and Minor W. *Methods Enzymol.* **1997**;276:307-326.
11. Boer, de JL and Duisenberg AJM. *Acta Cryst.* **1984**;A40:C-410.
12. Spek AL. HELENA. University of Utrecht, The Netherlands **1997**.
13. Sheldrick GM. SHELXS86. University of Göttingen, Germany **1985**.
14. Sheldrick GM. SHELXL97. University of Göttingen, Germany **1997**.

## Chapter 4

---

# Characterization of poly(L-lactic acid) microspheres loaded with holmium acetylacetonate

*in press (Biomaterials)*



**J.F.W. Nijsen<sup>1</sup>, M.J. van Steenbergen<sup>2</sup>, H. Kooijman<sup>3</sup>, H. Talsma<sup>2</sup>,  
L.M.J. Kroon-Batenburg<sup>3</sup>, M. van de Weert<sup>2</sup>, P.P. van Rijk<sup>1</sup>,  
A. de Witte<sup>1</sup>, A.D. van het Schip<sup>1</sup> and W.E. Hennink<sup>2</sup>**

<sup>1</sup>*Department of Nuclear Medicine, University Medical Center, Utrecht, The Netherlands*

<sup>2</sup>*Department of Pharmaceutics, Utrecht Institute for Pharmaceutical Sciences, Utrecht University, Utrecht, The Netherlands*

<sup>3</sup>*Department of Crystal and Structural Chemistry, Bijvoet Center for Biomolecular Research, Utrecht University, Utrecht, The Netherlands*

**Abstract:**

Holmium loaded PLLA microspheres are useful systems in radio-embolization therapy of liver metastases because of their low density, biodegradability and favourable radiation characteristics. Neutron activated Ho loaded microspheres showed a surprisingly low release of the relatively small holmium complex. In this paper factors responsible for this behavior are investigated, in particular by the use of differential scanning calorimetry, scanning electron microscopy, infrared spectroscopy and X-ray diffraction. The holmium complex is soluble in PLLA up to 8% in films and 17% in microspheres. Interactions between carbonyl groups of PLLA, and the Ho-ion in the holmium complex, explain very satisfactorily the high stability of holmium loaded microspheres.

## 4.1 Introduction

Injectable glass microspheres loaded with a radioactive compound have been investigated as systems in the treatment of hepatic metastases [1]. After introduction into the hepatic artery, these microspheres accumulate in the capillary bed of the liver, resulting in a high dose of radioactivity into the area of tumor cells. Studies on selective radio-embolization therapy of colorectal liver metastases using yttrium-90 ( $^{90}\text{Y}$ ) glass beads have shown encouraging results [1,2]. However, their high density (3.29 g/ml) and non-biodegradability are obvious disadvantages of this system [3,4]. Also, the choice of the radionuclide  $^{90}\text{Y}$  which lacks  $\gamma$ -emission for imaging can be considered as a disadvantage [4,5]. As an alternative for glass particles, microspheres of poly(L-lactic acid) (PLLA) containing holmium-166 ( $^{166}\text{Ho}$ ) were proposed [4]. The main advantages of this system are the reduced density when compared with glass beads and the well-known biocompatibility and biodegradability of PLLA microspheres. Moreover,  $^{166}\text{Ho}$  has a distinct advantage over  $^{90}\text{Y}$ . It has a relatively short physical half-life (26.8h compared with 64.1h for  $^{90}\text{Y}$ ) and is  $\gamma$ -emitting.

By increasing the incorporation of holmium acetylacetonate (HoAcAc), combined with a higher neutron flux during irradiation, we succeeded in preparing microspheres with a substantially higher dose of radioactivity than the preparation described by Mumper et al. [6], thus making clinical trials feasible. We were able to show that more than 98% of the  $^{166}\text{Ho}$  activity was retained in the microspheres (after 192h incubation at 37°C, in several physiological media) [7]. This is a favourable characteristic of these microspheres for the proposed application, but it is also surprising, since generally low molecular weight compounds are released to a great extent, and relatively rapidly from PLLA microspheres [8-10]. PLLA, instead of e.g. poly(lactic-co-glycolic acid) was selected for the preparation of HoAcAc-loaded microspheres because the crystalline domains of this polymer guarantee a good dimensional stability of the spheres once they are irradiated in a nuclear reactor, which can be accompanied with temperatures of 50–60°C. An additional advantage is the lower susceptibility of the crystalline state of PLLA to radiation induced degradation compared with the amorphous state [11]. The aim of the present study is to obtain insight into the factors responsible for the low-release properties of the holmium loaded microspheres.

## 4.2 Materials and Methods

### 4.2.1 Materials

All chemicals were commercially available and used as obtained. Acetylacetone, 2,4-pentanedione, (AcAc; MW 100.12; >99%) was obtained from Sigma Aldrich (Steinheim, Germany). Holmium(III) chloride hexahydrate ( $\text{HoCl}_3 \cdot 6\text{H}_2\text{O}$ ; MW 379.38; 99.9%) was obtained from Phase Separations BV (Waddinxveen, The Netherlands). Polyvinyl alcohol (PVA, average MW 30,000-70,000) was obtained from Sigma Chemical Co. (St. Louis, Mo). Poly(L-lactic acid) (end-capped, molecular weight as indicated by supplier 26,000 g/mol; intrinsic viscosity 0.9 dl/g (chloroform 25°C)) was obtained using stannous octoate as initiator (residual amount <100 ppm) and was supplied by Purac Biochem BV (Gorinchem, The Netherlands). Ethylene dinitrilotetraacetic acid disodium salt dihydrate (EDTA,  $\geq 99.0\%$ ) and zinc sulfate heptahydrate ( $\text{ZnSO}_4 \cdot 7\text{H}_2\text{O}$ , >99.5%) were obtained from Merck (Darmstadt, Germany).

### 4.2.2 Methods

#### 4.2.2.1 Preparation of the Ho-acetylacetonate complex

The complex of holmium with acetylacetone (further abbreviated as HoAcAc) was prepared and characterized as described previously [7,12]. In short, acetylacetone (180 g) was dissolved in 1080 g water. The pH of this solution was brought to 8.5 with an aqueous solution of  $\text{NH}_3$  (28.4% (v/v)). Holmium chloride (10 g in 30 ml water) was added to this solution, and HoAcAc crystals were formed at room temperature in 24h. The crystals were collected by filtration, washed with water and dried under nitrogen.

#### 4.2.2.2 Preparation of HoAcAc-loaded microspheres

HoAcAc-loaded poly(L-lactic acid) microspheres with different HoAcAc amounts were prepared by solvent evaporation as described previously [7]. As an example: HoAcAc (0-10 g) and PLLA (6 g) were dissolved in 186 g chloroform. The resulting homogeneous solution was added to an aqueous solution of PVA (1000 g water, 2% (w/w)). The mixture was stirred for 48h under nitrogen and the formed microspheres were collected by centrifugation and washed with water, 0.1 N HCl and water, respectively. The microspheres were suspended in water (around 4 g in 200 ml) and fractionated according to size using stainless steel sieves of 20 and 50  $\mu\text{m}$  with a sprinkler system (Analysette 3 system, Fritsch GmbH, Idar-Oberstein, Germany) and dried under nitrogen.

#### 4.2.2.3 Preparation of holmium loaded poly(L-lactic acid) films

In order to achieve a standardized and exact loading of poly(L-lactic acid) (PLLA) with HoAcAc, films of PLLA loaded with HoAcAc were prepared and obtained by

the following method: PLLA (0-2.5 g) and HoAcAc (0-1.6 g) were dissolved in chloroform (22.5 g). The resulting homogeneous and viscous solutions were poured onto a glass plate and the solvent was evaporated, resulting in films of 1-2 mm thickness, and a holmium loading ranging from 0-20% (w/w). All films were duplicated.

#### *4.2.2.4 Characterization of the microspheres and films*

##### *4.2.2.4.1 Determination of the holmium and chlorine content*

The holmium content in the PLLA film and microspheres was determined by titration based on the method described for aluminum sulphate [13]. About 50 mg microspheres (accurately weighed) were dissolved in 10 ml dichloromethane. To this solution, 2 ml 1M HCl and 50 ml water were added. The resulting two phase system was stirred for two minutes and boiled until the dichloromethane had evaporated. After cooling to room temperature, 3 ml 0.04 M EDTA-solution and four droplets of methylene-red were added. Thereafter, an aqueous solution of 1 M NH<sub>4</sub>OH was added until the solution changed from reddish to yellow. The solution was then kept at 100°C for 11 minutes. After cooling to room temperature, 50 mg xylenol-orange and 5 g hexamethylenetetramine were added. The solution was brought to a pH of 5.0 with 1 M HCl, and titrated with zinc sulfate heptahydrate (0.01 M).

Chlorine content was determined by neutron activation (NRG, Petten, The Netherlands) [14].

##### *4.2.2.4.2 Scanning electron microscopy*

Surface morphology of HoAcAc-loaded PLLA microspheres and films was evaluated by scanning electron microscopy using a Philips XL30 FEGSEM. A voltage of 5 or 10 kV was applied. Samples of PLLA microspheres and films, as well as HoAcAc crystals, were mounted on aluminum stubs and sputter-coated with a Pt/Pd layer of about 10 nm. Holmium distribution on the surface of the microspheres was analyzed by an energy dispersive x-ray spectrometer (EDX).

##### *4.2.2.4.3 Differential scanning calorimetry*

The modulated DSC (MDSC) analysis was performed with a DSC 2920 (TA Instruments, Inc., New Castle, DE, USA, division of Waters Inc.). Samples of approximately 6 mg were transferred into aluminum pans. A small pin hole in the lid avoided possible pressure build-up during measurement. The sample compartment was purged with helium. Scans were recorded under “heating only” conditions, with a heating rate of 2°C/min and cooling rate of 1°C/min. The settings were periods of 60s and a temperature modulation amplitude of 0.32°C. The universal analysis software version V2.5.M was used in evaluation. The T<sub>g</sub>-values were determined by taking the

half height between the baseline below and above the temperature range of the glass transition.

#### *4.2.2.4.4 Thermo-gravimetric analysis (TGA)*

HoAcAc-loaded microspheres and films, together with HoAcAc crystals, were analyzed with a TGA51 thermogravimetric analyzer (TA Instruments, Inc., New Castle, DE, USA, division of Waters Inc.). Samples of about 15 mg were heated under nitrogen at a rate of 2°C/min, up to 1000°C.

#### *4.2.2.4.5 X-ray diffraction studies*

X-ray diffraction experiments were carried out on a Nonius  $\kappa$ -CCD diffractometer with sealed tube (powder diffraction experiments) or rotating anode (single-crystal diffraction experiments), using MoK $\alpha$  radiation with a graphite monochromator. Powder patterns were recorded at a sample-to-detector distance of 75 mm and the maximum scattering angle ( $2\theta$ ) was 22°. Separate blank patterns were recorded in order to allow the subtraction of air-scattering. Single-crystal diffraction experiments were carried out under temperature control, with an Oxford Cryosystems Cryostream Cooler.

#### *4.2.2.4.6 Infrared spectroscopy*

Infrared spectra were recorded on a Bio-Rad FTS 6000 spectrometer (Cambridge, MA, USA), in the range of 400-4000 cm<sup>-1</sup> (scan number 256, resolution 2 cm<sup>-1</sup>). Samples of microspheres, crushed HoAcAc crystals and films were prepared by mixing with spectroscopy grade KBr grain. The KBr mixture was then pressed into a pellet. Acetylacetonate was prepared by adding acetylacetone to an aqueous solution of NH<sub>3</sub> (28.4% (v/v)), resulting in a concentrated acetylacetonate solution. Acetylacetone and prepared acetylacetonate were brought to the surface of KBr pellets. In addition to solid state IR experiments, samples of HoAcAc, films and microspheres were analyzed, in deuterated chloroform using a liquid cell with KBr windows.

### **4.3 Results and Discussion**

#### *4.3.1 Preparation of HoAcAc-loaded microspheres*

As reported previously, X-ray crystallography revealed that per mol HoAcAc, 3 moles of water are present (2 moles of water directly coordinated to Ho and 1 mole uncoordinated water) [12]. The microspheres prepared by the solvent evaporation method, with a size distribution (20-50  $\mu\text{m}$ ) suitable for radio-embolization therapy, were obtained with a yield of about 30% of the starting materials PLLA and HoAcAc. The loading of the microspheres with Ho was 17.0 $\pm$ 0.6% holmium (w/w) (average

$\pm$ s.d.,  $n=5$ ). Less than 0.3% (w/w) chloroform, based on chlorine content, was found in the holmium loaded microspheres.

#### 4.3.2 Scanning electron microscopy (SEM)

Fig. 1 shows representative SEM pictures of films with 8 and 20% Ho loading. It is obvious that HoAcAc crystals are present in films with 20% Ho (Fig. 1b). In contrast, in films containing 8% Ho (w/w), no crystals could be observed. SEM analysis of films differing in HoAcAc content revealed that crystals were present at a loading  $\geq 12\%$ . This indicates that below this concentration HoAcAc molecules are dispersed in the PLLA matrix, and it suggests the presence of PLLA/HoAcAc interactions.

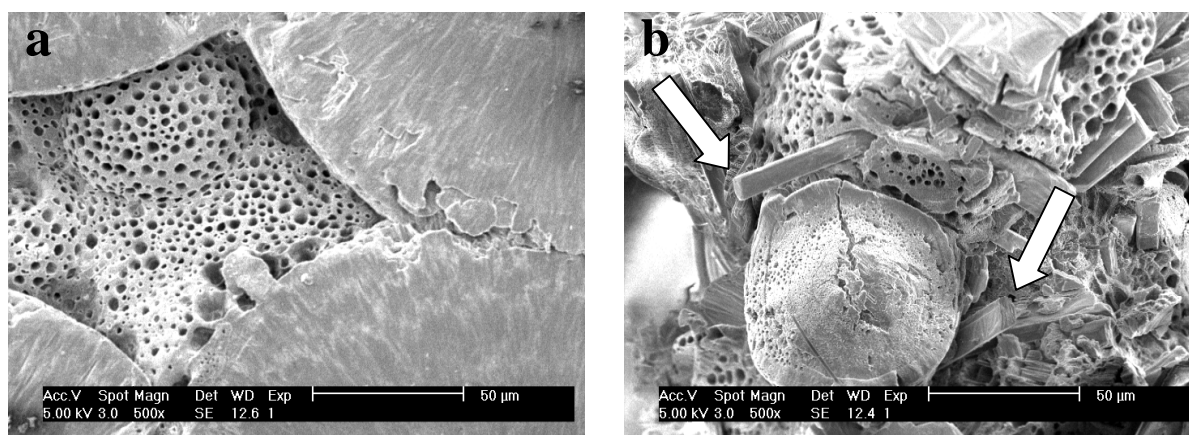


**Fig. 1.** Electron micrographs of films illustrating the forming of HoAcAc crystals at high loadings of holmium in the PLLA matrix (magnification 500x). (a) film with 8% holmium (w/w). (b) film with 20% Ho (w/w) loading resulted in crystals of HoAcAc (white arrows) surrounded with PLLA.

In Fig. 2 a representative SEM picture of microspheres with a diameter of 20-50  $\mu\text{m}$  is shown. It demonstrates that the particles are spherical and smooth. There were no HoAcAc crystals present on the surface of the microspheres, even at a Ho loading of 17%. EDX showed a homogeneous dispersion of Ho on the surface layer of the microspheres.



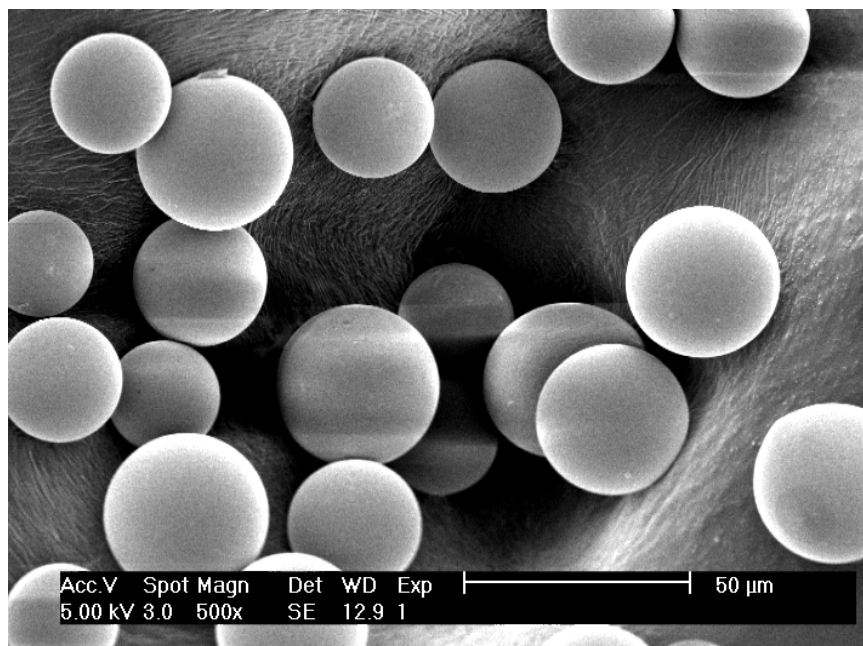


**Fig. 2.** Electron micrograph of microspheres with a loading of 17% (w/w) Ho demonstrating the spherical structure and the smooth surface of the particles.

#### *4.3.3 Differential scanning calorimetry and thermo-gravimetric analysis*

##### *4.3.3.1 PLLA films and microspheres without holmium*

Representative MDSC scans of PLLA films and microspheres, with and without HoAcAc, are shown in Figs. 3 and 4; Table 1 summarizes the results. MDSC thermograms of PLLA (as received), a PLLA film and microspheres without holmium, showed a melting temperature ( $T_m$ ) of about 176°C and melting enthalpy of 54, 46 and 57 J/g, respectively. The melting enthalpy and  $T_m$  for PLLA is in complete agreement with data published previously [15-17], and suggests a high degree of crystallinity ( $\Delta H$  for fully crystalline monodisperse lactic acid oligomers amounted to 93 J/g [18]). During the first heating a small  $T_g$  was observed at 66°C for PLLA (as received), at 49°C for PLLA film and at 58°C for empty microspheres (Table 1). During cooling following the first heating, which means that the thermal history of the samples was destroyed, a  $T_g$  of around 66°C was observed in all three PLLA samples.

**Table 1.** Transition temperatures of PLLA samples with varying HoAcAc loadings (n=2-5)

appearance	T <sub>g</sub> (°C)	T <sub>1</sub> max (°C)	ΔH <sub>1</sub> (J/g)	T <sub>2</sub> max (°C)	ΔH <sub>2</sub> (J/g)	T <sub>m</sub> max PLLA (°C)	*enthalpy (J/g)
PLLA (as recieved )	66±1	---	---	---	---	176±0	54±3
PLLA film 0% Ho	49±2	---	---	---	---	177±0	46±1
PLLA film 4% Ho	50±6	nd	nd	nd	nd	168±1	62±6
PLLA film 8% Ho	52±10	54±10	6±2	88±5	8.8±2	165±0	60±3
PLLA film 12% Ho	nd	44±6	18±4	84±6	29±16	164±1	64±4
PLLA film 16% Ho	nd	40±5	24±2	87±2	84±7	163±1	53±9
PLLA film 20% Ho	nd	44±8	29±14	87±4	112±28	163±1	51±6
Microspheres without Ho	58±2	---	---	---	---	176±0	57±4
Microspheres with Ho 7%	56±3	nd	nd	nd	nd	163±0	41±7
Microspheres with Ho 17%	59±2	nd	nd	nd	nd	159±1	25±12

\*Corrected for HoAcAc loading. nd = not detectable. T<sub>g</sub> in the first heating; Tmax, ΔH: as in Fig. 3.

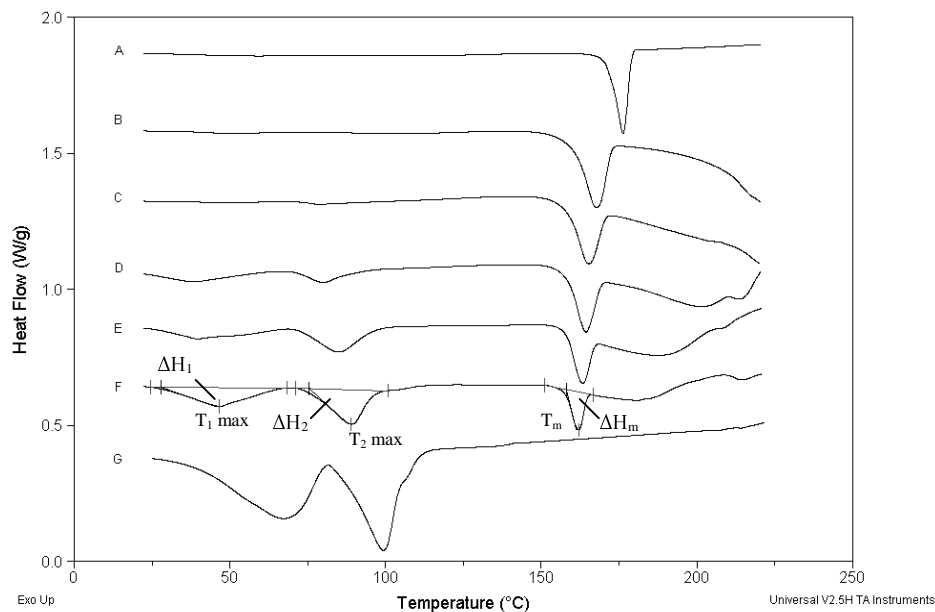


**Fig. 3.** MDSC thermograms of films with 0% (A), 4% (B), 8% (C), 12% (D), 16% (E) and 20% (w/w) Ho loading (F). Trace G shows HoAcAc.  $T_1 \text{ max}$  and  $T_2 \text{ max}$ : peak maximum of first and second endotherm,  $\Delta H_1$  and  $\Delta H_2$ : enthalpy of first and second endotherm,  $T_m$ : melting temperature,  $\Delta H_m$ : enthalpy of melting endotherm.

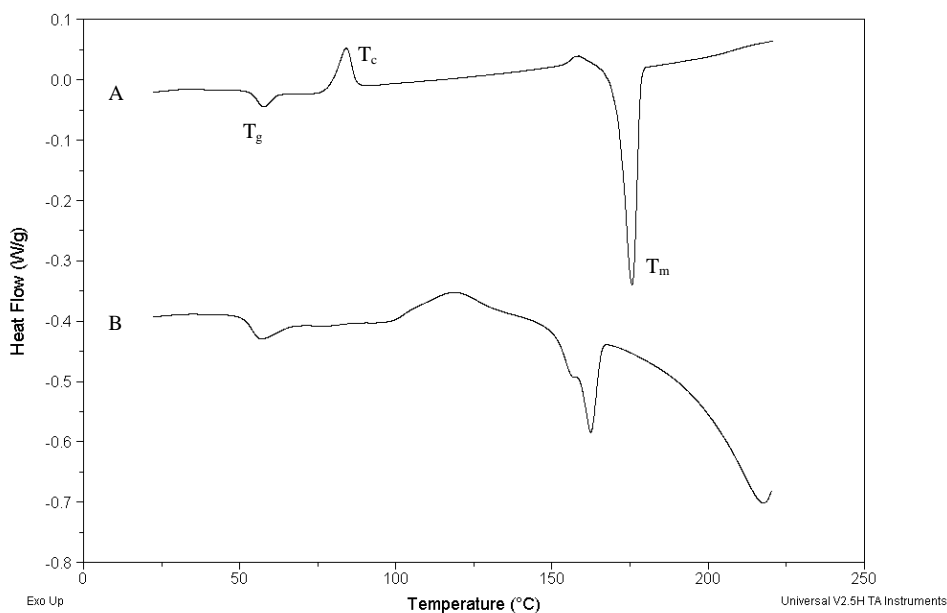


**Fig. 4.** MDSC thermograms of PLLA microspheres with 0% (A) and 17% (w/w) Ho loading (B).

### 4.3.3.2 Holmiumacetylacetonate

A weight loss of about 10-14% was observed from TGA analysis of freshly prepared HoAcAc crystals beginning at a temperature of 50°C, when this sample was heated from room temperature to 120°C. This is most likely ascribed to the loss of the three water molecules present in the HoAcAc asymmetric unit cell [12]. TGA showed a substantial weight loss above 200°C, indicating decomposition of HoAcAc. The residual weight is around 40% and indicates the presence of Ho<sub>2</sub>O<sub>3</sub>. MDSC thermograms (Fig. 5) of freshly prepared HoAcAc crystals showed two endotherms at temperatures around 64 and 95°C and  $\Delta H$  of 78 J/g and 149 J/g, respectively (Table 2). These endotherms were almost totally present in the non-reversing signal and not in the reversing signal, and were not detected in the second heating run (Fig. 5).

**Table 2.** Transition temperatures of HoAcAc crystals (n=3-8)

appearance	T <sub>g</sub> cooling (°C)	T <sub>1</sub> max (°C)	$\Delta H_1$ (J/g)	T <sub>2</sub> max (°C)	$\Delta H_2$ (J/g)
HoAcAc <sup>1</sup>	47±3	64±5	78±20	95±4	149±9
HoAcAc <sup>2</sup>	60±3	55±6	76±9	91±1	103±11

T<sub>g</sub>: glass transition temperature observed by cooling down the sample (Fig. 5), Tmax: peak maximum of first or second endotherm,  $\Delta H$ : enthalpy of first or second endotherm (Fig. 3, trace f). <sup>1</sup>HoAcAc freshly prepared, <sup>2</sup>HoAcAc recrystallized in chloroform.

Additionally, in the cooling curve and in the second heating a strong T<sub>g</sub> was observed in the reversing heat flow signal at around 47°C. This indicates that the first endotherm is due to the evaporation of the non-coordinating water molecule, whereas the second endotherm is due to evaporation of the two coordinating water molecules. We have recently deployed X-ray diffraction in the investigation of the effect of HoAcAc monohydrate crystals upon heating. The crystallographic unit cell of this compound contains 4 non-coordinating water molecules and 4 Ho-complexes, with a total of 8 coordinated water molecules [12]. At 40°C the unit cell volume is 1999.9±1.0 Å<sup>3</sup>, slightly higher than the value found at -123°C (1966.1±0.9 Å<sup>3</sup> [12]). When the crystals are heated to 50°C, the diffraction pattern changes dramatically. The high resolution reflections all become very weak and most of them can no longer be observed. The volume of the unit cell drops to 1873±3 Å<sup>3</sup>.

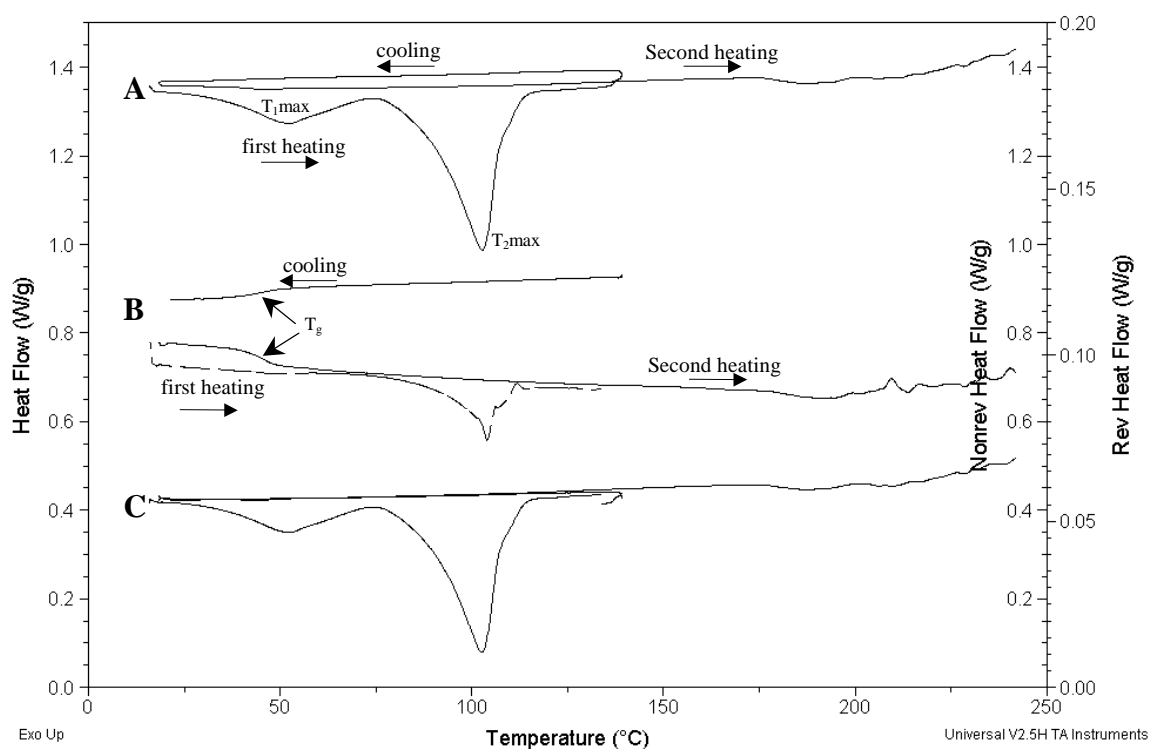


**Fig. 5.** MDSC thermograms of holmiumacetylacetonate. Heat flow (curve A).  $T_{1max}$  and  $T_{2max}$ : peak maximum of first and second endotherm of HoAcAc. Reversing heat flow (curve B) is given in an enlarged scale, shown on the right y-axis (first heating: dotted line),  $T_g$  is glass transition temperature. Non-reversing heat flow (curve C).

Interestingly, this decrease in volume of  $127 \text{ \AA}^3$  corresponds with the volume of 4 water molecules in liquid water ( $119.7 \text{ \AA}^3$ ). Unfortunately, the modification of HoAcAc obtained at  $50^\circ\text{C}$  is unstable. After a few minutes even the low resolution reflections can no longer be observed. Collection of a full data set and complete structure determination is therefore impossible.

It is interesting to note that, in the MDSC thermograms of HoAcAc aged at room temperature for 4 months, only an endotherm around  $95^\circ\text{C}$  ( $\Delta H=153 \text{ J/g}$ ) was observed. This means that with ageing the non-coordinating water molecule is removed. When HoAcAc crystals (either freshly prepared or aged) were dissolved in chloroform, followed by slow evaporation of the solvent, a powder-like material was obtained. MDSC analysis showed the same two endotherms as in freshly prepared crystals. From the results presented above, it can be concluded that by heating the HoAcAc crystals to  $50^\circ\text{C}$ , the non-coordinating water is removed, and this is associated with a concomitant conversion of the crystalline to the amorphous state, which underscores the important role of this water molecule for the crystal structure of HoAcAc [12]. We observed that the loss of crystal water occurs at a higher

temperature (120°C), when the heating rate was increased from the routinely applied 2°C/min to 10°C/min. Mumper et al. [6] also observed a thermal effect at 121°C,  $\Delta H$  104 J/g, using the latter heating rate, but erroneously ascribed this to a melting endotherm.

Fig. 6 (trace A-C) shows the IR bands of acetylacetone, acetylacetonate and HoAcAc in the C=C and C=O region (1700-1500  $\text{cm}^{-1}$ ) [19-22]. The results are summarized in Table 3.

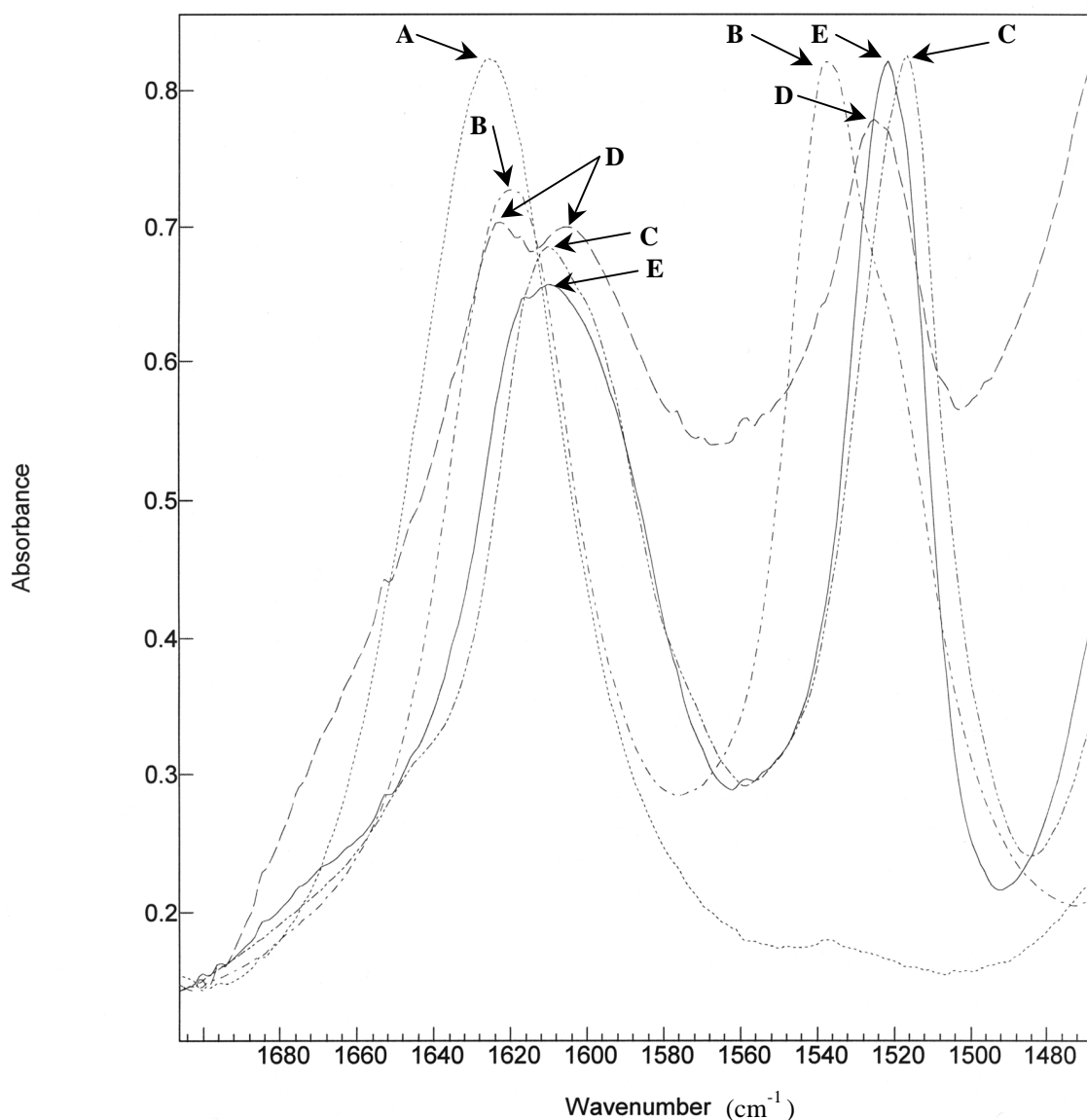


**Fig. 6.** IR spectra of acetylacetone (A), acetylacetonate (B), HoAcAc (C) and films with 4% (D) and 16% (w/w) Ho loading (E).

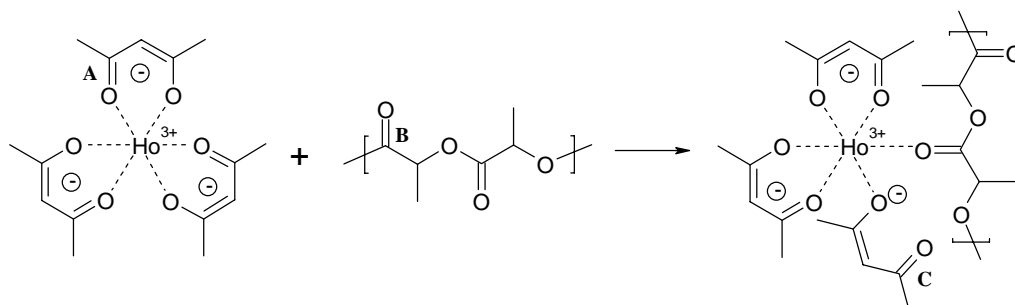
After addition of an aqueous solution of  $\text{NH}_3$ , by which the acetylacetonate anion is formed, as well as a carbonyl band ( $1620\text{ cm}^{-1}$ ), the stretching vibration  $\text{C}=\text{C}$  ( $1537\text{ cm}^{-1}$ ) band is also observed. In HoAcAc the  $\text{C}=\text{O}$  and  $\text{C}=\text{C}$  stretching vibrations are shifted to lower wave numbers ( $1610$  and  $1517\text{ cm}^{-1}$ ). When HoAcAc crystals were heated to  $80^\circ\text{C}$  (15 min), by which method amorphous HoAcAc is formed as seen by X-ray diffraction and MDSC, no difference in  $\text{C}=\text{O}$  and  $\text{C}=\text{C}$  vibration bands was observed (not shown). HoAcAc crystals dissolved in deuterated chloroform gave two bands at  $1621$  and  $1603\text{ cm}^{-1}$  respectively, indicating that in solution one of the three acetylacetonate anions (partially) dissociates from the complex, resulting in  $\text{Ho}^{3+}$  coordinated by two acetylacetonate anions.

#### 4.3.3.3 HoAcAc-loaded films

Ho loaded PLLA microspheres and films were prepared from a solution of PLLA and HoAcAc in chloroform. Fig. 3 shows the MDSC thermograms of PLLA films, with varying Ho loading. Due to the irreversible changes which HoAcAc undergoes, thermograms were recorded over the first run only. It appears that up to 8% Ho content no signal due to HoAcAc was observed (Fig. 3 trace B and C). This suggests that, in agreement with SEM analysis, HoAcAc is molecularly dispersed in the PLLA matrix at concentrations of  $<8\%$  Ho (w/w). The dispersed HoAcAc in the PLLA matrix explains very well the observed decreased  $T_m$  of the PLLA phase (from  $176^\circ\text{C}$  to  $163^\circ\text{C}$ , Table 1). At higher loadings of Ho ( $\geq 12\%$ ) clear endotherms (evaporation of crystal water, Fig. 3 trace D-F) were observed. This demonstrates that, in agreement with SEM (Fig. 1b), above this loading HoAcAc is also present in its crystalline form. The melting enthalpy of PLLA increased from  $46\text{ J/g}$  to around  $60\text{ J/g}$  in films with a relatively low HoAcAc loading (Table 1) and this suggests that HoAcAc acts as a crystallization nucleus for PLLA. Due to the high crystallinity of the PLLA matrix no clear  $T_g$  could be detected.

IR spectra of films with 16% holmium loading showed that the  $\text{C}=\text{O}$  vibration of AcAc was detected at the same wave number as for HoAcAc crystals ( $1610\text{ cm}^{-1}$ , Fig. 6 trace C, E and Table 3). In contrast, in films with a low loading (4%) the  $\text{C}=\text{O}$  vibration was observed at both  $1622$  and  $1606\text{ cm}^{-1}$ , Fig. 6 trace D and Table 3). Since the band at  $1622$  is indicative of the acetylacetonate anion (Fig. 6 trace B, Table 3), this suggests that in films with the 4% loading, some of the carbonyl groups of AcAc do not interact with the  $\text{Ho}^{3+}$  ion. The remaining positive charge is then a candidate for interaction with carbonyl oxygens present in PLLA of which only a minor portion can interact due to their large molar excess over holmium (seven-fold in case of the highest holmium loading of 17%). As expected, no detectable changes in the  $\text{C}=\text{O}$  band of PLLA ( $1760\text{ cm}^{-1}$ ) were observed since any shift will be obscured by the

strong absorption band of the remaining, non-coordinating C=O bonds. The reactions that are supposed to occur are:



C=O band of **A)** HoAcAc at  $1610\text{ cm}^{-1}$ ; **B)** PLLA at  $1760\text{ cm}^{-1}$ ; **C)** acetylacetonate anion at  $1623\text{ cm}^{-1}$

**Table 3.** Summary of infrared data

appearance	$\nu_{(\text{C}=\text{O})}$ ( $\text{cm}^{-1}$ )	$\nu_{(\text{C}=\text{C})}$ ( $\text{cm}^{-1}$ )
Acetylacetone	1626	np
Acetylacetonate	1620	1537
HoAcAc	1610	1517
PLLA film 4% Ho	1622, 1606 db	1525
PLLA film 16% Ho	1610	1522
Microspheres with Ho 17%	1623, 1610 db	1525

$\nu_{(\text{C}=\text{O})}$ ,  $\nu_{(\text{C}=\text{C})}$ : stretching vibrations, np = not present, db = double band.

#### 4.3.3.4 Microspheres

Fig. 4 shows the MDSC thermograms of empty as well as HoAcAc-loaded microspheres. MDSC thermograms of microspheres with 7% holmium loading showed no signals, due to HoAcAc, thus indicating that correspondingly with HoAcAc-loaded films, HoAcAc is dissolved in the microspheres. Interestingly, microspheres with a high Ho loading, 17%, (Fig. 4 trace B) did not show signals ascribable to crystalline HoAcAc. This means that in contrast to films with a comparable Ho loading (Fig. 3 trace E), HoAcAc was present in an amorphous state.



SEM analysis also suggested the absence of HoAcAc crystals in PLLA microspheres (Fig. 2). Furthermore, a strong decrease in enthalpy of fusion of the PLLA phase was observed ( $\Delta H=25$  J/g, Table 1) and now a strong  $T_g$  ( $59^\circ\text{C}$ , with relaxation peak in the first heating run [23], Fig. 4) was present, especially in the reversing heat-flow. These factors indicate that the PLLA phase has a low degree of crystallinity, and this accords well with powder diffraction, (see section 4.3.4). The apparently better dispersion of HoAcAc in PLLA microspheres, when compared with PLLA films, may be ascribed to the relatively faster removal of the solvent during microsphere preparation. This results in a more rapid solidification of the PLLA matrix, which will impede the crystallization of both PLLA and HoAcAc.

The IR spectrum of HoAcAc loaded microspheres showed, as in the films with a low loading, a C=O vibration of HoAcAc at both  $1623$  and  $1610\text{ cm}^{-1}$ . This again suggests that carbonyl groups of PLLA can interact with the HoAcAc complex, resulting in the immobilization of this complex in the PLLA matrix. This in turn explains the low release characteristics of the HoAcAc loaded microspheres.

#### *4.3.4 X-ray powder diffraction*

X-ray diffraction on films with a relatively low HoAcAc loading showed the presence of a crystalline PLLA phase, whereas, as in both MDSC and SEM, no HoAcAc crystals were detected (Fig. 7). A broad peak appeared, which we assign to Ho-Ho interactions (due to their large scattering power) in the amorphous state. The distance associated with the peak maximum is about  $16\text{ \AA}$ , which does not correspond with normal Ho-Ho distances in crystalline HoAcAc. However, at a higher loading (16% Ho (w/w)) a crystalline PLLA phase, as well as crystalline and amorphous HoAcAc was observed. The crystalline form can be assigned to crystal form I as described in a previous paper [12]. In agreement with MDSC data, X-ray diffraction analysis showed a strongly reduced crystallinity of the PLLA matrix in HoAcAc loaded microspheres compared with unloaded microspheres. Interestingly, microspheres with a high HoAcAc loading again showed a large broad peak, which we ascribed to Ho-Ho interactions in the amorphous state. This means that in PLLA microspheres, HoAcAc is incorporated in an amorphous way. These observations suggest that it is associated with amorphous PLLA, and explains the amount of HoAcAc that can be accommodated in the PLLA matrix.

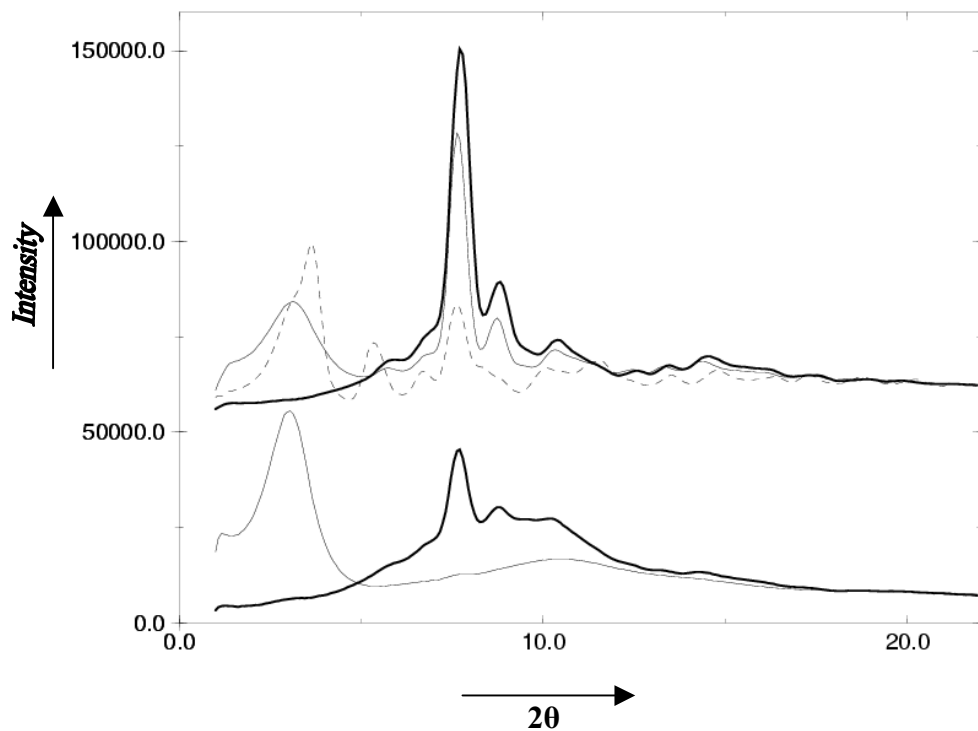


**Fig. 7.** X-ray scattered intensity as a function of the diffraction angle  $2\theta$ . Scaling is arbitrarily applied to the curves so as to match the intensities at  $2\theta$  of  $22^\circ$ . The upper three curves are shifted upwards by 55000 units. Lower curves: microspheres of PLLA (thick line) and microspheres of PLLA loaded with 17% Ho (thin line). Upper curves: film of PLLA (thick line), film of PLLA loaded with 4% Ho (thin line) and film of PLLA loaded with 16% Ho (thin dashed line). In the latter curve, peaks either correspond to crystalline PLLA, amorphous Ho-Ho or crystalline HoAcAc (crystal form I).

#### **4.4 Conclusions**

Poly(L-lactic acid) microspheres, films and microspheres with different holmium acetylacetonate contents were prepared, in order to get insight into factors responsible for the low release properties of the holmium loaded microspheres. MDSC, X-ray diffraction and SEM analysis revealed that HoAcAc is molecularly dispersed in PLLA up to 8% (w/w) holmium in films. This indicates that interactions are present between HoAcAc and PLLA. Above this concentration HoAcAc is also present in a crystalline form. In contrast, in PLLA microspheres HoAcAc is present in an amorphous form and is molecularly dispersed in the amorphous PLLA phase, even at higher HoAcAc loadings. IR spectroscopy produced evidence of the type of interaction between HoAcAc and PLLA. Carbonyl groups of PLLA are likely to interact with the Ho-ion in the HoAcAc complex, and as a result this complex is immobilized in the PLLA matrix. This interaction thus accounts for the high stability (= low release) found in HoAcAc-loaded microspheres.

#### **Acknowledgements**

The authors wish to thank D.W. Rook, S. Zielhuis and R. Lange from the Department of Nuclear Medicine, University Medical Center, Utrecht, The Netherlands for preparation of the microspheres and W.A.M. van Maurik from EMSA, Faculty of Biology, Utrecht University, Utrecht, The Netherlands for SEM acquisition. Financial support was provided by NRG and Mallinckrodt Medical BV, Petten, The Netherlands and the Dutch Technology Foundation STW (349-4431).

## References

1. Andrews JC, Walker SC, Ackermann RJ, Cotton LA, Ensminger WD and Shapiro B. Hepatic radioembolization with yttrium-90 containing glass microspheres, Preliminary results and clinical follow-up. *J. Nucl. Med.* **1994**;35:1637-1644.
2. Ho S, Lau WY, Leung TWT, Chan M, Johnson PJ and Li AKC. Clinical evaluation of the partition model for estimating radiation doses from yttrium-90 microspheres in the treatment of hepatic cancer. *Eur. J. Nucl. Med.* **1997**;24:293-298.
3. Wagner HN, Rhodes BA, Sasaki Y and Ryan JP. Studies of the circulation with radioactive microspheres. *Invest. Radiology* **1969**;4:374-386.
4. Mumper RJ, Ryo UY and Jay M. Neutron activated holmium-166-poly(L-lactic acid) microspheres: A potential agent for the internal radiation therapy of hepatic tumours. *J. Nucl. Med.* **1991**;32:2139-2143.
5. Turner JH, Claringbold PG, Klemp PFB, Cameron PJ, Martindale AA, Glancy RJ, Norman PE, Hetherington EL, Najdovski L and Lambrecht RM. <sup>166</sup>Ho-microsphere liver radiotherapy: a preclinical SPECT dosimetry study in the pig. *Nucl. Med. Commun.* **1994**;15:545-553.
6. Mumper RJ and Jay M. Poly(L-lactic acid) microspheres containing neutron-activatable holmium-165: A study of the physical characteristics of microspheres before and after irradiation in a nuclear reactor. *Pharmacol. Res.* **1992**;9:149-154.
7. Nijssen JFW, Zonnenberg BA, Woittiez JRW, Rook DW, Swildens-van Woudenberg IA, van Rijk PP and van het Schip AD. Holmium-166 poly lactic acid microspheres applicable for intra-arterial radionuclide therapy of hepatic malignancies: effects of preparation and neutron activation techniques. *Eur. J. Nucl. Med.* **1999**;26:699-704.
8. Jalil R and Nixon JR. Microencapsulation using poly(L-lactic acid) IV: Release properties of microcapsules containing phenobarbitone. *J. Microencapsul.* **1990**;7:53-66.
9. Miyajima M, Koshika A, Okada J, Ikeda M and Nishimura K. Effect of polymer crystallinity on papaverine release from poly(L-lactide acid) matrix. *J. Control. Release* **1997**;49:207-215.
10. Miyajima M, Koshika A, Okada J and Ikeda M. Mechanism of drug release from poly(L-lactic acid) matrix containing acidic or neutral drugs. *J. Control. Release* **1999**;60:199-209.
11. Sintzel MB, Merkli A, Tabatabay C and Gurny R. Influence of irradiation sterilization on polymers used as drug carriers A review. *Drug Dev. Ind. Pharm.* **1997**;23:857-878.
12. Kooijman H, Nijssen JFW, Spek AL and van het Schip AD. Diaquatrakis(pentane-2,4-dionato-O,O')holmium(III) monohydrate and diaquatrakis(pentane-2,4-dionato-O,O')-holmium(III) 4-hydroxypentan-2-one solvate dihydrate. *Acta Cryst.* **2000**;C56:156-158.
13. European Pharmacopoeia. Third edition, **1997**. p. 65.

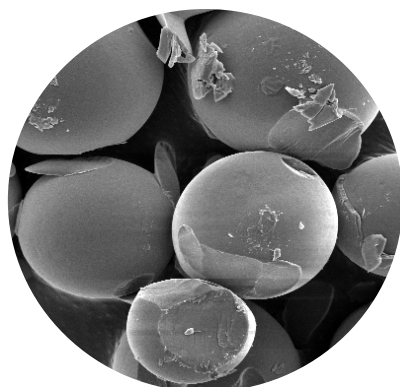
14. França YV, Leitão F, Shihomatsu HM, Scapin Jr. WS, de Moraes NMP, Salvador VL, Figueiredo AMG, Mucillo ENS and Muccillo R. Determination of yttrium and lanthanum in zirconium dioxide by HPLC, X-ray fluorescence and neutron activation analyses. *Chromatographia* **1999**;49:91-94.
15. Nakafuku C and Sakoda M. Melting and crystallization of poly(L-lactic acid) and poly(ethylene oxide) binary mixture. *Polym. J.* **1992**;25:909-917.
16. Sarasua J, Prud'homme RE, Wisniewski M, Le Borgne A and Spassky N. Crystallization and melting behavior of polylactides. *Macromolecules* **1998**;31:3895-3905.
17. van de Witte P, Boorsma A, Esselbrugge H, Dijkstra PJ, van den Berg JWA and Feijen J. Differential scanning calorimetry study of phase transitions poly(Lactide)-chloroform-methanol systems. *Macromolecules* **1996**;29:212-219.
18. de Jong SJ, van Dijk-Wolthuis WNE, Kettenes-van den Bosch JJ, Schuyl PJW and Hennink WE. Monodisperse enantiometric lactic acid oligomers: Preparation, characterization, and stereocomplex formation. *Macromolecules* **1998**;31:6397-6402.
19. Babich IV, Plyuto YU, Van Langeveld AD and Moulijn JA. Role of the support nature in chemisorption of Ni(acac)<sub>2</sub> on the surface of silica and alumina. *Appl. Surf. Sci.* **1997**;115:267-272.
20. Dunstan PO. Thermochemistry of adducts of nickel(II) acetylacetonate chelate with heterocyclic bases. *Thermochim. Acta* **1998**;317:165-174.
21. Dunstan PO. Thermochemistry of aniline-derivate adducts of nickel(II) acetylacetonate. *Thermochim. Acta* **1999**;333:5-11.
22. Irikura KK. Acetylacetonate (acac) anion in the gas phase: predicted structures, vibrational spectra, and photodetachment energies. *Int. J. Mass. Spectrom.* **1999**;185-7:577-587.
23. Coleman NJ and Craig DQM. Modulated temperature differential scanning calorimetry: a novel approach to pharmaceutical thermal analysis. *Int. J. Pharm.* **1996**;135:13-29.

## Chapter 5

---

# **Influence of neutron irradiation on holmium acetylacetonate loaded poly(L-lactic acid) microspheres**

*submitted (Biomaterials)*



**J.F.W. Nijsen<sup>1</sup>, A.D. van het Schip<sup>1</sup>, M.J. van Steenberg<sup>2</sup>,  
S.W. Zielhuis<sup>1</sup>, L.M.J. Kroon-Batenburg<sup>3</sup>, M. van de Weert<sup>2</sup>,  
P.P. van Rijk<sup>1</sup> and W.E. Hennink<sup>2</sup>**

<sup>1</sup>*Department of Nuclear Medicine, University Medical Center, Utrecht, The Netherlands*

<sup>2</sup>*Department of Pharmaceutics, Utrecht Institute for Pharmaceutical Sciences, Utrecht University, Utrecht, The Netherlands*

<sup>3</sup>*Department of Crystal and Structural Chemistry, Bijvoet Center for Biomolecular Research, Utrecht University, Utrecht, The Netherlands*

### **Abstract**

Holmium-loaded microspheres are useful systems in radio-embolization therapy of liver metastases. For administration to a patient, the holmium-loaded microspheres have to be irradiated in a nuclear reactor to become radioactive. In this paper the influence of neutron irradiation on poly(L-lactic acid) (PLLA) microspheres and films, with or without holmium acetylacetonate (HoAcAc), is investigated, in particular using differential scanning calorimetry (MDSC), scanning electron microscopy, gel permeation chromatography (GPC), infrared spectroscopy, and X-ray diffraction. After irradiation of the microspheres, only minor surface changes were seen using scanning electron microscopy, and the holmium complex remained immobilized in the polymer matrix as reflected by a relatively small release of this complex. GPC and MDSC measurements showed a decrease in molecular weight and crystallinity of the PLLA, respectively, which can be ascribed to radiation induced chain scission. Irradiation of the HoAcAc loaded PLLA matrices resulted in evaporation of the non-coordinated and one coordinated water molecule of the HoAcAc complex, as evidenced by MDSC and X-ray diffraction analysis. Infrared spectroscopy indicated that some degradation of the acetylacetonate anion occurred after irradiation. Although some radiation induced damage of both the PLLA matrix and the embedded HoAcAc-complex occurs, the microspheres retain their favourable properties (no/marginal release of Ho, preservation of the microsphere size), which make these systems interesting candidates for the treatment of tumours by radio-embolization.

## 5.1 Introduction

Poly(L-lactic acid) (PLLA) is a biodegradable and biocompatible, semi-crystalline polymer that can be used for the preparation of microspheres loaded with neutron-activatable Ho-complexes [1,2] or radioactive yttrium and rhenium salts [3-5]. These systems are presently under investigation in the field of internal radio-embolization. Especially liver metastases, which cause 25-50% of all cancer deaths [6-8], can potentially be treated with such radioactive particles through embolization of the hepatic artery [9-13]. Currently, both glass and resin-based microspheres with radioactive yttrium are applied for treatment of liver metastases and beneficial effects are reported [10,11,14]. However, glass has some drawbacks such as its high density and non-degradability. Therefore, biodegradable and biocompatible materials like PLLA are in favour over glass. In a previous paper we described the preparation and characterisation of PLLA microspheres loaded with holmium acetylacetonate (HoAcAc) [2]. For therapeutic application of these microspheres they have to be irradiated with neutrons to become radioactive. The radioactive microspheres are administered into the hepatic artery and will be trapped in the liver especially in and around tumours [2,5]. Only marginal leakage of radioactive holmium should occur. In a previous study only small amounts of free holmium (Ho) were found during in vitro experiments. For example, the retention of Ho in irradiated microspheres is over 98% after 192h (>7 half-lives) incubation in liver homogenate [2].

The neutron irradiation together with the simultaneously generated gamma rays, as well as secondary gamma rays caused by the  $H(n,\gamma)$  and  $Ho(n,\gamma)$  reactions [15,16], can result in damage to both the PLLA matrix and the entrapped HoAcAc complex.  $\gamma$ -Irradiation is applied as a sterilisation method for PLLA and therefore its effects on PLLA have been investigated extensively. After  $\gamma$ -irradiation of PLLA a decrease in molecular weight is observed [17,18], which is caused by chain scission due to radical formation [19]. Chain scission occurs predominantly in the amorphous phase of the polymer [1,19,20]. This could imply that after neutron irradiation similar processes in PLLA matrices would occur. However, irradiation in a nuclear reactor differs from  $\gamma$ -irradiation by higher linear energy transfer (LET) of nuclear interaction products leading to high radiation doses. Thus far, no systematic studies of the effect of neutron irradiation on PLLA have been published. Therefore, we investigated the influence of neutron irradiation on PLLA films and microspheres with and without HoAcAc using a variety of techniques: scanning electron microscopy (SEM), gel permeation chromatography (GPC), differential scanning calorimetry (MDSC), X-ray diffraction and infrared spectroscopy (IR).



## 5.2 Materials and Methods

### 5.2.1 Materials

All chemicals were commercially available and used as obtained. Acetylacetone, 2,4-pentanedione, (AcAc; MW 100.12; >99%) was obtained from Sigma Aldrich (Steinheim, Germany). Holmium(III) chloride hexahydrate ( $\text{HoCl}_3 \cdot 6\text{H}_2\text{O}$ ; MW 379.38; 99.9%) was obtained from Phase Separations BV (Waddinxveen, The Netherlands). Polyvinyl alcohol (PVA, average MW 30,000-70,000) was obtained from Sigma Chemical Co. (St. Louis, Mo, USA). Poly(L-lactic acid) (end-capped; intrinsic viscosity 0.9 dl/g (chloroform 25°C)) was supplied by Purac Biochem BV (Gorinchem, The Netherlands). Ethylenedinitrilotetraacetic acid disodium salt (dihydrate) (EDTA,  $\geq 99.0\%$ ) and zinc sulphate heptahydrate ( $\text{ZnSO}_4 \cdot 7\text{H}_2\text{O}$ , >99.5%) were obtained from Merck (Darmstadt, Germany).

### 5.2.2 Methods

#### 5.2.2.1 Preparation of the HoAcAc loaded films and microspheres

Films and microspheres of PLLA loaded with HoAcAc were prepared as described previously [2,21,22]. Briefly, acetylacetone was dissolved in water. The pH of this solution was brought to 8.5 with an aqueous solution of  $\text{NH}_3$ . Holmium chloride in water was added to this solution after which HoAcAc crystals were formed at room temperature. The crystals were collected by filtration. HoAcAc loaded films were prepared by dissolving PLLA and HoAcAc in chloroform. The resulting homogeneous and viscous solutions were poured onto a glass plate and the solvent was evaporated, resulting in films of 1-2 mm thickness, and a holmium loading range of 0, 4 and 16% (w/w). HoAcAc-loaded poly(L-lactic acid) microspheres with different HoAcAc amounts were prepared by solvent evaporation as described previously [2]. HoAcAc and PLLA were dissolved in chloroform. The resulting homogeneous solution was added to an aqueous solution of PVA. The mixture was stirred and the formed microspheres were collected by centrifugation. Microspheres with a size of 20-50  $\mu\text{m}$  were obtained by sieving.

#### 5.2.2.2 Irradiation

Irradiations were performed in the pneumatic rabbit system (PRS) in the reactor facilities in Petten, The Netherlands. The PRS (neutronflux  $5 \times 10^{13} \text{ cm}^{-2} \cdot \text{s}^{-1}$ ) irradiations were carried out on samples of 100-200 mg, which were packed in polyethylene vials. The irradiation time was 0.5 and 1h. The 1h irradiation resulted in an estimated radiation dose of 2 MGy (personal communication, NRG, Petten, The Netherlands) and gives an amount of microsphere associated radioactivity needed for the treatment of a patient. Analyses were performed after a cooling time of 1 month.

### 5.2.2.3 Characterization of microspheres and films

#### 5.2.2.3.1 Determination of holmium content

The holmium content in the PLLA film and microspheres was determined by titration based on the method described previously [22].

#### 5.2.2.3.2 Scanning electron microscopy

Surface morphology of HoAcAc-loaded PLLA microspheres and films was investigated by scanning electron microscopy using a Philips XL30 FEGSEM. A voltage of 5 or 10 kV was applied. Samples of PLLA microspheres and films as well as HoAcAc crystals were mounted on aluminium stubs and sputter-coated with a Pt/Pd layer of about 10 nm. Holmium distribution was analysed by an energy dispersive x-ray spectrometer (EDX) that was integrated in the scanning electron microscope.

#### 5.2.2.3.3 Differential scanning calorimetry

Modulated DSC (MDSC) analysis was performed with a DSC 2920 (TA Instruments, Inc., New Castle, DE, USA). Samples of approximately 6 mg were transferred into pierced aluminium pans. The sample compartment was purged with helium. Scans were recorded under “heating only” conditions, with a heating rate of 2°C/min and cooling rate of 1°C/min. The settings were periods of 60 s and temperature modulation amplitude of 0.32°C. The universal analysis software version V2.5.M was used for evaluation.

#### 5.2.2.3.4 Infrared spectroscopy

Infrared spectra were recorded on a Bio-Rad FTS 6000 spectrometer (Cambridge, MA, USA), in the range of 400-4000  $\text{cm}^{-1}$  (scan number 256, resolution 2  $\text{cm}^{-1}$ ). Samples of microspheres, HoAcAc crystals and films (irradiated or non-irradiated) were prepared by mixing with spectroscopy grade KBr grain and then pressed into a pellet. Acetylacetonate was prepared by adding acetylacetone to an aqueous solution of  $\text{NH}_3$ , resulting in a concentrated acetylacetonate solution. Acetylacetone and prepared acetylacetonate were brought on to the surface of KBr pellets. In addition to solid-state IR experiments, samples of HoAcAc, films and microspheres were analysed after dissolution in deuterated chloroform using a liquid cell with  $\text{CaF}_2$  windows.

#### 5.2.2.3.5 X-ray diffraction studies

X-ray diffraction experiments were carried out on a Nonius  $\kappa$ -CCD diffractometer with sealed tube (powder diffraction experiments) or rotating anode (single-crystal diffraction experiments), using MoK $\alpha$  radiation with a graphite monochromator. Powder patterns were recorded at a sample-to-detector distance of 75 mm and the maximum scattering angle ( $2\theta$ ) was  $22^\circ$ . Separate blank patterns were recorded in order to allow the subtraction of air-scattering.

#### 5.2.2.3.6 Molecular weight determinations

The weight-average molecular weight ( $M_w$ ) and number-average molecular weights ( $M_n$ ) of PLLA were determined by gel permeation chromatography (GPC). GPC measurements were performed with two thermostated ( $35^\circ\text{C}$ ) columns in series (PLgel Mixed-B, Polymer Laboratories) equipped with an evaporative light scattering refractive index detector (PL-ELS 1000, Polymer Laboratories). Samples of approximately 1 mg were dissolved in 2 ml HPLC-grade chloroform and filtered. Elution was performed with chloroform and the flow-rate was 1 ml/min. The columns were calibrated using poly(styrene) standards of known molecular weights (Polymer Laboratories, Shodex and Tosoh).

### 5.3 Results and Discussion

#### 5.3.1 Scanning electron microscopy

For therapeutic application of the HoAcAc loaded microspheres, the size has to be preferably between 20 and 50  $\mu\text{m}$  [23,24,25]. Therefore it was investigated whether the size distribution had altered after neutron irradiation. Since neutron irradiation is associated with an increase in temperature, fusion of microspheres may occur. SEM and particle size measurements demonstrated that no substantial particle fusion occurred. However, surface changes on the microspheres were seen with SEM giving rise to small PLLA fragments (Fig. 1). Similar fragments were seen on irradiated films. However, the amount of radioactivity in particles with a size  $<20\ \mu\text{m}$  is still marginal (1% and 3% before and after irradiation, respectively) [2].

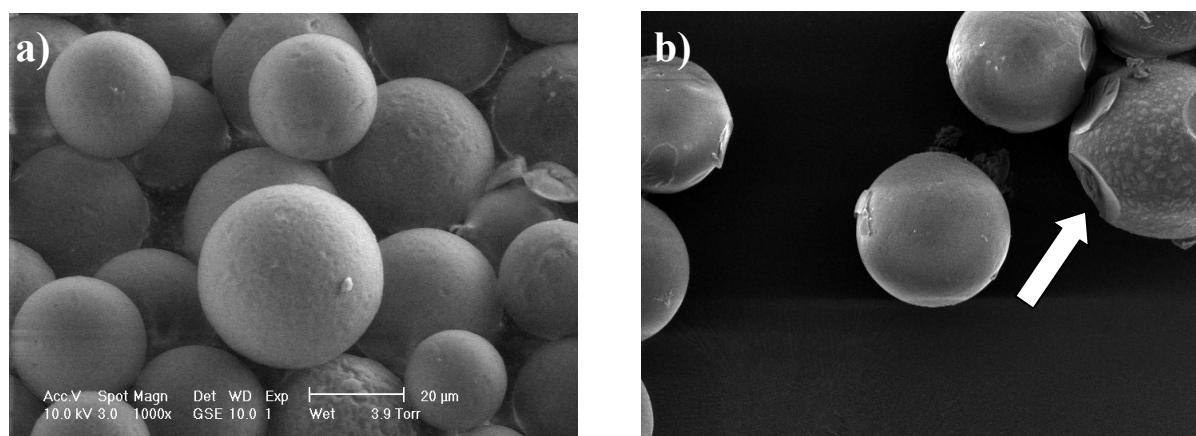


**Fig. 1.** Electron micrographs of microspheres with a loading of 17% (w/w) Ho, magnification 500x. Non-irradiated microspheres have a spherical structure and smooth surface (a). After irradiation only small surface changes were seen (white arrow; b).

### 5.3.2 Differential scanning calorimetry

Films and microspheres both with and without Ho loading were analysed with MDSC. Table 1 (films) and table 2 (microspheres) summarise the results. Irradiation of films without holmium resulted in a decreasing  $T_m$  and slightly decreased enthalpy of fusion with increasing irradiation time (Table 1 and Fig. 2 trace A) indicating impairment of the crystalline phase of PLLA after neutron irradiation [1,19]. In contrast to the non-irradiated films (small  $T_g$  observed at 66°C), in the irradiated film (1h) a clear  $T_g$  was seen at 35°C both during cooling and in the second run, indicating a loss in crystallinity. The PLLA film in which HoAcAc was molecularly dispersed (4% Ho (w/w) [22]) also showed a decreasing  $T_m$  of the PLLA phase with increasing irradiation dose (Fig. 2 trace B). Again, a  $T_g$  was seen during cooling and the second run for irradiated films (Table 1). In 1h irradiated PLLA films with HoAcAc present in its crystalline form (16% (w/w) Ho-loading) no  $T_m$  was observed, indicating a complete loss of crystallinity of the PLLA phase (Table 1). The decrease in  $T_m$  and enthalpy of fusion in Ho-loaded films was more extensive in comparison with unloaded films, which can probably be explained by secondary irradiation damage due to the radioactive holmium. In the non-irradiated films with 16% Ho (w/w) two other endotherms were observed besides the PLLA melting endotherm: the first endotherm (40°C) is due to the evaporation of the non-coordinating water molecule, and the second endotherm (87°C) is due to evaporation of the two coordinating water molecules [22]. After irradiation the first endotherm at 40°C was absent (Fig. 2 trace C) which can be explained by a rise in temperature up to 50°C (personal communication, NRG, Petten, The Netherlands) during irradiation resulting in evaporation of the non-coordinating water molecule. The second endotherm showed a 50-60% reduction in enthalpy which suggests that one of the coordinated water molecules did evaporate resulting in only one water molecule firmly attached to the Ho-ion, which in turn can explain the increase in  $T_{2\max}$  (Table 1). The loss of this one

coordinated water molecule is most likely caused by irradiation damage and not by heating, since the reactor temperature does not rise above 50°C.

**Table 1.** Transition temperatures of PLLA films with varying HoAcAc loadings (n=4-10)

Irradiation time (h)	Appearance	T <sub>g</sub> (°C)	T <sub>g</sub> c/2 (°C)	T <sub>1</sub> max (°C)	ΔH <sub>1</sub> (J/g)	T <sub>2</sub> max (°C)	ΔH <sub>2</sub> (J/g)	T <sub>m</sub> max PLLA (°C)	*enthalpy (J/g)
0	PLLA film 0% Ho	49±2	66/nd	---	---	---	---	177±0	46±1
0.5	PLLA film 0% Ho	nd	nd	---	---	---	---	154±1	47±2
1	PLLA film 0% Ho	nd	35/35	---	---	---	---	136±2	32±7
0	PLLA film 4% Ho	50±6	nd	nd	nd	nd	nd	168±1	62±6
0.5	PLLA film 4% Ho	nd	55/55	nd	nd	nd	nd	149±1	44±3
1	PLLA film 4% Ho	nd	46/46	nd	nd	127±7	9±12	133±1	28±3
0	PLLA film 16% Ho	nd	nd	40±5	24±2	87±2	84±7	163±1	53±9
0.5	PLLA film 16% Ho	nd	55/57	nd	nd	93±3	35±5	138±3	39±8
1	PLLA film 16% Ho	nd	54/54	nd	nd	97±2	37±3	nd	nd

\*Corrected for HoAcAc loading. nd = not detectable. T<sub>g</sub> c/2= T<sub>g</sub> cooling/ T<sub>g</sub> second heating, Tmax, ΔH: as in Fig. 2.

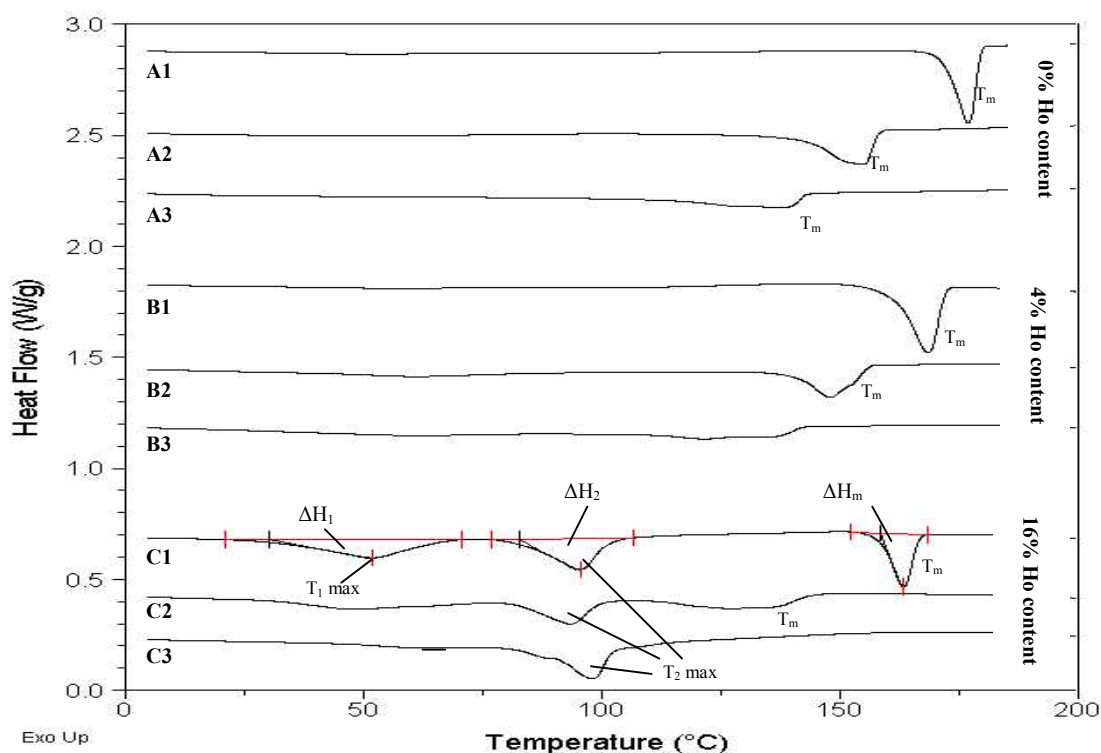


**Fig. 2.** MDSC thermograms of films with 0% (A), 4% (B) and 16% (C) Ho (w/w) loading irradiated for 0 (1), 0.5 (2) and 1h (3) in a nuclear reactor. For example: thermogravimetric signals of HoAcAc and PLLA are both seen in the 16% (w/w) Ho loading marked with  $T_1\text{max}$  and  $T_2\text{max}$ : peak maximum of first and second endotherm,  $\Delta H_1$  and  $\Delta H_2$ : enthalpy of first and second endotherm, the thermogravimetric signals of PLLA:  $T_m$ : melting temperature,  $\Delta H_m$ : enthalpy of melting endotherm.

Representative MDSC scans of empty microspheres irradiated for 0, 0.5 and 1h are shown in Fig. 3 trace A. As observed for PLLA films, irradiated non-loaded microspheres showed a decreased  $T_m$  and enthalpy of fusion with increasing irradiation time (Table 2, Fig. 3). Further, the relaxation peak (at  $58^\circ\text{C}$ ) and recrystallisation exotherm were not observed after irradiation for 0.5h (Fig. 3, compare trace A1 and A2). When the microspheres were irradiated for 1h a strong  $T_g$  ( $34^\circ\text{C}$ ) in the second heating was observed (Fig. 4). As observed for HoAcAc loaded films, microspheres with molecularly dispersed HoAcAc (7 and 17% Ho (w/w)) showed a decreased  $T_m$  and enthalpy of fusion of the PLLA phase with increasing irradiation time (Table 2, Fig. 3 trace B). Irradiation of holmium loaded microspheres for 1h showed no melting endotherm of PLLA indicating a total loss of crystallinity.

**Table 2.** Transition temperatures of PLLA microspheres with varying HoAcAc loadings (n=4-10)

Irradiation time (h)	appearance	T <sub>g</sub> (°C)	T <sub>g</sub> second heating (°C)	T <sub>m</sub> max PLLA (°C)	*enthalpy (J/g)
0	Microspheres without Ho	58±2	66±1	176±0	57±4
0.5	Microspheres without Ho	51±1	46±0	151±1	40±1
1	Microspheres without Ho	nd	34±2	133±0	30±1
0	Microspheres with Ho 7%	56±3	nd	163±0	41±7
0.5	Microspheres with Ho 7%	52±2	60±1	147±4	3±2
1	Microspheres with Ho 7%	nd	60±3	nd	nd
0	Microspheres with Ho 17%	59±2	nd	159±1	25±12
0.5	Microspheres with Ho 17%	57±3	57±2	147±2	4±2
1	Microspheres with Ho 17%	58±4	62±2	nd	nd

\*Corrected for HoAcAc loading. nd = not detectable. T<sub>g</sub>, T<sub>m</sub>max, ΔH: as in Fig. 3.

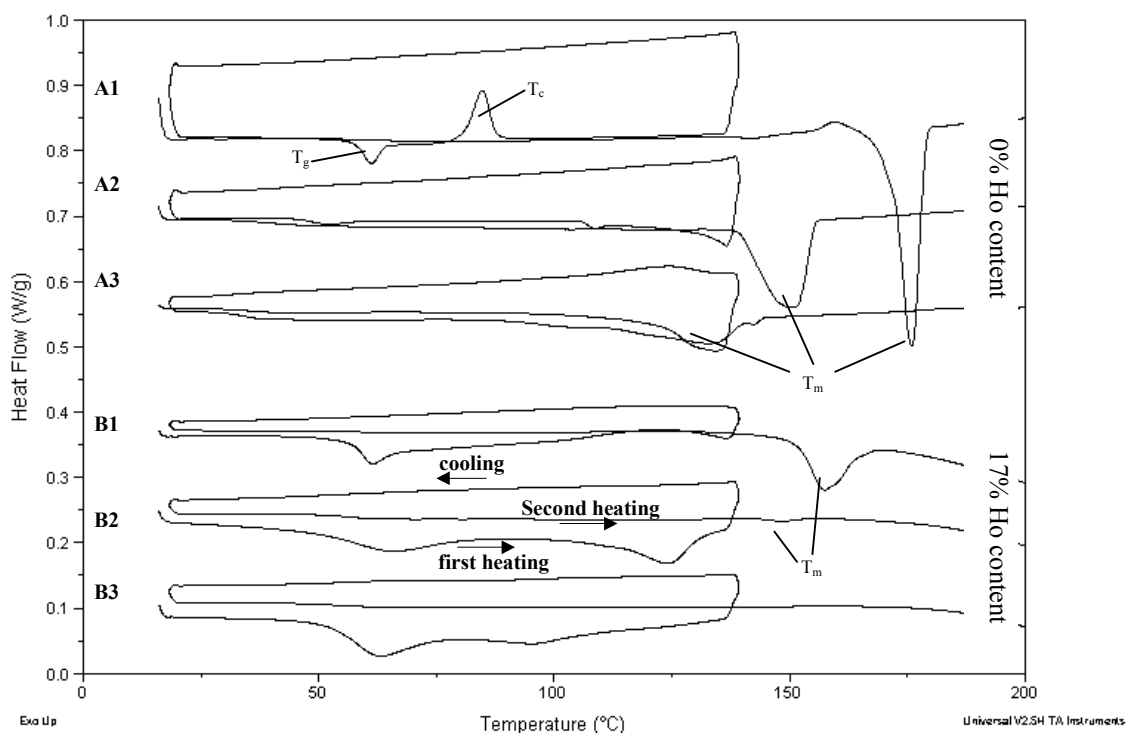


**Fig. 3.** MDSC thermograms of microspheres without (A) and with (B) 17% Ho (w/w) irradiated for 0 (1), 0.5 (2) and 1h (3). Given is the heat flow for first heating, cooling and second heating.  $T_g$  is glass transition temperature,  $T_c$  is recrystallisation temperature and  $T_m$  is melting temperature.

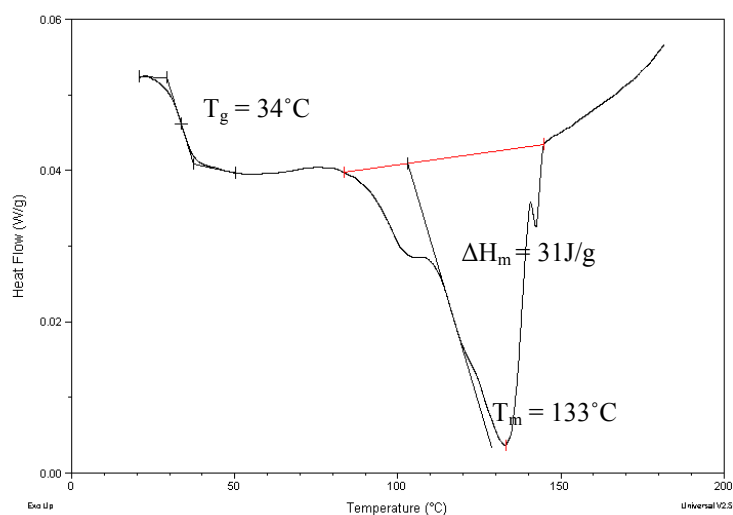


**Fig. 4.** Enlargement of the MDSC thermogram of microspheres without holmium (irradiation 1h). Given is the heat flow for second heating.  $T_g$  is glass transition temperature,  $T_m$  is melting temperature,  $\Delta H_m$  is enthalpy of melting endotherm. Clearly visible is the broad peak (80-145°C) existing of several peaks, indicating a collection of polymer chains with their own melting temperatures.

### 5.3.3 Infrared spectroscopy

With increasing irradiation time of PLLA and holmium loaded PLLA microspheres and films the intensity of a broad peak (range 3000-3600  $\text{cm}^{-1}$ , corresponding to stretching vibrations of COOH end groups of PLLA chains) in the IR spectrum



increased and can be explained by radiation induced chain scission [26]. Tables 3A and B summarise the observed frequencies of the C=O and C=C bands of AcAc in different forms (non-complexed and complexed with Ho, and in PLLA matrices) before and after neutron irradiation for 1h. Stretching vibrations of the C=O and C=C bands of acetylacetonate in HoAcAc were observed at 1610 and 1517  $\text{cm}^{-1}$ , respectively [22,27,28]. Remarkable was the additional peak observed around 1622/3  $\text{cm}^{-1}$  of the C=O stretching vibration of acetylacetonate in PLLA films (4% loading) and microspheres (17% Ho loading) [22]. Likely, some of the carbonyl groups of acetylacetonate do not interact with the  $\text{Ho}^{3+}$  ion leaving the remaining positive charge available for interaction with carbonyl oxygens present in PLLA [22]. After irradiation of HoAcAc loaded films and microspheres the 1622/3  $\text{cm}^{-1}$  due to the C=O stretching vibration band was absent. The C=O band around 1600 and C=C stretching band (around 1520  $\text{cm}^{-1}$ ) showed a shift to lower wave number and a decrease in intensity with increasing irradiation time. In contrast to non-irradiated Ho-loaded PLLA matrices, in which two C=O bands were observed (1600/1 and 1620/1, Table 3B) after dissolution, irradiated Ho-containing films and microspheres showed only one C=O band at 1601/2  $\text{cm}^{-1}$ . Moreover, the C=C stretching vibration observed in irradiated films and microspheres after dissolution decreased in intensity (Table 3B). The IR data indicate that some radiation induced structural changes of the acetylacetonate anion had occurred.

**Table 3A.** Summary of solid state infrared data in the C=O and C=C region of AcAc of non irradiated and irradiated (1h) samples.

Irradiation time (h)	appearance	$\nu_{(\text{C}=\text{O})}$ ( $\text{cm}^{-1}$ )	$\nu_{(\text{C}=\text{C})}$ ( $\text{cm}^{-1}$ )
0	PLLA film 4% Ho	1622, 1606 db	1525
1	PLLA film 4% Ho	1603 b	1521*
0	PLLA film 16% Ho	1610	1522
1	PLLA film 16% Ho	1605b	1520*
0	Microspheres with Ho 17%	1623, 1610 db	1525
1	Microspheres with Ho 17%	1597	1523*
0	Acetylacetonate	1620	1537
0	HoAcAc	1610	1517

$\nu_{(\text{C}=\text{O})}$ ,  $\nu_{(\text{C}=\text{C})}$ : stretching vibrations, db = double band, b = broad band, \*lower intensity than non-irradiated sample

**Table 3B.** Summary of infrared data of samples dissolved in deuterated chloroform in the C=O and C=C region of AcAc of non-irradiated and irradiated (1h) samples.

Irradiation time (h)	appearance	$\nu_{(C=O)}$ ( $\text{cm}^{-1}$ )	$\nu_{(C=C)}$ ( $\text{cm}^{-1}$ )
0	PLLA film 4% Ho	1620, 1601db	1522
1	PLLA film 4% Ho	1602	nd
0	PLLA film 16% Ho	1621, 1600db	1522
1	PLLA film 16% Ho	1601	1520*
0	Microspheres with Ho 17%	1620, 1601db	1522
1	Microspheres with Ho 17%	1601	1522*
0	Acetylacetonate	1620	1537
0	HoAcAc	1621, 1603db	1523

$\nu_{(C=O)}$ ,  $\nu_{(C=C)}$ : stretching vibrations, db = double band, \*lower intensity as non-irradiated sample, nd = not detectable

#### 5.3.4 X-ray diffraction studies

X-ray diffraction analysis has been performed on non-irradiated PLLA-films with and without HoAcAc [22]. X-ray analysis of irradiated (1h) PLLA films without Ho and 4% Ho loading showed only a small change in diffraction pattern indicating a preserved crystallinity of the PLLA matrix (Fig. 5). This is in agreement with the MDSC analysis (Table 1, Fig. 2). X-ray analysis also showed that HoAcAc complex was strongly affected by neutron irradiation. The broad peak (Fig. 5) in films with 4 % Ho (w/w) loading assigned to amorphous Ho-Ho interactions has disappeared, indicating an increased disorder of Ho-Ho distances. After irradiation (1h) of the 16% Ho-loaded (w/w) film the initially low crystallinity of PLLA was not detected anymore. The amorphous HoAcAc component showed the same transformation as was observed for films with 4% Ho (w/w). The crystalline form had changed after irradiation in another unknown form. The diffraction pattern of crystalline HoAcAc in the PLLA matrix changed after irradiation (Fig. 5). Now, a pattern was detected which resembles the pattern of HoAcAc heated at 80°C. It was shown that upon heating 2 to 3 of the (non-)coordinated water molecules were lost. Therefore, it is concluded, and also evidenced by MDSC (Fig. 2), that similar conversions occur by neutron irradiation in crystalline HoAcAc within the PLLA matrix.

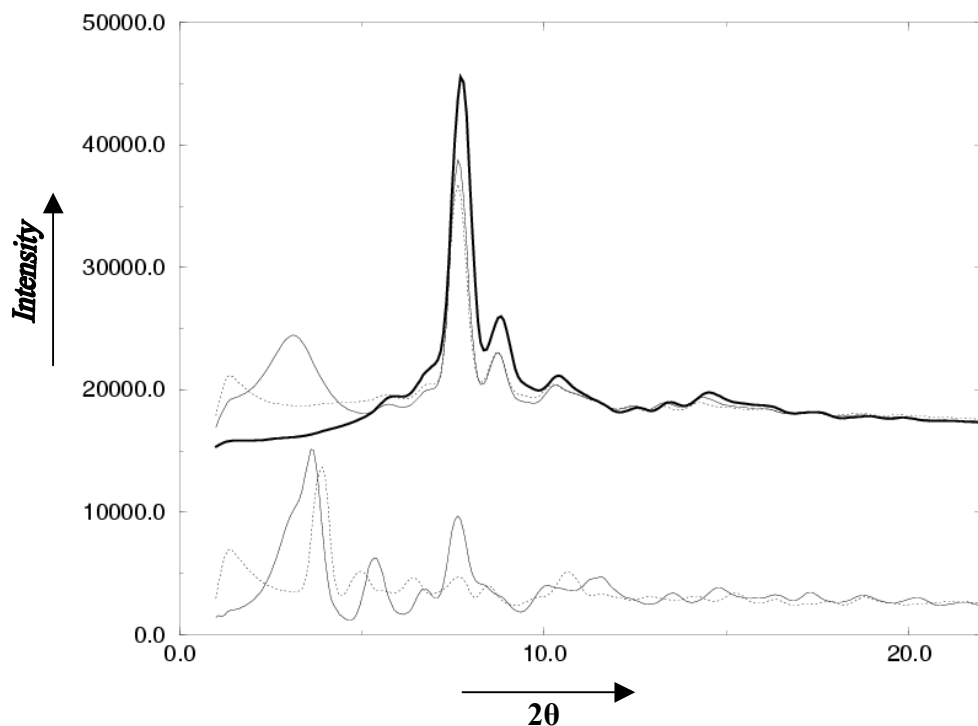


**Fig. 5.** X-ray scattered intensity as a function of the diffraction angle  $2\theta$ . Scaling is arbitrarily applied to the curves so as to match the intensities at  $2\theta$  of  $22^\circ$ . The upper three curves are shifted upwards by 15000 units. Lower curves: films of PLLA loaded with 16% HoAcAc (thin line) and loaded with 16% HoAcAc and irradiated (thin dotted line). Upper curves: film of PLLA (thick line), film of PLLA loaded with 4% Ho (thin line) and film of PLLA loaded with 4% Ho and subsequently irradiated (thin dotted line).

### 5.3.5 Molecular weight determinations

Table 4 summarizes the  $M_w$  and  $M_n$  of PLLA in non-irradiated and irradiated (1h) films and microspheres. As reported for gamma irradiation of PLLA [19,26,29,30,31,32] neutron irradiation of films and microspheres resulted in a substantial decrease of the molecular weights. This indicates that chain scissions are predominant over cross-linking when PLLA is irradiated with neutrons. In line herewith, no gel fraction was found after dissolution of the irradiated PLLA films with or without holmium in  $\text{CHCl}_3$ . Radiation induced chain scission of the polymers can occur by two mechanisms, namely via unzipping [19,33], and by random chain cleavage of the polymer chain. Since the polydispersity ( $M_w/M_n$ ) was hardly affected after irradiation (1h) this indicates that chain scission occurs randomly [19,34].

**Table 4.** GPC data of films and microspheres with varying HoAcAc loadings

Irradiation time (h)	appearance	M <sub>w</sub> (g/mol)	M <sub>n</sub> (g/mol)	poly dispersity
0	PLLA film 0% Ho	93,000	45,000	2.1
1	PLLA film 0% Ho	6,500	2,700	2.4
0	PLLA film 4% Ho	*50,000	25,000	2.0
1	PLLA film 4% Ho	9,200	4,300	2.1
0	PLLA film 16% Ho	*45,000	*24,000	1.9
1	PLLA film 16% Ho	6,000	2,100	2.9
0	microspheres 0% Ho	94,000	*44,000	2.1
1	microspheres 0% Ho	5,200	2,400	2.2
0	microspheres 17% Ho	*21,000	*10,000	2.1
1	microspheres 17% Ho	3,400	1,500	2.3

\*Apparent decrease in M<sub>w</sub> and M<sub>n</sub> is probably caused due to interactions of PLLA and HoAcAc

#### 5.4 Conclusions

This study shows that neutron irradiation of PLLA results in similar processes as found for gamma-irradiation, namely a decrease in molecular weight and loss in crystallinity. When the PLLA matrices were loaded with HoAcAc, besides damage to the PLLA also some damage of the HoAcAc complex occurs. This paper demonstrates that although some radiation induced damage of both the PLLA matrix and the loaded HoAcAc-complex occurs, the microspheres retain their favourable properties (no/marginal release of Ho, preservation of the microsphere size) which makes these systems interesting candidates for the treatment of tumours by radio-embolization.

#### Acknowledgements

The authors wish to thank D.W. Rook, from the Department of Nuclear Medicine, University Medical Center, Utrecht, The Netherlands for preparation of the microspheres, T. Uitslag from Purac Biochem BV (Gorinchem, The Netherlands) for his support in GPC analysis and W.A.M. van Maurik from EMSA, Faculty of Biology, Utrecht University, Utrecht, The Netherlands for SEM acquisition. The authors also wish to thank P. Snip and J. Woittiez of the nuclear reactor, NRG, Petten, The Netherlands for sample irradiations. Financial support was provided by NRG and Mallinckrodt Medical BV, Petten, The Netherlands.

**References**

1. Mumper RJ and Jay M. Poly(L-lactic acid) microspheres containing neutron-activatable holmium-165: A study of the physical characteristics of microspheres before and after irradiation in a nuclear reactor. *Pharmacol. Res.* **1992**;9:149-154.
2. Nijssen JFW, Zonnenberg BA, Woittiez JRW, Rook DW, Swildens-van Woudenberg IA, van Rijk PP and van het Schip AD. Holmium-166 poly lactic acid microspheres applicable for intra-arterial radionuclide therapy of hepatic malignancies: effects of preparation and neutron activation techniques. *Eur. J. Nucl. Med.* **1999**;26:699-704.
3. Häfeli UO, Sweeney SM, Beresford BA, Sim EH and Macklis RM. Magnetically directed poly(lactic acid) <sup>90</sup>Y-microspheres: Novel agents for targeted intracavitary radiotherapy. *J. Biomed. Res.* **1994**;28:901-908.
4. Häfeli UO, Sweeney SM, Beresford BA, Humm JL and Macklis RM. Effective targeting of magnetic radioactive <sup>90</sup>Y-microspheres to tumor cells by an externally applied magnetic field. Preliminary in vitro and in vivo results. *Nucl. Med. Biol.* **1995**;22:147-155.
5. Häfeli UO, Casillas S, Dietz DW, Pauer GJ, Rybicki LA, Conzone SD and Day DE. Hepatic tumor radioembolization in a rat model using radioactive rhenium (<sup>186</sup>Re/<sup>188</sup>Re) glass microspheres. *Int. J. Radiation Oncology Biol. Phys.* **1999**;44:189-199.
6. Ehrhardt GJ and Day DE. Therapeutic use of <sup>90</sup>Y microspheres. *Nucl. Med. Biol.* **1987**;14:233-242.
7. Cady B. Natural history of primary and secondary tumours of the liver. *Seminars in Oncology* **1983**;10:127-135.
8. Stribley KV, Gray BN, Chmiel RL, Heggie JCP and Bennett RC. Internal radiotherapy for hepatic metastases I: The homogeneity of hepatic arterial blood flow. *J. Surg. Res.* **1983**;34:17-24.
9. Gray BN, Burton MA, Kelleher D, Klemp P and Matz L. Tolerance of the liver to the effects of yttrium-90 radiation. *Int. J. Radiation Oncology Biol. Phys.* **1990**;18:619-623.
10. Andrews JC, Walker SC, Ackermann RJ, Cotton LA, Ensminger WD and Shapiro B. Hepatic radioembolization with yttrium-90 containing glass microspheres. Preliminary results and clinical follow-up. *Eur. J. Nucl. Med.* **1994**;35:1637-1644.
11. Lau WY, Ho S, Leung TWT, Chan M, Ho R, Johnson PJ and Li AKC. Selective internal radiation therapy for nonresectable hepatocellular carcinoma with intraarterial infusion of <sup>90</sup>yttrium microspheres. *Int. J. Radiation Oncology Biol. Phys.* **1998**;40:583-592.
12. Herba MJ, Illescas FF, Thirlwell MP, Boos GJ, Rosenthal L, Atri M and Bret PM. Hepatic malignancies: improved treatment with intraarterial Y-90. *Radiology* **1988**;169:311-314.

13. Tian J-H, Xu B-X, Zhang J-M, Dong B-W, Liang P and Wang X-D. Ultrasound-guided internal radiotherapy using yttrium-90-glass microspheres for liver malignancies. *J. Nucl. Med.* **1996**;37:958-963.
14. Ho S, Lau WY, Leung TWT and Johnson P.J. Internal radiation therapy for patients with primary or metastatic hepatic cancer. *Am. Cancer Soc.* **1988**;83:1894-1907.
15. Raaijmakers CPJ, Konijnenberg MW and Mijnheer BJ. Clinical dosimetry of an epithermal neutron beam for neutron capture therapy: dose distributions under reference conditions. *Int. J. Radiation Oncology Biol. Phys.* **1997**;37:941-951.
16. Kegel GHR and DeSimone D. Facilities for gamma and neutron irradiations. *Nucl. Instr. Meth. Physics. Res. A* **1999**;426:61-67.
17. Esselbrugge H, Grootoink J and Feijen J.  $\gamma$ -irradiation of poly(L-lactide) hollow fibers. Thesis, University of Twente, The Netherlands: *Biodegradable hollow fibres for controlled drug delivery.* **1992**;Appendix A:245-258.
18. Montanari L, Costantini M, Signoretti EC, Valvo L, Santucci M, Bartolomei M, Fattibene P, Onori S, Faucitano A, Conti B and Genta I. Gamma irradiation effects on poly(DL-lactide-co-glycolide) microspheres. *J. Control. Release* **1998**;56:219-229.
19. Sintzel MB, Merkli A, Tabatabay C and Gurny R. Influence of irradiation sterilization on polymers used as drug carriers-A review. *Drug Develop. Ind. Pharm.* **1997**;23:857-878.
20. Athanasiou A K, Niederauer GG and Agrawal CM. Sterilization, toxicity, biocompatibility and clinical applications of polylactic acid/polyglycolic acid copolymers. *Biomaterials* **1996**;17:93-102.
21. Kooijman H, Nijsen JFW, Spek AL, and van het Schip AD. Diaquatrakis(pentane-2,4-dionato-O,O') holmium(III) monohydrate and diaquatrakis(pentane-2,4-dionato-O,O') holmium(III) 4-hydroxypentan-2-one solvate dihydrate. *Acta Cryst.* **2000**;C56:156-158.
22. Nijsen JFW, van Steenberg MJ, Kooijman H, Talsma H, Kroon-Batenburg LMJ, van de Weert M, van Rijk PP, de Witte A, van het Schip AD and Hennink WE. Characterization of poly(L-lactic acid) microspheres loaded with holmium acetylacetonate. *Biomaterials* **in press**.
23. Meade VM, Burton MA, Gray BN and Self GW. Distribution of different sized microspheres in experimental hepatic tumours. *Eur. J. Clin. Oncol.* **1987**;23:37-41.
24. Bastian P, Bartkowski R, Köhler H and Kissel T. Chemo-embolization of experimental liver metastases. Part I: distribution of biodegradable microspheres of different sizes in an animal model for the locoregional therapy. *Eur. J. Pharm. Biopharm.* **1998**;46:243-254.
25. Campbell A.M, Bailey IH and Burton MA. Analysis of the distribution of intra-arterial microspheres in human liver following hepatic yttrium-90 microsphere therapy. *Phys. Med. Biol.* **2000**;45:1023-1033.

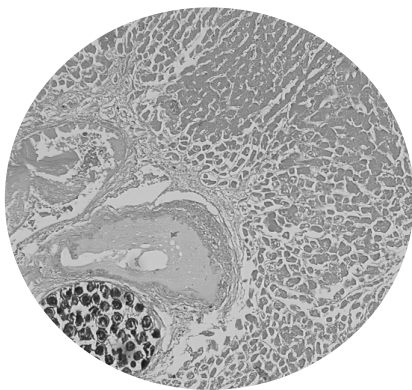
26. Merkli A, Heller J, Tabatabay C and Gurny R. Gamma sterilization of a semi-solid poly(ortho ester) designed for controlled drug delivery-validation and radiation effects. *Pharm. Res.* **1994**;11:1485-1491.
27. Irikura KK. Acetylacetonate (acac) anion in the gas phase: predicted structures, vibrational spectra, and photodetachment energies. *Int. J. Mass Spectrom.* **1999**;185:577-587.
28. Nakamoto K, McCarthy PJ, Ruby A and Martell AE. Infrared spectra of metal chelate compounds. II. Infrared spectra of acetylacetonates of trivalent metals. *J. Am. Chem. Soc.* **1961**;83:1066-1069.
29. Collet JH, Lim LY and Gould PL. Gamma-irradiation of biodegradable polyesters in controlled physical environments. *Polymer Reprints* **1989**;30:468-469.
30. Henn GG, Birkinshaw C, Buggy M and Jones E. A comparison of the effects of  $\gamma$ -irradiation and ethylene oxide sterilization on the properties of compression moulded poly-d,l-lactide. *J. Mat. Sciences; Mat. in Med.* **1996**;7:591-595.
31. Rothen-Weinhold A, Besseghir K and Gurny R. Analysis of the influence of polymer characteristics and core loading on the in vivo release of a somatostin analogue. *Eur. J. Pharm. Sciences* **1997**;5:303-313.
32. Yoshioka S, Aso Y and Kojima S. Drug release from poly (*dl*-lactide) microspheres controlled by  $\gamma$ -irradiation. *J. Control. Release* **1995**;37:263-267.
33. Gilding DK and Reed AM. Biodegradable polymers for use in surgery-polyglycolic/poly(lactic acid) homo- and copolymers. *Polymer* **1979**;20:1459-1464.
34. Volland C, Wolff M and Kissel T. The influence of terminal gamma-sterilization on captopril containing poly (D,L-lactide-co-glycolide) microspheres. *J. Control. Release* **1994**;31:293-305.

## Chapter 6

---

# Targeting of liver tumour in rats by selective delivery of holmium-166 loaded microspheres: a biodistribution study

*in press (European Journal of Nuclear Medicine)*



**J.F.W. Nijsen<sup>1</sup>, D.W. Rook<sup>1</sup>, C.J.W.M. Brandt<sup>2</sup>, R. Meijer<sup>3</sup>,  
H.F.J. Dullens<sup>4</sup>, B.A. Zonnenberg<sup>1</sup>, J.M.H. de Klerk<sup>1</sup>, P.P. van  
Rijk<sup>1</sup>, W.E. Hennink<sup>5</sup> and A.D. van het Schip<sup>1</sup>**

<sup>1</sup>*Department of Nuclear Medicine, University Medical Center, Utrecht, The Netherlands*

<sup>2</sup>*Central Laboratory Animal Institute, University of Utrecht, Utrecht, The Netherlands*

<sup>3</sup>*Department of Radiology, University Medical Center, Utrecht, The Netherlands*

<sup>4</sup>*Department of Pathology, University Medical Center, Utrecht, The Netherlands*

<sup>5</sup>*Department of Pharmaceutics, Utrecht Institute for Pharmaceutical Sciences,  
Utrecht University, Utrecht, The Netherlands*



### **Abstract**

Intra-arterial administration of beta-emitting particles that become trapped in the vascular bed of a tumour and remain there while delivering high doses, comprises a unique application in the treatment of both primary and metastatic liver tumours. Studies on selective internal radiation therapy of colorectal liver metastases using yttrium-90 glass microspheres have shown encouraging results. This study describes the biodistribution of 37  $\mu\text{m}$  poly lactic acid microspheres loaded with radioactive holmium-166, after intra-arterial administration into the hepatic artery of rats with implanted liver tumours. Radioactivity measurements showed >95% retention of injected activity in the liver and its resident tumour. The average activity detected in other tissues was  $\leq 0.1$  %ID/g, with incidental exceptions in lungs and stomach. Very little  $^{166}\text{Ho}$  activity was detected in kidneys ( $< 0.1$  %ID/g), thereby indicating the stability of the microspheres in vivo. Tumour targeting was very effective, with a mean tumour to liver ratio of  $6.1 \pm 2.9$  for rats with tumour ( $n=15$ ), versus  $0.7 \pm 0.5$  for control rats ( $n=6$ ;  $p < 0.001$ ). These ratios were not significantly affected by the use of adrenaline. Histological analysis showed that 5 times as many large ( $>10$ ) and medium-sized (4-9) clusters of microspheres were present within tumour and peritumoural tissue, compared with normal liver. Single microspheres were equally dispersed throughout the tumour, as well as normal liver parenchyma.

## 6.1 Introduction

The liver is one of the most common sites of metastatic cancer in human beings, especially for metastases of colon and rectum carcinoma. Despite the advances in radiotherapy, chemotherapy and immunotherapy, surgical excision of localised disease is currently the only means of improving the survival in these patients [1]. However, surgical resection of liver metastases of colorectal carcinomas is possible in only 10-30% of all cases [2,3]. There is therefore a great need for the development of an effective therapy. A promising alternative is intra-arterial radionuclide therapy. This depends upon the arterial blood supply to the liver metastases, and the subsequent infusion of the metastases with well-defined sized [4,5], radioactive microspheres.

Tumours from 1-2 mm acquire their oxygen and nutrients by diffusion and transportation, thereafter the growth of the tumour depends mainly on angiogenesis [6]. Newly formed vessels behave differently from the surrounding, well-established vascular structures of the host tissue [7]. Tumour vessels are morphologically irregular and have larger lumen. As the liver tumour grows, the new vessels derive their blood (mainly) from the hepatic artery [8]. Administration of radioactive microspheres therefore takes place via this artery. Administration of a vasoconstrictor results in the constriction of vessels of the normal liver, while tumour vessels may not or may only partially react to vasoconstrictors [9,10]. This results in an enhancement of the blood flow to the tumour, since the increased resistance of the liver's vascularization enhances the blood flow to the open vascularization of the tumour vessels. The radiation dose may consequently be maximised to the tumour and minimised to the normal liver [9-11].

Encouraging results were obtained with yttrium-90 ( $^{90}\text{Y}$ ) glass and resin microspheres [11-13]. The use of neutron activated holmium-166 ( $^{166}\text{Ho}$ ) for this type of therapy is particularly suitable because of its favourable radiation characteristics ( $E_{\text{max}}=1.84$  MeV,  $E_{\gamma}=81$  keV,  $t_{1/2}=26.8\text{h}$ ) and the 100% natural abundance of  $^{165}\text{Ho}$ . This led us to produce therapeutic amounts of  $^{166}\text{Ho}$  loaded poly lactic acid microspheres of uniform size and high chemical stability in vitro illustrated by the fact that more than 99.3% of  $^{166}\text{Ho}$  activity was retained in the microspheres after 192-h (>7 half-lives) incubation in PBS, plasma and leucocytes suspended in PBS [14].

The purpose of this study was to investigate the biodistribution of  $^{166}\text{Ho}$  loaded poly lactic acid microspheres of 20-50  $\mu\text{m}$  (average diameter 37  $\mu\text{m}$ ) under influence of the vasoconstrictor adrenaline in a tumourous rat model. Biodistribution was examined by scintigraphic imaging and radioactivity measurements of rat livers, with and without tumour, and of other organs. Microscopic distribution of the microspheres was investigated after histological staining of dissected liver and tumour tissue, and this corroborated the radioactivity data.

## 6.2 Materials and methods

### 6.2.1 Animals

All experiments were performed in agreement with The Netherlands Experiments on Animals Act (1977) and the European Convention for the Protection of Vertebrate Animals used for Experimental Purposes (1986). Approval was obtained from the University Animal Experiments Committee (FDC/DEC-GNK nr. 70044). The experiments were performed using 21 male pathogen-free, inbred WAG/Rij rats (WAG/Rij CrI BR; Charles River, Someren, The Netherlands) weighing 225-360 g. The rats were housed in Macrolon cages with sawdust provided as bedding, 2 or 3 animals/cage. A standard pelleted rat maintenance diet (RMH-TM, Hope Farms, Woerden, The Netherlands) and water were provided *ad libitum*.

### 6.2.2 Tumour cells

The medullary thyroid cell line was derived from the Department of Internal Medicine (University Medical Center, Utrecht, The Netherlands). The original tumour cells were obtained from a spontaneous medullary thyroid carcinoma of an aging WAG/Rij-rat. The medullary thyroid cell line was propagated by subcutaneous passage of the back of the rat. To facilitate implantation the donor rat was killed and the tumour tissue was dissected. Small parts of firm tumour tissue were chosen for implantation.

### 6.2.3 Tumour implantation

The rats were anaesthetised with an intraperitoneal injection of Hypnorm<sup>®</sup> (0.1 ml/100 g, Janssen Pharmaceutical Beerse, Belgium) and intramuscular injection of Dormicum<sup>®</sup> (0.05 ml/100 g, Roche Nederland B.V. Mijdrecht, The Netherlands). A laparotomy was performed by ventral mid-line incision in order to expose the lobes of the liver. In fifteen rats an incision was made in the cranial brim of the *lobus sinister lateralis* and 0.5-1 mm<sup>3</sup> tumour-tissue was implanted, together with a piece of titanium to serve as localisation marker for ultrasound. Control rats (n=6) were sham implanted by the injection of 0.5 ml saline. After approximately 20 days an ultrasound investigation (HDI 3000 ATL, Entos<sup>™</sup> CL10-5 transducer) was performed to check tumour growth.

#### 6.2.4 Preparation of microspheres

Radioactive microspheres (Fig. 1) were prepared as previously described [14]. Briefly, holmiumacetylacetonate is incorporated into poly lactic acid by solvent evaporation, resulting in microspheres of 20-50  $\mu\text{m}$  after sieving (mean 37  $\mu\text{m}$ ). Neutron activation of the holmium loaded microspheres was performed by irradiation in the high-flux nuclear reactor in Petten, The Netherlands. A neutron flux was used of  $5 \times 10^{13} \text{ cm}^{-2} \cdot \text{s}^{-1}$  (PRS-facility) for 1h. Neutron activated microspheres (80 MBq in 25 mg) were suspended in 0.5 ml Gelofusine<sup>®</sup> (Vifor Medical SA, Switzerland) prior to administration.

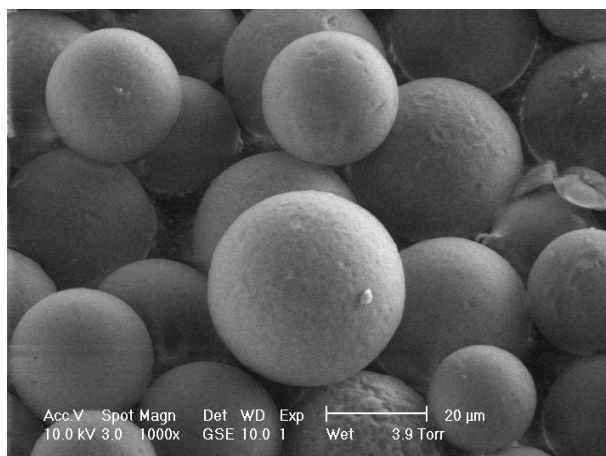


**Fig. 1.** Scanning electron micrograph of  $^{166}\text{Ho}$  microspheres demonstrating their spherical shape. Average diameter is 37  $\mu\text{m}$  (magnification 1000x).

#### 6.2.5 Administration of radioactive microspheres

When the tumour had reached a diameter of  $\geq 5$  mm, a second laparotomy was performed in order to administer the  $^{166}\text{Ho}$  microspheres. The hepatic artery and the gastroduodenal branch were identified and isolated at the three-way junction (Fig. 2). The gastroduodenal artery and the coeliac artery to the aorta were ligated with two wires (a1 and a2) and one wire (b), respectively. The gastroduodenal artery was cannulated with a 27G needle with a blunt tip (Anterior Chamber Cannula 5006; Visitec, USA). The wires a1 and b were tightened, obstructing the backflow of blood to the gastroduodenal artery and the blood flow from the aorta. The needle was moved up into the artery so that its tip layed just in the hepatic artery. In order to check the flow to the liver, Gelofusine<sup>®</sup> (Vifor Medical SA, Switzerland) was administered through the pre-flushed administration system. If backflow occurred, wire a2 (over the needle) was tightened. The suspended radioactive microspheres were administered with or without a bolus of 0.3 ml adrenaline (1mg/ml, Kombivet V.P. Etten- Leur, The Netherlands) and the syringe with needle was measured for activity pre- and post-injection, in order to calculate the injected dose exactly. The sling around the coeliac artery was removed and the hepatic arterial circulation was restored.

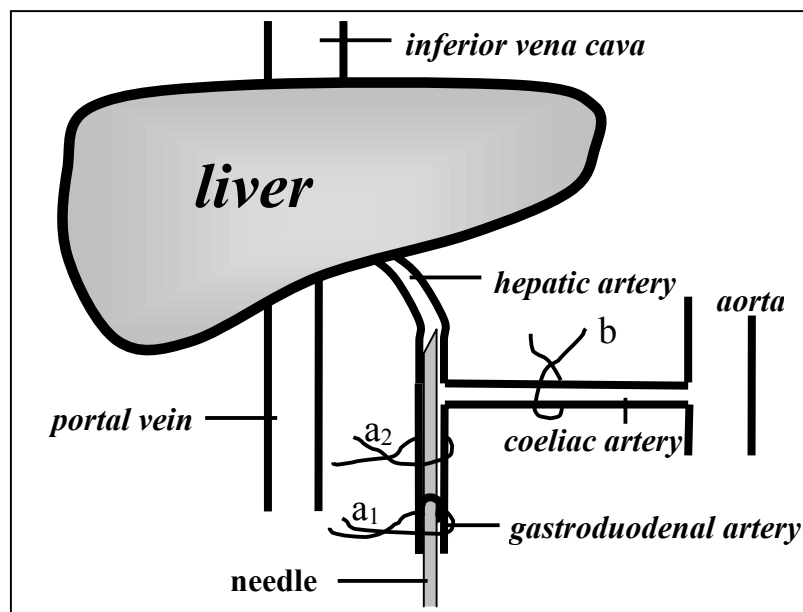


**Fig. 2.** Scheme of the administration technique. The gastroduodenal artery was cannulated with a needle with blunt tip and moved up into the hepatic artery. During administration wires a<sub>1</sub> and b were ligated.

#### 6.2.6 Biodistribution studies

The rats were monitored by planar imaging, using a gamma camera (Elscont, Apex 609, Elscint Ltd., Israel) with pinhole collimator. A whole body scintigram was made 30 min and one day after administration, in order to determine gross distribution and redistribution of radioactive microspheres. The rats were subsequently killed and the activity in liver, tumour, heart, lungs, intestine, stomach, spleen, kidneys and the rest of the rat was determined in a low background  $\gamma$ -counter. The results were expressed as a percentage of injected dose/gram of tissue (%ID/g). Tumour and 2 mm of its surrounding liver tissue was dissected to determine radioactivity, and defined as the target tissue. The target to non-target ratio (T/N ratio) was calculated as the ratio between activity per gram tumour target tissue, or tissue of the sham implantation site in the control group, and activity per gram liver tissue.

Autoradiography of tissue samples was carried out using PhosphorImager exposure cassettes (Molecular Dynamics GmbH, Krefeld, Germany). In order to investigate the microscopic distribution of the microspheres, organs were fixed in phosphate-buffered 4% formaldehyde. The liver lobe with tumour (*lobus sinister lateralis*) was embedded in paraffin wax, sectioned in 6  $\mu$ m coupes, taken every 60  $\mu$ m transversal on the embedded tissue, and stained with haematoxylin-eosin. Spheres were counted in tumour tissue, peripheral tumour tissue and liver parenchyma.

#### 6.2.7 Statistical analysis

Variables were expressed as mean $\pm$ SD. Study groups were compared with the unpaired Student's *t* test in the case of independent samples. The non-parametric Mann-Whitney test for two-group comparisons was used when indicated. Paired samples were analysed using the paired *t* test, or the Wilcoxon matched-pairs test

when indicated. A *P* value of less than 0.05 was considered to be indicative of a significant difference.

### 6.3 Results

#### 6.3.1 Tumour implantation and administration of $^{166}\text{Ho}$ microspheres

Implantation of the tumour resulted in a 100% "take"-rate. To avoid expulsion of the tumour, a relatively deep incision (2-6 mm) was made in the liver and closed afterwards with tissue glue. After 16-27 days the tumour had grown from 1-2 mm into a well-vascularized tumour of 5-12 mm in diameter, as measured by ultrasound, which gave accurate information about tumour size and form. The tumour appeared as deviations of rounded tissue in a relatively flat liver image. As a result of the recovery from the first laparotomy, the omentum was hypervascularized and merged with the liver and the stitches in the abdomen. All rats survived the operations and were in good physical condition after their last intervention.

The microspheres showed a tendency to adhere to the wall of the syringe during administration. This was overcome by agitation and flushing of the syringe, which enabled the injection of a fixed amount of microspheres to the individual animals.

#### 6.3.2 Biodistribution

On scintigraphic images no radioactivity was visible in tissues other than the tumour and the liver (Fig. 3).

Radioactivity measurements showed that the average %ID/g in organs other than liver (control group) or liver with tumour (experimental group) was very low or negligible (Fig. 4). The %ID/g was highest in the lungs being  $0.4\pm 0.7$  and  $0.3\pm 0.4$  in the experimental and control group, respectively. For the stomach these values were  $0.2\pm 0.1$  in the tumour group and  $0.1\pm 0.1$  in the control group. The %ID/g of other tissues was  $\leq 0.1\%$  in both study groups.

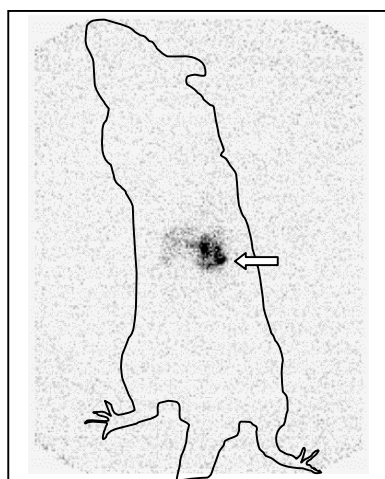


**Fig. 3.** Whole body scintigraphic image of a tumour-bearing rat 1 day after the injection of  $^{166}\text{Ho}$  poly lactic acid microspheres into the hepatic artery. Contour of the rat was merged with the image to show the imaging set-up.

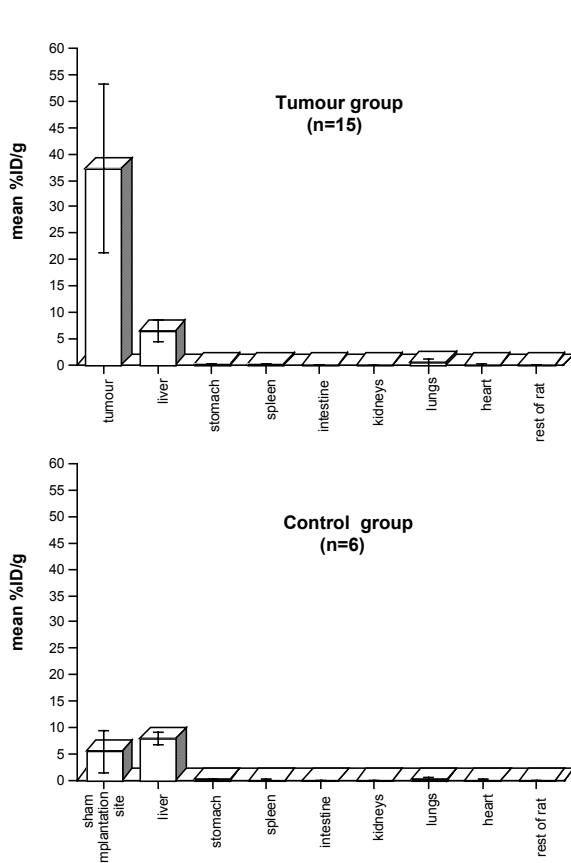


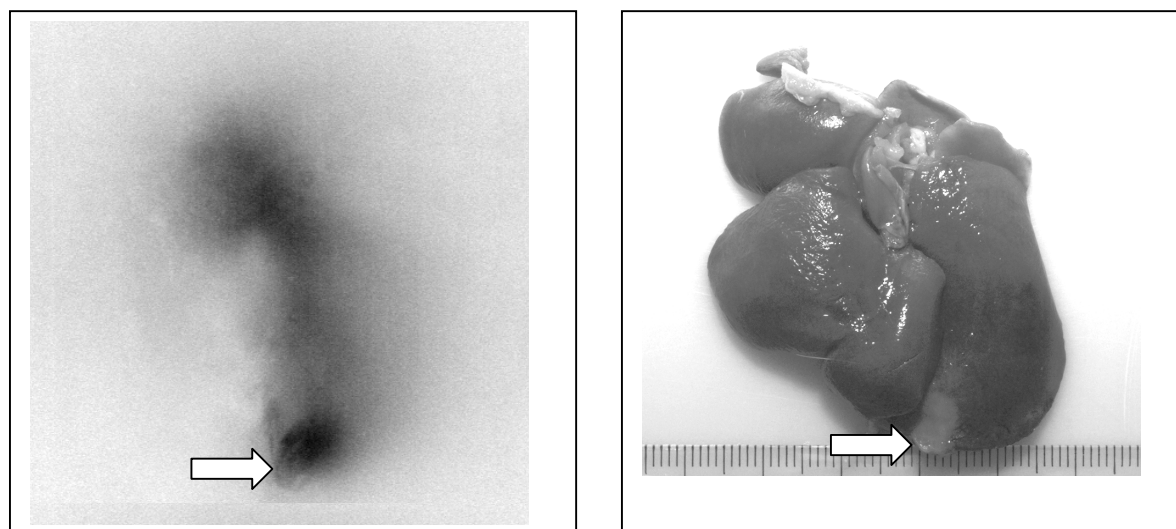
**Fig. 4.** Biodistribution of  $^{166}\text{Ho}$  microspheres in rats with implanted liver tumour (upper panel) and in control rats without tumour (lower panel). Mean uptake values are given in %ID/g  $\pm$  sd.

In Table 1 the tumour to liver ratio's obtained for the different study groups are given. The use of adrenaline during administration did not show a significant effect on the tumour targeting of the microspheres. Overall a mean T/N ratio of  $6.1 \pm 2.9$  for the rats with tumour ( $n=15$ ) versus  $0.7 \pm 0.5$  for the sham-implanted control rats ( $n=6$ ) was found, which proved to be a highly significant difference ( $p < 0.001$ ).

Within the liver itself the distribution of the  $^{166}\text{Ho}$  microspheres appeared to be confined predominantly to the tumour and the liver lobe in which the tumour was implanted, as is clearly illustrated in Fig. 5. As a result the %ID/g in this liver lobe is higher than in the liver as a whole. Consequently, the mean T/N ratio significantly ( $p=0.003$ ) decreased to  $4.0 \pm 1.6$  ( $n=13$ ) if just the liver lobe instead of the whole liver was taken as the non-target region.

**Table 1.** Tumour/liver-ratio's in rats with implanted liver tumour and in sham-implanted rats after administration of  $^{166}\text{Ho}$  loaded microspheres with or without adrenaline

	Tumour		Sham-implanted	
	+ adrenaline (n=9)	- adrenaline (n=6)	+ adrenaline (n=3)	- adrenaline (n=3)
	2.1	5.0	0.1	0.5
	4.5	2.6	0.6	1.5
	5.4	12.8	0.6	0.8
	7.1	7.9		
	2.2	8.1		
	5.9	9.4		
	7.5			
	6.0			
	4.4			
Mean	5.0	7.6	0.4	0.9
SD	1.9	3.5	0.3	0.5

**Fig. 5.** Autoradiogram on phosphor imaging plate of a rat liver with tumour illustrating preferential accumulation in the liver lobe with resident tumour (left panel, white arrow) and photograph of the same liver showing the tumour (right panel, white arrow). Scale bar: 1 mm per division.

Histological analysis showed characteristically small irregular vessels inside the tumour and a plexus of vessels around the tumour. The microspheres appeared to accumulate predominantly in medium-sized (4-9 microspheres) or large (>10 microspheres) clusters within these vascular structures, in and around the tumour (Fig. 6B). In the normal liver parenchyma these clusters virtually were absent and mainly isolated microspheres were observed (Fig. 6A).



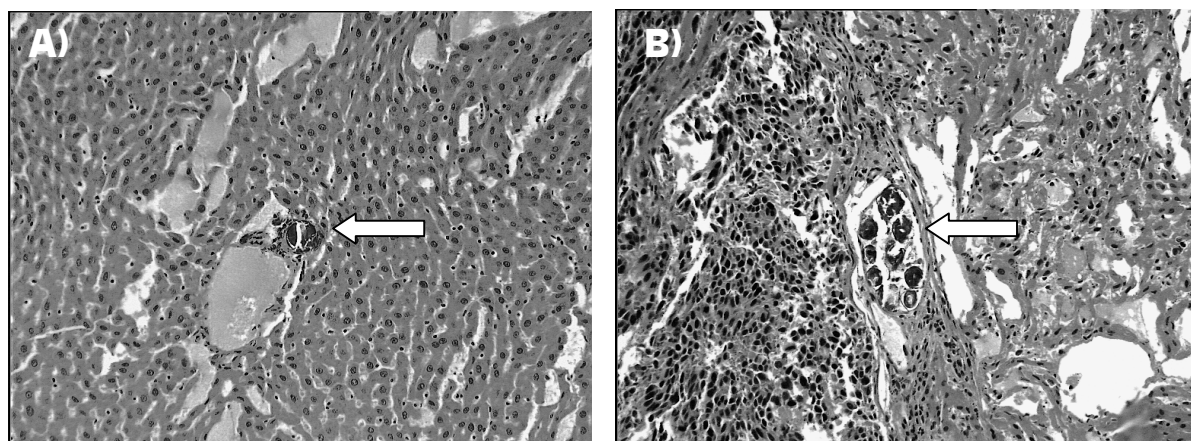


**Fig. 6A-B.** Single  $^{166}\text{Ho}$  microsphere in normal liver parenchyma (A) and cluster of microspheres in tumour tissue (B), HE stained 6  $\mu\text{m}$  coupes. Microscopic magnification: 200x.

#### 6.4 Discussion

The average life expectation of patients following diagnosis of liver metastases is very poor. There are no conventional therapies that can be used to treat these metastases adequately. Because of the tumour and liver biology the administration of radioactive microspheres into the hepatic artery with a vasoconstrictor has been considered as a therapy [11]. As an alternative for the  $^{90}\text{Y}$  glass microspheres, which are currently available for this kind of internal radionuclide therapy, we have recently described a straightforward method for the production of radioactive  $^{166}\text{Ho}$  loaded microspheres of poly lactic acid [14]. These microspheres are advantageous in that they combine biocompatibility and low density with the favourable physical characteristics of  $^{166}\text{Ho}$ , thus enabling image-guided radionuclide therapy. Moreover, production costs would be reduced due to the 100% natural abundance of  $^{165}\text{Ho}$  and its cross-section of 64 barn, which allows for short neutron activation times.

In this study the biodistribution of  $^{166}\text{Ho}$ -PLLA microspheres was investigated, after intra-arterial administration into the hepatic artery of rats with implanted liver tumours.

Whole body images showed that virtually all injected activity (>95%) had accumulated in tumour and liver and that no substantial redistribution or shunting to other tissues had occurred. The average activity detected in other tissues was generally very low ( $\leq 0.1$  %ID/g) with occasional exceptions in lungs and stomach. The maximum activity measured for stomach was 0.8 %ID/g, and observed in two animals, which was probably due to retrograde flow within the hepatic artery resulting in spill over to the stomach. Shunting to the lungs was observed in another two animals, with values of 1.6 and 2.5 %ID/g respectively. In the therapeutic situation possible

arteriovenous shunts should be assessed with a tracer dose prior to the therapy, and during administration care must be taken to prevent backflow to the stomach.

No substantial amounts of activity were detected in kidneys ( $<0.1$  %ID/g), indicating that no release of  $^{166}\text{Ho}$  from the microspheres had occurred. This was confirmed by the absence of activity in urine and faeces.

Within the liver, entrapment of the  $^{166}\text{Ho}$  microspheres occurred predominantly in and around the tumour and was found to be approximately six times that found in the normal liver tissue. The use of adrenaline during administration showed no significant effect on the T/N ratio in this study. Conflicting evidence of the effect of vasoconstrictors on tumour blood flow and its effect on the T/N ratio in rat liver tumours has been published, varying from increase to no effect, or even decrease of the T/N ratio [15]. The interaction of adrenaline with both alpha- (vasoconstriction) and beta-adrenoceptors (vasodilatation) may result in a net effect on tumour blood flow, and hence the T/N ratio being the same in both groups with and without adrenaline [15].

There was a 6-fold variation in tumour to liver ratios ranging from 2.1 to 12.8 (Table 1). This variability is in accordance with results in rabbits with implanted liver tumours, where even substantially larger variations in T/N ratios were reported [15]. Also in patients with hepatic cancer variability in the T/N ratio was observed [16]. These variations may be explained by wide variation in tumour to liver blood flow ratios caused by variation in blood vessel density in and around the tumour between individuals, as reported by Dworkin et al. [17].

As visualized by autoradiography on phosphor imaging plates (Fig. 5) the  $^{166}\text{Ho}$  microspheres were not deposited homogeneously throughout the whole liver, but were restricted mainly to the liver lobe in which the tumour was situated. The activity more or less fades out when further away from the tumour. As a consequence, the T/N ratio decreased significantly from 6.1 to 4.0 when the liver lobe (which comprises about 25% of total liver weight [18]) instead of the whole liver, was regarded as the non-target tissue.

The fading out phenomenon of the microspheres was manifested by their spatial distribution on the microscopic level, and provided direct histological evidence of their embolization specific to tumour. About 5 times as many large ( $>10$  microspheres) and medium-sized (4-9 microspheres) clusters were observed within the tumour and the 0.5 mm layer of peritumoural tissue than in normal liver tissue, whilst individual microspheres were equally dispersed throughout tumour tissue as well as liver parenchyma. This is in agreement with the findings of Pillai et al. in rabbits [19].

In conclusion, this in vivo study has demonstrated the preferential embolization of liver tumours with  $^{166}\text{Ho}$  poly lactic acid microspheres, and their stability with regard to  $^{166}\text{Ho}$  release. The biodistribution of these microspheres which achieve average

concentrations in the tumour of up to 6 times higher than in the liver, and which are close enough to allow for the delivery of tumouricidal radiation doses to the target cells, whilst virtually preserving intact the normal hepatic parenchyma, is similar to that reported for  $^{90}\text{Y}$  carrying particles. Burton et al. [11] measured radioactivity in biopsy samples of tumour nodules and normal hepatic tissue of nine patients with liver metastases after injection of  $^{90}\text{Y}$  containing microspheres and found a mean T/N ratio of 6 (range: 0.4-45). In other studies T/N ratios of  $^{90}\text{Y}$  microspheres were assessed with  $^{99\text{m}}\text{Tc}$  macroaggregated albumin. The mean T/N ratios reported varied between 2.8 (range: 1.0-10.0) for ten hepatocellular carcinoma patients [20] and 4.8 (range: 0.2-26.5) for 377 patients with hepatocellular carcinoma and 4.3 (range: 2.3-7.2) for 25 patients with colorectal liver metastases [16].

The biodegradability of the poly lactic acid microspheres and their low density (1.4 g/ml) add extra value since it allows for repeated injections and diminishes the chance of settling during administration. Combined with the imageable gamma emission and low production costs of  $^{166}\text{Ho}$  these microspheres offer an attractive alternative for  $^{90}\text{Y}$  microspheres and warrant further research in this field.

### **Acknowledgements**

This study was financially supported by the Energy Research Foundation and Mallinckrodt Medical BV, Petten, The Netherlands. The authors would like to thank Drs. G. Voorhout for performing ultrasound studies, and J. Woittiez and P. Snip for their skilled technical assistance with the irradiation of the microspheres. The assistance of M. Gerrits with the rat-scintigraphy studies, and of R. Lange, and S. Zielhuis in preparing the holmium loaded microspheres is gratefully acknowledged. Finally, we are indebted to J.P Hoven and B. Westendorp for their assistance in the histological analysis.

**References**

1. Häfeli UO, Casillas S, Dietz DW, Pauer GJ, Rybicki LA, Conzone SD and Day DE. Hepatic tumor radioembolization in a rat model using radioactive rhenium ( $^{186}\text{Re}/^{188}\text{Re}$ ) glass microspheres. *Int. J. Rad. Oncol. Biol. Phys.* **1999**;44:189-199.
2. Farmer DG and Busuttill RW. The role of multimodal therapy in the treatment of hepatocellular carcinoma. *Cancer* **1994**;73:2669-2670.
3. Scheele J and Altendorf-Hofmann A. Resection of colorectal liver metastases. *Langenbeck's Arch. Surg.* **1999**;384:313-327.
4. Bastian P, Bartkowski R, Köhler H and Kissel T. Chemo-embolization of experimental liver metastases. Part I: distribution of biodegradable microspheres of different sizes in an animal model for the locoregional therapy. *Eur. J. Pharm. Biopharm.* **1998**;46:243-254.
5. Anderson JH, Angerson WJ, Willmott N, Kerr DJ, McArdle CS and Cooke TG. Regional delivery of microspheres to liver metastases: the effects of particle size and concentration on intrahepatic distribution. *Br. J. Cancer* **1991**;64:1031-1034.
6. Folkman J. What is the evidence that tumors are angiogenesis dependent? *J. Nat. Cancer Inst.* **1990**;82:2-4.
7. Ackerman NB and Hechmer PA. The blood supply of experimental liver metastases V. Increased tumor perfusion with epinephrine. *Am. J. Surg.* **1980**;140:625-631.
8. Wang LQ, Persson BG, Bergqvist L and Bengmark S. Rearterialization of liver tumors after various dearterialization procedures. *J. Surg. Res.* **1994**;57:454-459.
9. Andrews JC, Walker-Andrews SC, Juni JE, Warber S and Ensminger WD. Modulation of liver tumor blood flow with hepatic arterial epinephrine: A SPECT study. *Radiology* **1989**;173:645-647.
10. Sasaki Y, Imaoka S, Hasegawa Y, Nakano S, Ishikawa O, Ohigashi H, Taniguchi K, Koyama H, Iwanaga T and Terasawa T. Changes in distribution of hepatic blood flow induced by intra-arterial infusion of angiotensin II in human hepatic cancer. *Cancer* **1985**;55:311-316.
11. Burton MA, Gray BN, Klemp PF, Kelleher DK and Hardy N. Selective internal radiation therapy: Distribution of radiation in the liver. *Eur. J. Cancer Clin. Oncol.* **1989**;25:1487-1491.
12. Lau WY, Ho S, Leung TWT, Chan M, Ho R, Johnson PJ and Li AKC. Selective internal radiation therapy for nonresectable hepatocellular carcinoma with intraarterial infusion of  $^{90}\text{Y}$ trium microspheres. *Int. J. Rad. Oncol. Biol. Phys.* **1998**;40:583-592.
13. Ho S, Lau WY, Leung TWT and Johnson PJ. Internal radiation therapy for patients with primary or metastatic hepatic cancer. *Cancer* **1998**;83:1894-1907.
14. Nijsen JFW, Zonnenberg BA, Woittiez JRW, Rook DW, Swildens-van Woudenberg IA, van Rijk PP and van het Schip AD. Holmium-166 poly lactic acid microspheres applicable for intra-arterial radionuclide therapy of hepatic malignancies: effects of

- preparation and neutron activation techniques. *Eur. J. Nucl. Med.* **1999**;26:699-704.
15. Burton MA and Gray BN. Redistribution of blood flow in experimental hepatic tumours with noradrenaline and propranolol. *Br. J. Cancer* **1987**;56:585-588.
  16. Ho S, Lau WY, Leung TWT, Chan M, Chan KW, Lee WY, Johnson PJ and Li AKC. Tumour-to-normal uptake ratio of  $^{90}\text{Y}$  microspheres in hepatic cancer assessed with  $^{99\text{m}}\text{Tc}$  macroaggregated albumin. *Br. J. Radiology* **1997**;70:823-828.
  17. Dworkin MJ, Zweit J, Carnochan P, Deehan B and Allen-Mersh TG. Effect of regional angiotensin II infusion on the relationship between tumour blood flow and fluorouracil uptake in a liver metastasis animal model. *Eur. J. Cancer* **1996**;32A:1580-1584.
  18. Caster WO, Poncelet J, Simon AB and Armstrong WD. Tissue weights of the rat. I. Normal values determined by dissection and chemical methods. *Proc. Soc. Exp. Biol. Med.* **1956**;91:122-126.
  19. Pillai KM, McKeever PE, Knutsen CA, Terrio PA, Prieskorn DM and Ensminger WD. Microscopic analysis of arterial microsphere distribution in rabbit liver and hepatic VX2 tumor. *Sel. Cancer Therapeutics* **1991**;7:39-48.
  20. Shepherd FA, Rotstein LE, Houle S, Yip T-CK, Paul BA and Sniderman KW. A phase I dose escalation trial of yttrium-90 microspheres in the treatment of primary hepatocellular carcinoma. *Cancer* **1992**;70:2250-2254.

## Chapter 7

---

# Radioactive holmium loaded poly(L-lactic acid) microspheres for treatment of hepatic malignancies: efficacy in rabbits

*in preparation*



**J.F.W. Nijsen<sup>1</sup>, D.W. Rook<sup>1</sup>, B. Westendorp<sup>1</sup>, C.J.W.M. Brandt<sup>2</sup>,  
B.A. Zonnenberg<sup>1</sup>, P.P. van Rijk<sup>1</sup>, W.E. Hennink<sup>3</sup> and  
A.D. van het Schip<sup>1</sup>**

<sup>1</sup>*Department of Nuclear Medicine, University Medical Center, Utrecht, The Netherlands*

<sup>2</sup>*Central Laboratory Animal Institute, University of Utrecht, Utrecht, The Netherlands*

<sup>3</sup>*Department of Pharmaceutics, Utrecht Institute for Pharmaceutical Sciences, Utrecht University, Utrecht, The Netherlands*

### **Abstract**

In this chapter the therapeutic effect of  $^{166}\text{Ho}$  loaded poly(L-lactic acid) microspheres in rabbits with liver tumours was investigated. New Zealand White rabbits with an implanted VX2 tumour were divided in three groups: sham-treated (n=3), cold microspheres (n=3) and microspheres loaded with  $^{166}\text{Ho}$  (0.9-1.0 GBq; n=2). After administration of the microspheres into the hepatic artery the biodistribution was studied with a gamma camera and tumour growth was followed in time with ultrasound. The radioactive microspheres were heterogeneously distributed over the liver and accumulated preferentially in the tumour area, which was confirmed by histological analysis. A transient increase of hepatic enzyme activity was observed after (radio)embolization. Sham-treated rabbits and rabbits treated with “cold” microspheres showed an exponential tumour growth. Therapeutic doses (100 Gy to the whole liver) arrested growth and resulted in necrosis of the tumour. No histological signs of pathological radiation effects, such as hepatic fibrosis or necrosis of the normal liver, were detected. This feasibility study demonstrates that  $^{166}\text{Ho}$  loaded poly(L-lactic acid) microspheres are promising systems for the treatment of patients with liver tumours.

## 7.1 Introduction

Malignant neoplasms of the liver, both primary and metastatic, are among the most common tumours worldwide. In western countries the majority of liver metastases originates from colorectal cancer. Its prognosis is poor, with a median survival of approximately 6 to 12 months [1]. Currently, chemotherapy, either systemic or by hepatic arterial infusion, is the main approach of treatment. Nevertheless, side effects of chemotherapy are commonly reported while life extension is often marginal [1-3]. Long-term survivors are frequently documented after partial liver resection, but this is only possible in 10% of the patients [2,4].

In the last decade a new therapy, viz. selective internal administration of radioactive yttrium loaded glass or resin based microspheres, resulted in a useful treatment with minor side effects [5]. The microspheres are administered into the hepatic artery and will lodge in the end arterioles in the liver. Tumours are usually rich in vasculature and they derive most of their blood supply from the arterial side. Thus accumulation of spheres can be found in and around the tumour when administered by the hepatic artery [6]. Estimated tumour doses exceed 300 Gy while the absorbed doses to the liver range from 50 to 150 Gy [5,7]. Although increased longevity and long term survivors are reported, this treatment modality is certainly far from optimal. Especially the high density of glass microspheres, the absence of a gamma component for imaging and the non-biodegradability are major drawbacks of both the resin- and glass-based  $^{90}\text{Y}$  loaded microspheres [5,8].

These disadvantages are solved to a large extent by the use of a new type of microsphere and isotope, as first described by Mumper et al. [8]. Neutron activated Ho-PLLA microspheres have more favourable properties. A disadvantage of these organic types of spheres is their high susceptibility to degradation induced by neutron irradiation needed for the activation of the holmium [9,10]. By carefully defining the irradiation conditions and increasing the holmium content we succeeded in the preparation of useful microspheres loaded with a therapeutic amount of radioactive holmium [11]. Experiments in a rat tumour model showed an average tumour/liver ratio of six for these PLLA microspheres [12].

In order to use these microspheres for therapy in humans, distribution in the liver should be inhomogeneous with preference for the tumour area and the delivered radiation dose should be able to induce necrosis of the tumour with acceptable toxicity to the normal liver. The objective of the present study was to investigate the effects of PLLA microspheres, containing therapeutic amounts of  $^{166}\text{Ho}$ , in the treatment of liver tumours in rabbits. Rabbits were either sham-treated or received a diagnostic or therapeutic (100 Gy) dose of microspheres. The dose of 100 Gy to the whole liver was chosen since it is well tolerated and results in effective tumour kill or reduction [5,13,14]. Tumour growth was investigated by ultrasound.



## 7.2 Materials and methods

### 7.2.1 Animals

All experiments were performed in agreement with The Netherlands Experiments on Animals Act (1977) and the European Convention guidelines (86/609/EC). Approval was obtained from the University Animal Experiments Committee (FDC/DEC-GNK nr. 99042). Ten adult female or male specific pathogen free New Zealand White rabbits of 2000 to 3500 g were used (Harlan, Horst, The Netherlands). The rabbits were housed individually in steel or plastic cages and provided daily with approximately 100 g “complete diet” pellets for rabbits (LKK-20, Hope Farms BV, Woerden, The Netherlands). Water was provided *ad libitum*. Rabbits were sacrificed after three or four weeks or earlier, when clear inconvenience for the animal was observed.

### 7.2.2 Tumour cells

The VX2 cell line was obtained from the Department of Oral and Maxillofacial Surgery of the University Medical Center, Utrecht, The Netherlands [15]. The original tumour cells were obtained from a virus induced papilloma rabbit carcinoma [16]. The VX2 tumour was propagated by subcutaneous passage in the hip region of the rabbit or was derived from a part of the implanted tumour in the liver of a freshly killed rabbit. In order to facilitate implantation, the tumour tissue was dissected and small parts (2 mm in diameter) were chosen for implantation.

### 7.2.3 Tumour implantation

Prior to inhalation-anaestheticum, premedication of 0.5 ml methadon (10 mg/ml; Veterinary Pharmacy, University of Utrecht, The Netherlands) and 0.5 ml Vetranquil<sup>®</sup> (acepromazine, 10 mg/ml; Sanofi Sante Animale Benelux BV, Maassluis, The Netherlands) was given. Subsequently, the rabbits were anaesthetized by an intravenous injection of Hypnomidate<sup>®</sup> (2 mg/ml; B. Braun Melsungen AG, Melsungen, Germany) and N<sub>2</sub>O and halothane (Albic BV, Maassluis, The Netherlands) as inhalation anaestheticum. A laparotomy was performed by ventral mid-line incision in order to expose the lobes of the liver. Tumour tissue was implanted in the *lobus sinister lateralis* by injection with an Abbocath-T<sup>®</sup> 18G (Abbott Ltd., Ireland), together with a piece of titanium to serve as a localization marker for ultra sound. After approximately 12 days the first ultrasound investigation (HDI 3000 ATL, Entos<sup>™</sup> CL10-5 transducer) was performed to check tumour growth.

### 7.2.4 Preparation of microspheres

Radioactive holmium loaded microspheres were prepared as previously described [11]. Briefly, holmium acetylacetonate (HoAcAc) is incorporated into PLLA by

solvent evaporation, resulting in microspheres of 20-50  $\mu\text{m}$  after sieving. Neutron activation of the microspheres was performed by irradiation for 1h in the PRS facility of the high-flux nuclear reactor in Petten, The Netherlands. Neutron activated microspheres were used the next day for therapeutic purpose (900-1000 MBq in 35-40 mg) or as diagnostic, “cold” microspheres after decay for four to five days (40-80 MBq in 35-40 mg). Microspheres were sonicated for 10 min in an ultrasonic cleaner and suspended in Gelofusine® (Vifor Medical SA, Switzerland) prior to administration.

#### *7.2.5 Administration of microspheres*

When the tumour had reached a diameter of  $\geq 20$  mm, a second laparotomy was performed in order to administer the holmium loaded microspheres (or Gelofusine® in case of sham-treated rabbits). Administration of microspheres was similar as described for rats in chapter 6. The gastroduodenal artery was cannulated with an Abbocath-T® 24G (Abbott Ltd., Ireland). Back flow was checked with 0.1% methylene blue in 5% glucose. A pre-flushed administration system similar as described by Herba et al. [17] was connected to the Abbocath®. The suspended microspheres were administered and the administration system was measured for activity pre- and post injection, in order to calculate the injected dosage. The gastroduodenal artery was sealed with tissue glue (Histoacryl, B. Braun Melsungen AG, Melsungen, Germany) and wires were removed to restore the arterial hepatic circulation.

#### *7.2.6 Biodistribution and assessment of tumour growth*

Rabbits were divided in three treatment groups which received either Gelofusine® (control group, n=3), “cold” microspheres containing 40-100 MBq  $^{166}\text{Ho}$  for diagnostic imaging (n=3) or microspheres containing therapeutic amounts of activity (900-1000 MBq; n=2) resulting in approximately 100 Gy to the whole liver. The rabbits were monitored by planar and SPECT imaging, using a triple-head gamma camera (Prism 3000, Cleveland, USA). A whole body scintigram was made 5 days after administration of therapeutic and 1 day after diagnostic microspheres, in order to determine gross distribution.

Ultrasound studies were performed at approximately 4, 10, and 18 days after administration of Gelofusine® or microspheres and before sacrificing, and were evaluated by the same observer. Examination of the liver, stomach and part of the intestines was established by sagittal and transversal scanning of the abdominal region. The tumour was measured in three directions and its volume was calculated by applying the equation for the volume of an ellipsoid [18]. Ultrasound measurements before treatment and sacrificing were compared with calliper measurements at time of treatment and autopsy of the rabbit.

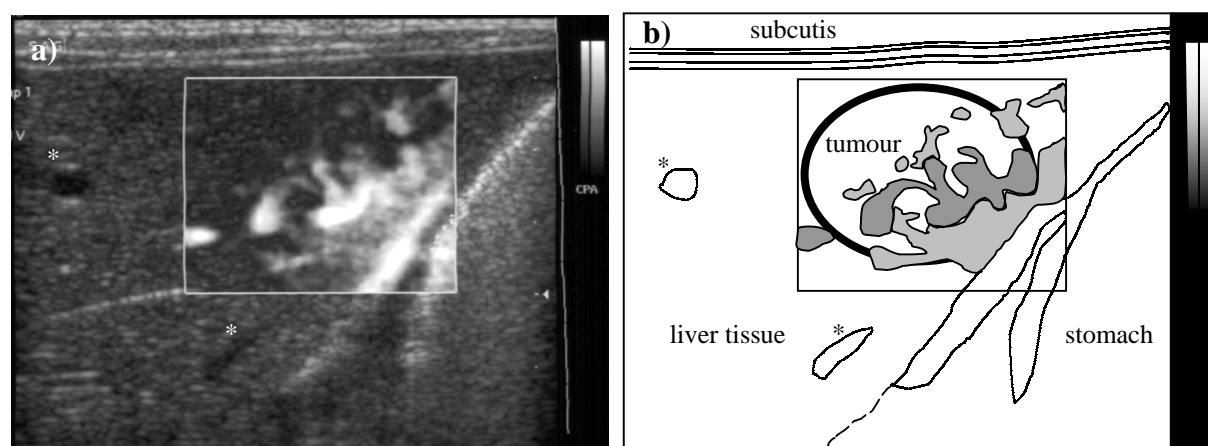
### 7.2.7 Toxicity evaluation

Blood samples were taken three or four times: prior to tumour implantation, before administration of microspheres, after administration and before sacrifice. Blood was centrifuged at 2500 g for 10 min and the plasma immediately frozen. The plasma samples were analysed for alkaline phosphatase as an indicator of biliary toxicity and for alanine aminotransferase (ALAT), gamma glutamyltransferase ( $\gamma$ -GT) and bilirubine as indicators of hepatocellular toxicity. At autopsy the thoracic and abdominal organs were inspected and fixed in phosphate-buffered 4% formaldehyde. In order to verify presence of microspheres, tissue samples from the tumour site, liver, lungs, spleen, and stomach were embedded in paraffin and histologically evaluated after staining with haematoxylin-eosin.

## 7.3 Results

### 7.3.1 Tumour growth and survival

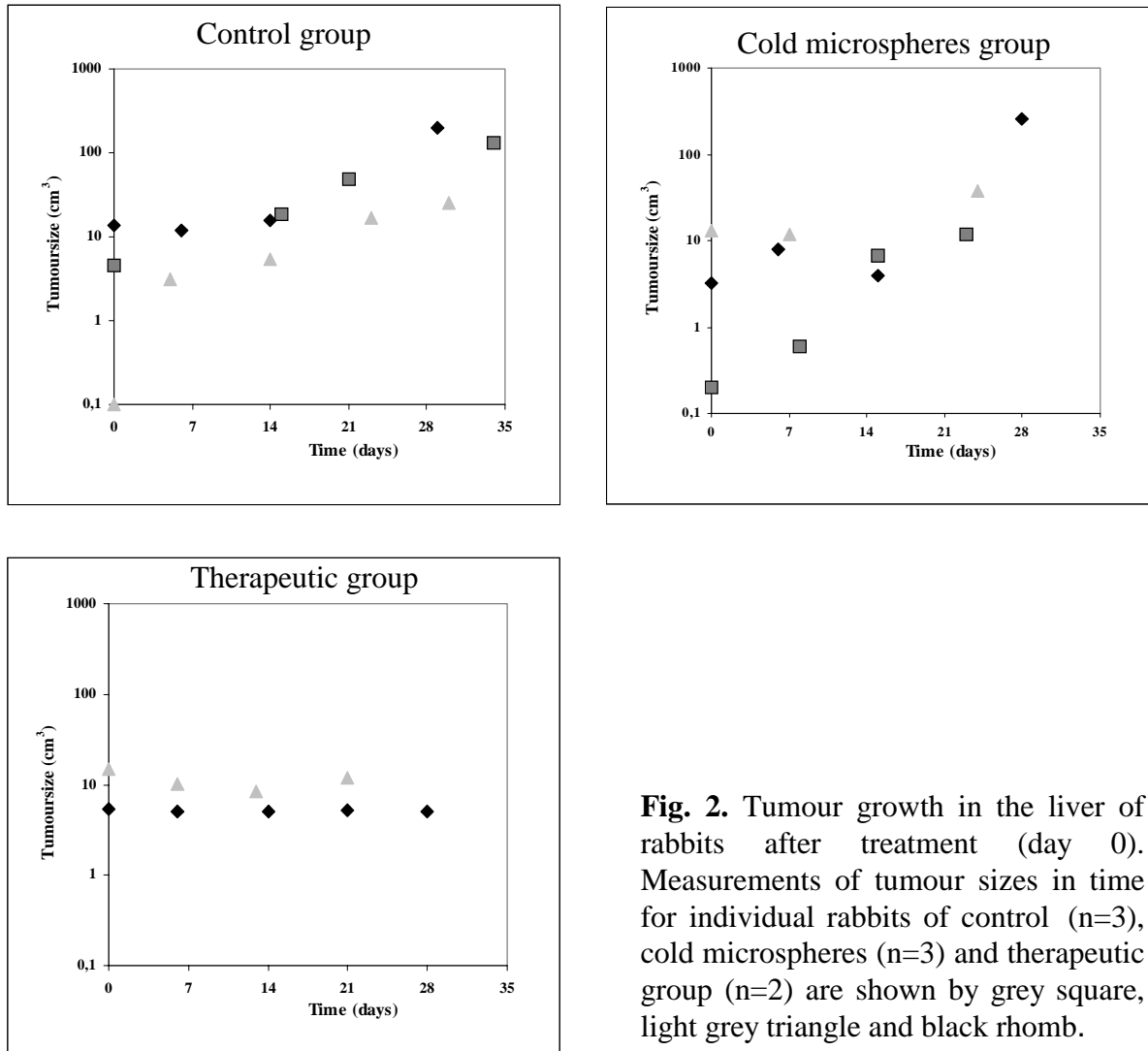
Implantation of the tumour resulted in a 100% “take-rate”. In tumours transplanted from subcutaneous site to liver a slower tumour growth was observed (approximately 21 days before reaching a diameter  $>20$  mm) compared with tumour tissue that was transplanted from liver to liver (approximately 16 days before reaching  $>20$  mm). Tumours  $>2$  mm in diameter were visible with ultrasound and were well vascularized as illustrated in Fig. 1.



**Fig. 1a-b.** Doppler ultrasound (square) of the vasculature of the VX2 tumour (1.2 x 1.3 cm) before treatment. The high blood flow in and around the tumour is indicated in the ultrasound graph in the white/light grey regions (a). In the schematic drawing the blood flow is indicated as grey regions (b). \*Branch of the portal vein.

Tumour growth was exponential in both the control group and the rabbits treated with “cold” microspheres (Fig. 2 and Table 1). No primary tumour growth was seen in the rabbits treated with 900 MBq of activity.

After the second operation most rabbits showed a decline in physical condition mainly manifested by a decrease in appetite.



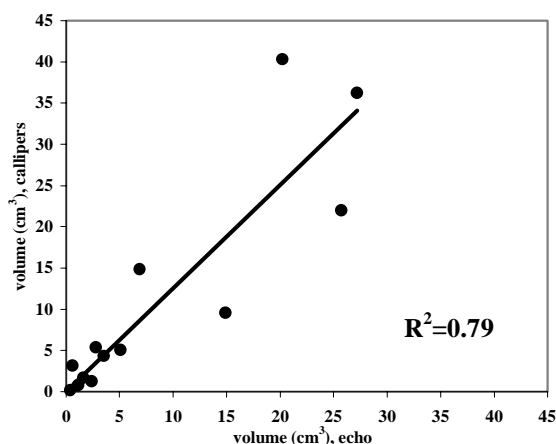
**Fig. 2.** Tumour growth in the liver of rabbits after treatment (day 0). Measurements of tumour sizes in time for individual rabbits of control (n=3), cold microspheres (n=3) and therapeutic group (n=2) are shown by grey square, light grey triangle and black rhomb.

Table 1. Tumour size at treatment and sacrifice.

Rabbit	$^{166}\text{Ho}$ (MBq)	Tumour size at treatment ( $\text{cm}^3$ )	Tumour size at sacrification ( $\text{cm}^3$ )	Day of sacrification	Increase of tumour size (%)
Control 1	---	4.8	132.8	34	2767
Control 2	---	13.6	201.1	29	1479
Control 3	---	0.1	25.7	30	25700
Cold 1	92	0.2	11.7	23	5850
Cold 2	123	3.2	254.9	28	7966
Cold 3	46	12.9	37.7	24	292
Therapeutic 1	900	5.4	5.2	28	-96
Therapeutic 2	928	14.9	11.8	21	-79

### 7.3.2 Metastatic disease

Ultrasound appeared to be a useful modality in predicting the size of the tumours (Fig. 3). In all treatment groups several massive lung and liver metastases were found with ultrasound or subsequently at autopsy. Histology showed high proliferation grade and necrotic centre indicative for non-differentiated and aggressive tumours. Also metastases on the exterior of the stomach and diaphragm were present in all three groups. Metastases on the incision wound were sometimes present and often visible before treatment. If possible this tumour tissue was resected during the second laparotomy.



**Fig. 3.** Correlation between tumour volume measured with ultrasound and calliper measurements during operation and autopsy of the rabbits.

### 7.3.3 Biodistribution and histological analysis

Cannulation of the liver artery resulted in deposition of 80-90% of the initial activity of microspheres. Based on SPECT and planar scintigraphic images radioactivity remained in the liver and tumour with preferential accumulation of activity in the tumour (Fig. 4). Activity in the liver was heterogeneously distributed which was

confirmed by microscopic analysis showing that microspheres were distributed unequally over liver and tumour. Although single spheres were found in similar amounts in tumour and liver tissue, the greater part of clustered microspheres had accumulated around the (primary) tumour and in the larger vessels (Figs. 5 and 6). No microspheres were found in lungs, stomach or spleen. Particularly in the rabbits that were embolized with (radioactive) microspheres cholestasis was noted in the liver and this was sometimes visualized as small ridges in the ultrasound image.

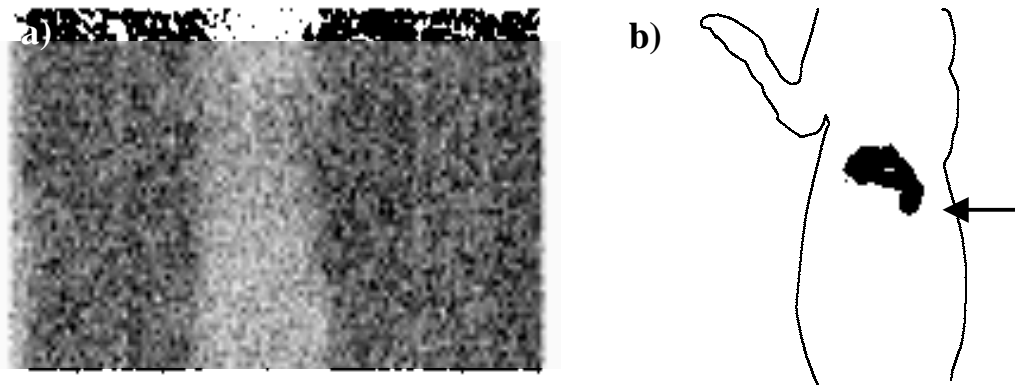


**Fig. 4a-b.** Whole body scintigraphic image of a tumour-bearing rabbit 3 days after injection of approximately 1GBq  $^{166}\text{Ho}$  poly(L-lactic acid) microspheres into the hepatic artery. Contour of the rabbit was obtained by using a “flood source”.

In the control group and the rabbits embolized with “cold” microspheres histology showed compression of liver parenchyma caused by the rapid expansion of the tumour. The tumour tissue appeared to be viable and was unaffected by the treatment. In contrast, in the therapeutic treated rabbits the primary tumour and the larger metastases were entirely necrotic. Also necrotic liver tissue was seen close to large blood vessels containing clusters of microspheres. Compression of normal liver tissue was scarcely observed.

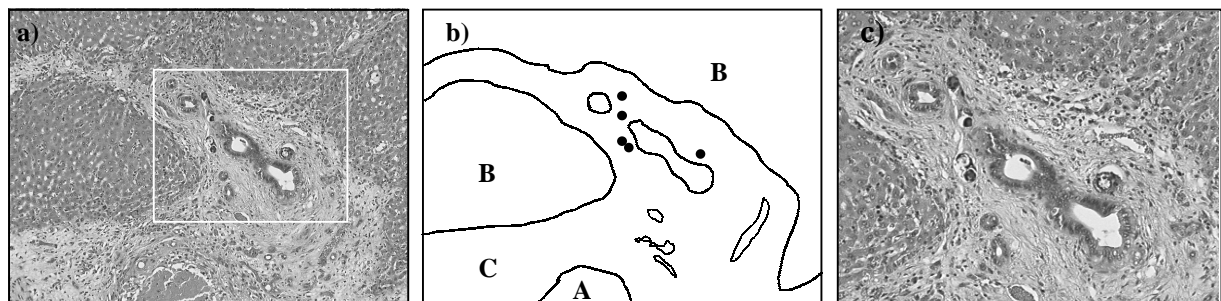


**Fig. 5a-b.** Typical example of a liver tissue section after embolization with cold microspheres in the liver artery (a). A schematic overview of the micrograph shows A) tumour tissue B) liver tissue and C) connective tissue with bile ducts and blood vessels (b). The magnification of the white square of (a) shows five microspheres in small arteries close to the tumour (schematic drawing 5 black circles) (c). Since microspheres were cold no damage is seen in liver or tumour tissue.

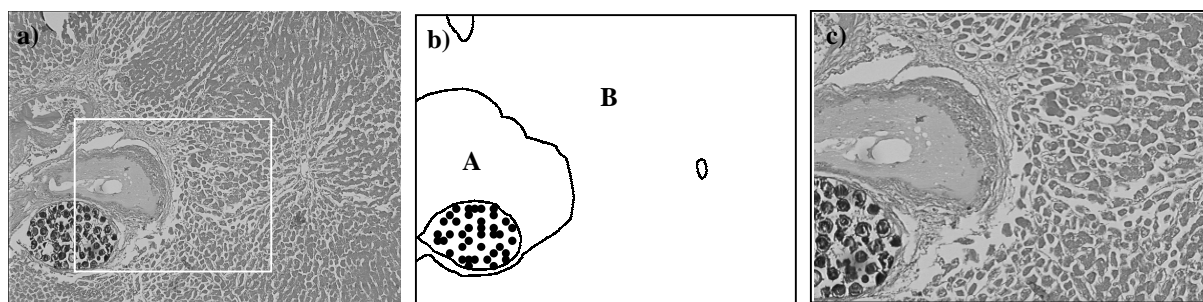


**Fig. 6a-b.** Typical example of a liver tissue section after embolization with microspheres with therapeutic amounts of activity (a). A schematic overview of the micrograph shows A) tumour tissue and B) liver tissue (b). A cluster of microspheres is seen in a large blood vessel in the tumour. No cell nucleus is seen in cells of both liver tissue and tumour tissue indicating necrotic tissue (c).

### 7.3.4 Hepatic toxicity

At this stage of the study plasma data were too incomplete to allow for statistical analysis of hepatic enzyme levels. Therefore only the trends observed in the individual animals can be described. Total bilirubin levels remained unchanged in all rabbits. For alkaline phosphatase, ALAT and  $\gamma$ -GT a transient elevation in activity was observed which is illustrated in Fig. 7 for a rabbit that was treated therapeutically with 928 MBq of radioactive microspheres. This phenomenon was not observed in sham-treated rabbits, which showed no change in activity of liver enzymes during the follow up until sacrificing.

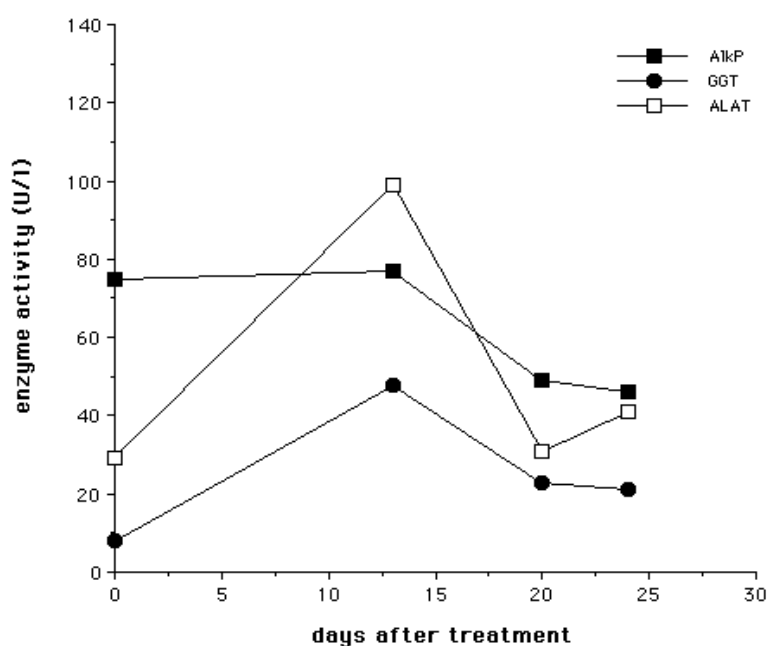


**Fig. 7.** Liver enzyme levels in a rabbit treated (at day 0) with 928 MBq  $^{166}\text{Ho}$ -microspheres.

## 7.4 Discussion

Treatment of liver malignancies in humans remains a challenge and prognosis of these patients is still poor. Conventional therapies such as systemic chemotherapy and external radiotherapy are insufficient [1,2]. New approaches such as regional chemotherapy result in increased survival and palliation [1,3,19]. Nevertheless, the side effects of regional chemotherapy are a considerable drawback.

A good alternative with less side effects are radioactive yttrium containing glass or resin based microspheres. Although these spheres showed some favourable clinical results, they have their own disadvantages such as a relatively high density, lack of  $\gamma$ -emission and non-biodegradability [5]. This is reflected in the risk that these microspheres are deposited into the gastroduodenal vasculature under gravity. The microspheres can not be tracked during and after administration and repeated administration of spheres is difficult. The use of neutron activated holmium loaded poly(L-lactic acid) microspheres may overcome these disadvantages.

In this study the proof of principle of this radioactive holmium loaded system was investigated in a rabbit tumour model. A major difference with human liver metastases and transplantable rodent tumours is the relatively slow doubling time in humans [20]. In the human situation microspheres can be administered via the femoral artery using standard radiological intervention techniques. The present rabbit model has the disadvantage of relatively rapid tumour growth, the concomitant spread of metastases and the need for two laparotomies.

The present study shows that holmium loaded microspheres infused into the hepatic artery do not give rise to backflow to the gastrointestinal vessels and that virtually all injected activity is deposited in the liver and tumour.

The high dose of activity in the liver and tumour was surprisingly well tolerated. This effect (external radiotherapy is limited to 30-35 Gy [5,21]) is similar as described for the radioactive yttrium loaded microspheres and is probably caused by the inhomogeneous distribution of activity in the liver [22,23]. Fox et al. [23] described for a patient that 86% of the normal liver parenchyma received less than the dose that would be expected for a uniform distribution, and 34% of the tissue received even less than one third of the dose [23]. Thus, approximately one third of the tissue receives less or equal to 30 Gy (total dose 90 Gy).

Histology as well as planar and SPECT imaging of the tumorous rabbit livers confirmed the high variability in microsphere and activity distribution for this embolization technique. In the rabbits embolized with microspheres at least two times more activity was found in and around the tumour compared with normal liver parenchyma based on SPECT imaging and histology. These values and variability are in accordance with results in other animal studies and clinical trials [13,24,25].



It was shown in this study that radioactive microspheres with therapeutic amounts of  $^{166}\text{Ho}$ , approximately 100 Gy to the whole liver, can arrest tumour growth and induce tumour necrosis. Studies, in other animal models, will be needed to further investigate the potential survival benefit of this therapy.

The administration of (radioactive) microspheres often gave rise to cholestasis in the liver and was also observed in one sham-treated rabbit. This phenomenon was probably caused by repeated halothane exposure during the two laparotomies. Impaired bile flow and cholestasis were reported as liver injury induced by halothane [26] and these effects may be enhanced by microsphere embolization.

In conclusion, this study has demonstrated that holmium loaded PLLA microspheres with a therapeutic dose of activity can arrest tumour growth and induce necrosis of tumour tissue while sparing normal liver tissue. These results warrant further studies in other models before this therapy can be tested in the human situation.

### **Acknowledgements**

The authors wish to thank P. Snip and J. Woittiez for their skilled technical assistance with the irradiation of the microspheres. The authors thank Adrie Versluis and Jeroen van Ark for assistance with and care of the rabbits. We also thank M. Gerrits, J. Buijs, C. Joosse, K. van de Ende and M. Wienia for their assistance with the rabbit-scintigraphy studies. Finally, we wish to thank M. El Ouamari for excellent performance of the ultrasound studies. This study was financially supported by the Energy Research Foundation and Mallinckrodt Medical BV, Petten, The Netherlands.

## References

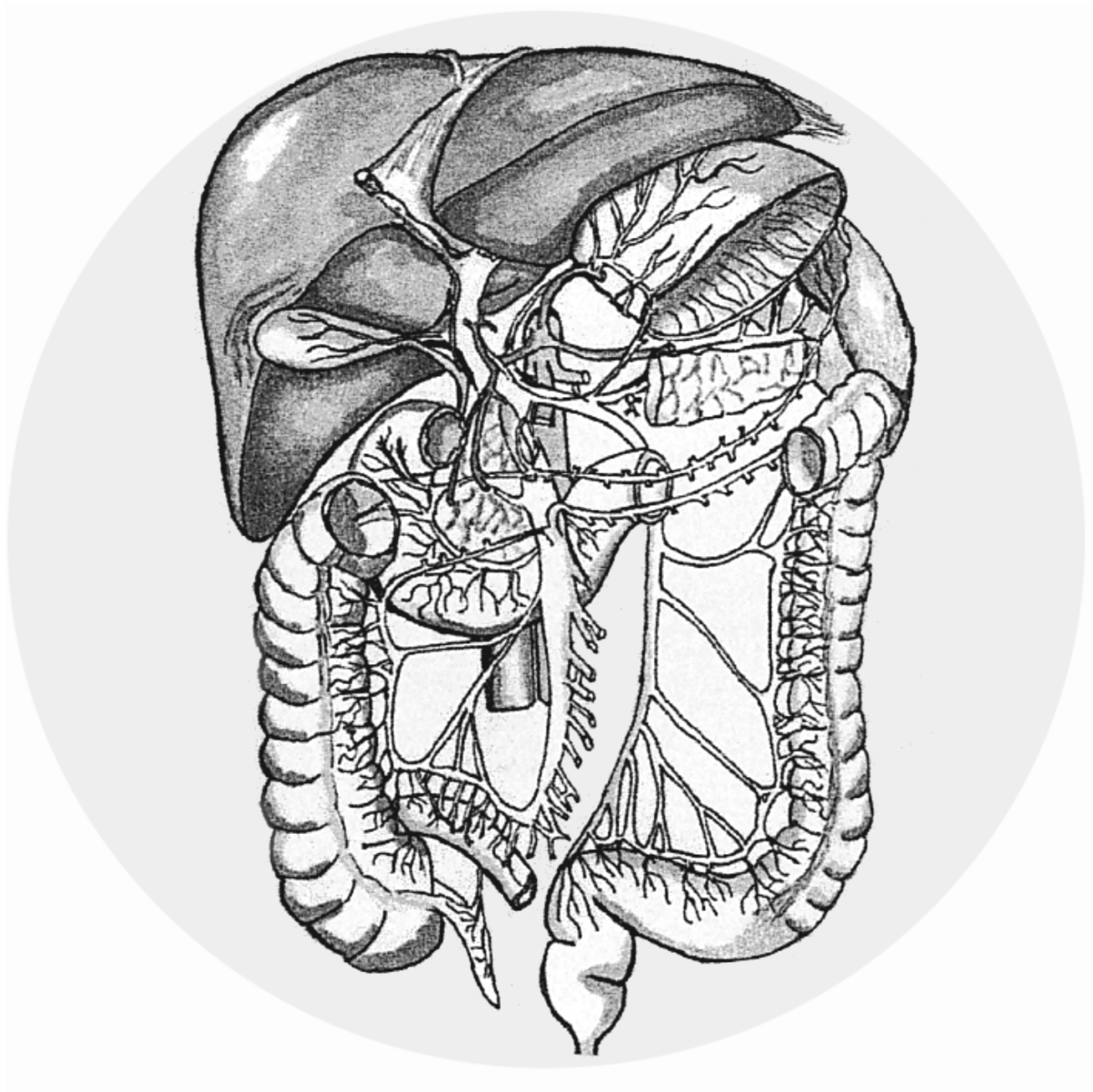
1. Kemeny NE and Ron IG. Hepatic arterial chemotherapy in metastatic colorectal patients. *Semin. Oncol.* **1999**;26:524-535.
2. Fong Y and Salo J. Surgical therapy of hepatic colorectal metastasis. *Semin. Oncol.* **1999**;26:514-523.
3. Giacchetti S, Itzhaki M, Gruia G, Adam R, Zidani R, Kunstlinger F, Brienza S, Alafaci E, Bertheault-Cvitkovic F, Jasmin C, Reynes M, Bismuth H, Misset JL and Lévi F. Long-term survival of patients with unresectable colorectal cancer liver metastases following infusional chemotherapy with 5-fluorouracil, leucovorin, oxaliplatin and surgery. *Ann. Oncol.* **1999**;10:663-669.
4. Wallace JR, Chistians KK, Pitt HA, and Quebbeman EJ. Cryotherapy extends the indications for treatment of colorectal liver metastases. *Surgery* **1999**;126:766-774.
5. Ho S, Lau WY, Leung TWT and Johnson PJ. Internal radiation therapy for patients with primary or metastatic hepatic cancer. *Cancer* **1998**;83:1894-1907.
6. Stribley KV, Gray BN, Chmiel RL, Heggie CP and Bennett RC. Internal radiotherapy for hepatic metastases II: The blood supply to hepatic metastases. *J. Surg. Res.* **1983**;34:25-32.
7. Yorke ED, Jackson A, Fox RA, Wessels BW and Gray N. Can current models explain the lack of liver complications in Y-90 microsphere therapy? *Clin. Cancer Res.* **1999**;5:3024-3030.
8. Mumper RJ, Ryo UY and Jay M. Neutron activated holmium-166-poly(L-lactic acid) microspheres: A potential agent for the internal radiation therapy of hepatic tumours. *J. Nucl. Med.* **1991**;32:2139-2143.
9. Sintzel MB, Merkli A, Tabatabay C and Gurny R. Influence of irradiation sterilization on polymers used as drug carriers-A review. *Drug. Develop. Ind. Pharm.* **1997**;23:857-878.
10. Nijsen JFW, van het Schip AD, van Steenberg MJ, Zielhuis S, Kroon-Batenburg LMJ, van de Weert M, van Rijk PP and Hennink WE. Influence of neutron irradiation on holmium acetylacetonate loaded poly(L-lactic acid) microspheres. **Submitted.**
11. Nijsen JFW, Zonnenberg BA, Woittiez JRW, Rook DW, Swildens-van Woudenberg IA, van Rijk PP and van het Schip AD. Holmium-166 poly lactic acid microspheres applicable for intra-arterial radionuclide therapy of hepatic malignancies: effects of preparation and neutron activation techniques. *Eur. J. Nucl. Med.* **1999**;26:699-704.
12. Nijsen F, Rook D, Brandt C, Meijer R, Dullens H, Zonnenberg B, de Klerk J, van Rijk P, Hennink W and van het Schip F. Targeting of liver tumour in rats by selective delivery of holmium-166 loaded microspheres: a biodistribution study. **In press.**
13. Yan ZP, Lin G, Zhao HY and Dong YH. An experimental study and clinical pilot trials on yttrium-90 glass microspheres through the hepatic artery for treatment of primary liver cancer. *Cancer* **1993**;72:3210-3215.

14. Wollner I, Knutsen C, Smith P, Prieskorn D, Chrisp C, Andrews J, Juni J, Warber S, Klevering J, Crudup J and Ensminger W. Effects of hepatic arterial yttrium 90 glass microspheres in dogs. *Cancer* **1988**;61:1336-1344.
15. van Es RJJ, Franssen O, Dullens HFJ, Bernsen MR, Bosman F, Hennink WE and Slootweg PJ. The VX2 carcinoma in the rabbit auricle as an experimental model for intra-arterial embolization of head and neck squamous cell carcinoma with dextran hydrogel microspheres. *Lab. Animals* **1999**;33:175-184.
16. Kidd JG and Rous P. A transplantable rabbit carcinoma originating in a virus induced papilloma and containing the virus in a masked or altered form. *J. Exp. Med.* **1940**;71:813-837.
17. Herba MJ, Illescas FF, Thirlwell MP, Boos GJ, Rosenthal L, Atri M and Bret PM. Hepatic malignancies: improved treatment with intraarterial Y-90. *Radiology* **1988**;169:311-314.
18. Tomayko MM and Reynolds CP. Determination of subcutaneous tumour size in athymic (nude) mice. *Cancer Chem. Pharmacol.* **1989**;24:148-154.
19. Civalleri D, Pector J-C, Håkansson L, Arnaud J-P, Duez N and Buyse M. Treatment of patients with irresectable liver metastases from colorectal cancer by chemo-occlusion with degradable starch microspheres. *Brith. J. Surg.* **1994**;81:1338-1341.
20. Steel GG. Growth kinetics of tumors. *Oxford Clarendon Press* **1977**.
21. Ingold J, Reed G, Kaplan H and Bagshaw M. Radiation hepatitis. *Am. J. Rontgenol. Radium Ther. Nucl. Med.* **1965**;93:200-208.
22. Burton MA, Gray BN, Kelleher DK and Klemp PF. Selective internal radiation therapy: validation of intraoperative dosimetry. *Radiology* **1990**;175:253-255.
23. Fox RA, Klemp PFB, Egan G, Mina LL, Burton MA and Gray BN. Dose distribution following selective internal radiation therapy. *Int. J. Radiation Oncology Biol. Phys.* **1991**;21:463-467.
24. Lau WY, Leung WT, Ho S, Leung NWY, Chan M, Lin J, Metreweli C, Johnson P and Li AKC. Treatment of inoperable hepatocellular carcinoma with intrahepatic arterial yttrium-90 microspheres: a phase I and II study. *Br. J. Cancer* **1994**;70:994-999.
25. Häfeli UO, Casillas S, Dietz W, Pauer GJ, Rybicki LA, Conzone SD and Day DE. Hepatic tumor radioembolization in a rat model using radioactive rhenium ( $^{186}\text{Re}/^{188}\text{Re}$ ) glass microspheres. *Int. J. Radiation Oncology Biol. Phys.* **1999**;44:189-199.
26. Frost L, Mahoney J, Field J and Farell GC. Impaired bile flow and disordered hepatic calcium homeostasis are early features of halothane-induced liver injury. *Hepatology* **1996**;23:80-86.

## Chapter 8

---

### Summary and concluding remarks



### 8.1 Summary and concluding remarks

Liver metastases frequently occur during the progression of various solid tumours, especially colorectal cancers, and are the cause of 25-50% of all cancer deaths [1-3]. In particular in patients with colorectal cancer the liver is the main metastatic site. Median survival of patients with liver metastases is approximately 6-12 months, and in the presence of extensive hepatic metastases survival is reported to be less than 6 months with no 5-year survivors [1,4,5]. Systemic chemotherapy results in only limited increase in life span with a median survival of around 1 year. In addition to systemic chemotherapy, local hepatic arterial chemotherapy, chemo-occlusion or combination therapies have resulted in some extension of life span of approximately 12-24 months [5-7]. Although loco-regional chemotherapy showed good palliative properties, a number of side effects such as nausea, vomiting and diarrhoea has been reported. In addition, hepatic toxicity associated with these therapies is often observed [5,8]. Surgery is still the only accepted treatment with curative intention, but only a minority of the patients can be subjected to this treatment [9,10]. Other newly developed surgical modalities like cryo-ablation and radiofrequency ablation have resulted in refinement of the surgical techniques which can be applied to a greater number of patients. Nevertheless, surgical therapies are only possible in approximately 10% of the patients [11,12].

External beam radiotherapy in the treatment of hepatic malignancies is limited by the radiosensitivity of normal liver tissue, which can tolerate doses of only up to 30 Gy for whole liver irradiation [3,13,14]. Therefore, investigators have searched for ways to utilise the arterial vascularization of hepatic metastases in order to inject local radioactive deposits. Yttrium-90 ( $^{90}\text{Y}$ ) labelled microspheres which can be administered intra-arterially, became available in the late 1980s and resulted in the start of a new safe therapy for treatment of liver cancer [2,15]. Livers of patients can receive up to 150 Gy without developing radiation hepatitis; a safety limit of 80 to 100 Gy is used in most studies [16,17]. The median survival in a study of 17 patients with liver metastases from colorectal cancer treated with  $^{90}\text{Y}$  microspheres was 14 months and there were 3 long-term survivors of 4 years [18]. As important as longevity, the treatment has very little morbidity [8].

Although studies with  $^{90}\text{Y}$  labelled microspheres, either based on glass or resin, showed promising results, their high density (3.3 g/ml for glass and 1.6 g/ml for resin), apparent non-biodegradability and the lack of  $\gamma$ -emission of  $^{90}\text{Y}$  ( $E_{\text{max}}=2.28$  MeV,  $t_{1/2}=64.1\text{h}$ ) for imaging can be considered as disadvantages. Therefore, Mumper et al. [19] proposed the use of poly(L-lactic acid) (PLLA) microspheres loaded with the  $\beta$ -emitter holmium-166 ( $^{166}\text{Ho}$ ) as alternative for the glass or resin based systems.  $^{166}\text{Ho}$ -loaded microspheres have favourable characteristics above the  $^{90}\text{Y}$  glass and resin based systems because of their relatively low density and biodegradability.

Moreover,  $^{166}\text{Ho}$  also emits  $\gamma$ -photons, which makes image-guided radionuclide therapy possible. However, because of the relatively low contents of holmium, 10% (w/w), Mumper et al. were not able to produce a patient dose with sufficient activity.

In chapter 2 of this thesis it was shown that adjustment of the irradiation parameters used by Mumper et al. to increase the radioactivity was not successful. However, optimisation of the formulation and process parameters resulted in PLLA microspheres with a substantially higher loading (16-17% (w/w) Ho) than obtained by Mumper et al. Further, the irradiation parameters were studied to result in microspheres with high activity and acceptable irradiation damage. Thus, we were able to produce stable radioactive holmium loaded PLLA microspheres with therapeutic amounts of activity (chapters 2-5). This thesis concludes with two animal studies that show the successful targeting of the Ho-loaded microspheres to liver tumours in rats (chapter 6) and, importantly, in a feasibility study a good therapeutic effect of these microspheres in rabbits with liver tumours was demonstrated (chapter 7).

**Chapter 1** reviews the current literature on radioactive microspheres used for the treatment of liver malignancies. The first usable microspheres for clinical application were  $^{90}\text{Y}$ -glass microspheres which now have a proven efficacy in the treatment of especially liver tumours. Resins with  $^{90}\text{Y}$  bound to the carboxylate anions of an acrylic copolymer also showed good clinical results. PLLA microspheres with  $^{165}\text{Ho}$ -acetylacetonate (HoAcAc) which can be activated by neutron irradiation (by which  $^{165}\text{Ho}$  is converted into radioactive  $^{166}\text{Ho}$ ) were introduced as an improved system as compared with glass and resin based particles. The size, stability, toxicity, density, radio-isotope and other requirements which the optimal microsphere formulation for radio-embolization of liver malignancies should meet, are discussed in this chapter. This chapter concludes with the scope, aims and outline of the thesis.

In **Chapter 2** the preparation of  $^{165}\text{Ho}$ -loaded PLLA microspheres with a solvent evaporation technique is described. The optimisation of the formulation and process parameters resulted in a standard method which yielded PLLA microspheres with a diameter of 20-50  $\mu\text{m}$  and a loading of 17% holmium (w/w). Furthermore, the effect of the neutron irradiation parameters on the microsphere integrity and Ho-release has been evaluated. In order to produce an amount of activity which is sufficient for a patient dose (estimated activity of 20 GBq per 400 mg microspheres) the microspheres have to be free of water and irradiation with a relatively low neutron flux ( $5 \times 10^{13} \text{ cm}^{-2} \cdot \text{s}^{-1}$ ) for 1h has to be performed. Irradiation has to be performed preferably in a container (e.g. made of polyethylene) which by itself is not activated by the

irradiation. The structural integrity of the microspheres was maintained in terms of form and size. In vitro analyses showed that >98% of  $^{166}\text{Ho}$  activity was retained in the microspheres after 192h incubation in PBS, plasma, a leucocyte suspension, and liver homogenate.

In **Chapter 3** the crystal structures of two HoAcAc complexes were identified with X-ray diffraction. The structures of the two complexes,  $[\text{Ho}(\text{C}_5\text{H}_7\text{O}_2)_3(\text{H}_2\text{O})_2] \cdot \text{H}_2\text{O}$  (complex I; prepared at pH 8.5) and  $[\text{Ho}(\text{C}_5\text{H}_7\text{O}_2)_3(\text{H}_2\text{O})_2] \cdot \text{C}_5\text{H}_8\text{O}_2 \cdot 2\text{H}_2\text{O}$  (complex II; prepared at pH 9.0), both show an eight-coordinate holmium(III) ion. In both structures (I and II), hydrogen bonds between the complexes join them into a chain. In complex I the non-coordinating water molecule links these chains in a two-dimensional network. In complex II two non-coordinating water molecules and a free 4-hydroxypentan-2-one molecule also form a hydrogen-bonded chain. Diaquatris-(pentane-2,4-dionato-O,O')holmium(III) monohydrate (complex I) is the HoAcAc complex that is used for the preparation of holmium loaded microspheres.

In **Chapter 4** the preparation and characterisation of poly(L-lactic acid) microspheres and films loaded with HoAcAc are described. The factors responsible for the low release described in chapter 2 are investigated by modulated differential scanning calorimetry (MDSC), scanning electron microscopy (SEM), infrared spectroscopy (IR) and X-ray diffraction. MDSC analysis of HoAcAc crystals shows two endotherms which were ascribed to evaporation of the non-coordinated water molecule (first endotherm), and the second endotherm is due to evaporation of the two coordinated water molecules. Both MDSC and X-ray diffraction revealed that HoAcAc is molecularly dispersed in the PLLA matrix up to a loading of 8% in films and 17% Ho (w/w) in microspheres. Crystalline HoAcAc was present in films with high loading of holmium >12% (w/w). IR suggested that interactions between carbonyl groups of PLLA and the Ho-ion in the HoAcAc complex occurs, which might explain the high stability (=low release) of holmium loaded microspheres.

**Chapter 5** describes the influence of neutron irradiation on HoAcAc loaded PLLA microspheres. The PLLA matrices before and after irradiation, with and without HoAcAc, were analysed by MDSC, SEM, gel permeation chromatography (GPC), IR-spectroscopy and X-ray diffraction. GPC and MDSC measurements showed a decrease in molecular weight and crystallinity of the PLLA, respectively, which can be ascribed to radiation induced chain scission. Irradiation of HoAcAc loaded PLLA matrices resulted in evaporation of the non-coordinated and one coordinated water molecule of the HoAcAc complex, as shown by DSC and X-ray diffraction analysis. IR spectroscopy indicated that radiation caused some degradation of the

acetylacetonate anion. This chapter shows that although radiation-induced damage of both the PLLA matrix and the loaded HoAcAc-complex occurs, the microspheres retain their favourable properties (size and low Ho release) which makes these systems interesting candidates for the treatment of tumours by radio-embolization.

The selective delivery of the  $^{166}\text{Ho}$ -loaded PLLA microspheres to liver tumours was studied in rats (**Chapter 6**). The biodistribution of microspheres (20-50  $\mu\text{m}$ ; 17% Ho (w/w), activity of 15-20 MBq for imaging) after administration into the hepatic artery of WAG/Rij rats, with implanted liver tumours, was investigated. More than 95% retention of the injected activity was found in the liver and its tumour. A marginal amount of radioactivity was detected in the kidneys, indicating no leakage of  $^{166}\text{Ho}$ . Histological analysis showed that many large (>10) and medium sized (4-9) clusters of microspheres were present within the tumour and the peritumoural tissue, as compared with normal liver tissue. However, individual microspheres were equally dispersed through liver and tumour. The mean tumour-to-liver activity ratio was 6 (sham operated rats 0.7) which demonstrates a successful targeting of microspheres to the tumour. The use of the vasoactive agent adrenaline, which has been reported to enhance the blood flow to the tumour [20,21], did not result in an increased tumour-to-liver activity ratio.

**Chapter 7** shows the therapeutic effect of  $^{166}\text{Ho}$ -loaded PLLA microspheres in rabbits with hepatic malignancies. New Zealand White rabbits with an implanted VX2 (virus induced papilloma rabbit carcinoma) tumour were treated with cold microspheres or microspheres with a therapeutic amount of activity. The control group of sham-treated animals served as reference. The activity, and thus the microspheres, was heterogeneously distributed over the liver, as was confirmed by a gamma camera and histological analysis. Interestingly, a “hot spot” of activity corresponding with the location of the implanted tumour was observed, again indicating a successful targeting of microspheres to the tumour. Microscopic analysis also showed a high accumulation of microspheres within the tumour and peritumoural tissue. A transient increase of the liver enzymes was detected after administration of microspheres, indicating some liver toxicity. A normal exponential growth of the tumours was observed in the two control groups (sham-treated and rabbits which received cold microspheres). In animals which received a therapeutic dose of Ho-loaded microspheres growth of the tumour was arrested. Moreover, the therapeutic dose of activity induced necrosis of tumour tissue while sparing normal liver tissue. This is a very promising result for the further development and application of Ho-PLLA systems.



## 8.2 Prospects

This thesis has demonstrated that  $^{166}\text{Ho}$ -loaded poly(L-lactic acid) microspheres are very attractive systems for the therapeutic treatment of patients with liver malignancies. Before these systems can be fully exploited in clinical practice, a number of items deserves further attention. As mentioned in chapter 1, the preferred diameter of the microspheres for internal radiotherapy is approximately 30  $\mu\text{m}$ . Although the in vivo experiments in this thesis were done with a sub-optimal size of spheres (20-50  $\mu\text{m}$ ), both the retention in liver and tumour, and the tumour-to-liver ratio were quite high (chapters 6 and 7). Probably, microspheres with a narrower size distribution (25-35  $\mu\text{m}$ ) will show an even higher tumour-to-liver ratio. The solvent evaporation production process applied in this thesis results in microspheres with a relatively large size distribution of 5-100  $\mu\text{m}$ . This means that the yield of particles with the preferred size (~25-35  $\mu\text{m}$ ) is rather low. It is therefore recommended to investigate whether particles with the right average size and distribution can be obtained in a single step by adjustment of the process conditions. Also, other preparation methods like spray drying are recommended for further investigation. It is likely that the encapsulation efficiency will be improved by using this technique. In addition, for large scale production of Ho-loaded microspheres spray drying is preferred above the solvent evaporation technique, because spray drying is a continuous process, whereas solvent evaporation is a batch process. Moreover, spray drying results in less waste production as compared to solvent evaporation. A preliminary investigation revealed that the microspheres produced by spray drying could not easily be resuspended in saline, most likely because of the hydrophobic character of the surface of the microspheres. Probably, the wettability of the microspheres can be improved by resuspending the particles in saline in which a surface active agent (e.g. Pluronic<sup>®</sup>) is dissolved. However, the production of relatively large microspheres (20-50  $\mu\text{m}$ ) with spray drying, is another difficulty.

In present clinical practice, patients with liver tumours receive 2-4 GBq  $^{90}\text{Y}$ -particles. When an equivalent dose of  $^{166}\text{Ho}$ -loaded PLLA microspheres has to be administered to patients, the total radioactivity should be a factor 2.4 higher [22], because of its shorter half-life (3 days for  $^{90}\text{Y}$  and 1 day for  $^{166}\text{Ho}$ ). Moreover, for logistic reasons, the time between neutron irradiation and administration of the microspheres to the patient is about 1 day. This implies that one patient dosage should have an activity of 10-20 GBq off reactor preferably with the highest specific activity attainable. From the data described in chapter 7, it can be calculated that 100 mg PLLA microspheres with 17%  $^{165}\text{Ho}$  loading, yielded an activity of 3.5 GBq directly after irradiation. This means that with the current batches of microspheres in combination with the irradiation schedule, patient dosages with the required activity can be prepared. However, when clinical data would reveal that higher amounts of

activity are required, it can be evaluated whether greater amounts of microspheres can be administered to patients. If this is not possible, further investigation into the development of microspheres with higher specific activity is recommended. It should be noted that a 'simple' increase of the irradiation time can be associated with unacceptable aggregation and fragmentation of the microspheres (chapter 2). This means that higher radioactivity has to be achieved by an increase of  $^{165}\text{Ho}$ -loading. As described in chapter 4, HoAcAc is molecularly dispersed in the amorphous phase of the PLLA matrix. Thus, the use of for example fully amorphous poly(dl-lactic acid) (PDLA) will probably result in microspheres with a higher holmium loading. However, experimental evidence should demonstrate whether microspheres based on this polymer remain their structural integrity after neutron irradiation.

In chapter 5, it is demonstrated that neutron irradiation of Ho-loaded PLLA microspheres resulted in a radiation-induced chain scission of PLLA chains. This radiation damage was associated with a decrease of polymer molecular weight and of crystallinity. However, this does not need to be a disadvantage. It has been reported that the degradation time of PLLA matrices strongly depends on the molecular weight and the presence of a crystalline phase [23]. For highly crystalline PLLA a degradation time of 1-2 years has been reported [23]. Therefore, it can be expected that irradiated microspheres will degrade faster compared with non-irradiated spheres. PLLA is a biodegradable polymer which finally yields lactic acid as the sole degradation product. Although neutron irradiation causes chain scission in PLLA, it can not be excluded that also some recombination of radicals formed during irradiation occurs. It can be expected that upon degradation of irradiated PLLA microspheres under physiological conditions, also other degradation products (originating from recombination reactions) will be formed besides lactic acid. It is therefore recommended to perform *in vitro* degradation studies on (non-)irradiated PLLA microspheres with and without HoAcAc to gain more insight into the degradation kinetics as well as the nature of the degradation products. The amount and identity of degradation products other than lactic acid can probably be established by a combination of HPLC and mass spectroscopy. Furthermore, it is necessary to perform *in vivo* biocompatibility/degradation studies to establish the *in vivo* degradation behaviour as well as to investigate whether radiation-induced damage of PLLA adversely affects its favourable biocompatibility.

Acute toxicity caused by holmium ions is probably negligible since the holmium complex is immobilized in the polymeric matrix, possibly because of interactions with PLLA (chapters 4 and 5). Release of holmium will therefore occur upon microsphere degradation. Since the degradation/dissolution phase of PLLA matrices is extended over time (a few days to weeks), the release of Ho will be gradual and therefore only small amounts of holmium ions will enter the circulation. Furthermore, data

concerning holmium chloride show a low toxicity (LD50 in mice ip 312 mg/kg) and holmium is not noticed as carcinogenic (material safety data sheet; 91/155EEG).

For the preparation of Ho-loaded microspheres organic solvents are required. In this thesis the commonly used volatile solvent chloroform was applied. It was demonstrated that its residual content in the microsphere batches was 0.3% (w/w) (chapter 4). Lowering the residual solvent by heating for 24 hours at 80°C resulted in a substantial reduction in residual chloroform (~0.01% (w/w)). Although this method appeared to be highly efficient, the effects of heating of the PLLA microspheres have to be further investigated.

Since the microspheres are administered into the blood stream, they must be sterile. However, it is highly unlikely that non-sterile microspheres receiving a dose of 2 MGy during neutron irradiation still contain living microbes. The sterilising effect of neutron irradiation was evaluated by contaminating holmium loaded microspheres with a suspension of *Bacillus subtilis* bacteria [24]. After neutron irradiation, no living bacteria could be detected and it can be concluded that the neutron irradiation for the production of radioactive  $^{166}\text{Ho}$ -PLLA microspheres is a very effective sterilisation method as well.

In vivo studies were performed in relatively small animals like rats (chapter 6) and rabbits (chapter 7). However, administration by catheterisation of the hepatic artery via the femoral artery similar to the method used in humans was impossible. Nevertheless, the direct administration into the liver artery of rats and rabbits was a useful model for studying the biodistribution and efficacy of the  $^{166}\text{Ho}$ -loaded PLLA microspheres. A major problem was the obstruction of the microspheres in the needle of the administration system used in rats. It can be expected that these problems do not occur in humans or larger animals because then a relatively large volume of suspended PLLA-microspheres can be administered in a relatively short time. Moreover, the lumen of the catheters used in human embolizations have a three to four fold larger diameter. Obstruction by the microspheres is therefore hardly imaginable, as was indeed observed in a recent pilot study in pigs.

Minimal radiation exposure to personnel who administer the  $^{166}\text{Ho}$ -PLLA microspheres is also important. We designed and patented a new vial (polyethylene based) in which irradiation of the microspheres in a nuclear reactor is performed. Subsequently, the microspheres are suspended in saline after which the vial is connected to the administration system, and the spheres can be introduced into the hepatic artery of the patient via a catheter [25]. With this combined irradiation/administration system it is possible to customize the amount of radioactivity for the individual radiotherapeutic indication.

In chapter 7 it was shown that the  $^{166}\text{Ho}$ -loaded PLLA microspheres are very suitable for treatment of liver malignancies. No back flow of the microspheres, as

frequently encountered with the currently used  $^{90}\text{Y}$ -systems, occurred and the growth of primary tumours was inhibited, which is a very encouraging result for future clinical application of these systems. Currently, an efficacy study in dogs with spontaneous tumours is being planned in co-operation with the Faculty of Veterinary Medicine, Utrecht.

In conclusion, this pre-clinical study of the preparation and application of  $^{166}\text{Ho}$ -loaded microspheres for the treatment of liver metastases showed encouraging results. Human phase-I studies have to answer the questions about dosimetry, efficacy and administration technique in more detail. Other applications of holmium loaded microspheres such as the treatment of head-and-neck cancer [26,27], bone metastases and ovarian cancer are subject of recent and future studies. It is expected that internal radionuclide therapy using Ho-loaded PLLA microspheres will play a substantial role in the treatment of hepatic and other types of cancer in the near future.

**References**

1. Cady B. Natural history of primary and secondary tumours of the liver. *Semin. Oncol.* **1983**;10:127-135.
2. Ehrhardt GJ and Day DE. Therapeutic use of  $^{90}\text{Y}$  microspheres. *Nucl. Med. Biol.* **1987**;14:233-242.
3. Stribley KV, Gray BN, Chmiel RL, Heggie JCP and Bennett RC. Internal radiotherapy for hepatic metastases I: The homogeneity of hepatic arterial blood flow. *J. Surg. Res.* **1983**;34:17-24.
4. Jaffe BM, Donegan WL, Watson F and Spratt JS. Factors influencing survival in patients with untreated hepatic metastases. *Surg. Gyn. Obst.* **1968**;127:1-11.
5. Kemeny NE and Ron IG. Hepatic arterial chemotherapy in metastatic colorectal patients. *Semin. Oncol.* **1999**;26:524-535.
6. Civalieri D, Pector J-C, Håkansson L, Arnaud J-P, Duez N and Buyse M. Treatment of patients with irresectable liver metastases from colorectal cancer by chemo-occlusion with degradable starch microspheres. *Br. J. Surg.* **1994**;81:1338-1341.
7. Giacchetti S, Itzhaki M, Gruia G, Adam R, Zidani R, Kunstlinger F, Brienza S, Alafaci E, Bertheault-Cvitkovic F, Jasmin C, Reynes M, Bismuth H, Misset JL and Lévi F. Long-term survival of patients with unresectable colorectal cancer liver metastases following infusional chemotherapy with 5-fluorouracil, leucovorin, oxaliplatin and surgery. *Ann. Oncol.* **1999**;10:663-669.
8. Lau WY, Ho S, Leung TWT, Chan M, Ho R, Johnson PJ and Li AKC. Selective internal radiation therapy for nonresectable hepatocellular carcinoma with intraarterial infusion of  $^{90}\text{yttrium}$  microspheres. *Int. J. Radiation Oncology Biol. Phys.* **1998**;40:583-592.
9. Fong Y and Salo J. Surgical therapy of hepatic colorectal metastasis. *Semin. Oncol.* **1999**;26:514-523.
10. Scheele J and Altendorf-Hofmann A. Resection of colorectal liver metastases. *Langenbeck's Arch. Surg.* **1999**;384:313-327.
11. Wallace JR, Chistians KK, Pitt HA and Quebbeman EJ. Cryotherapy extends the indications for treatment of colorectal liver metastases. *Surgery* **1999**;126:766-774.
12. Bastian P, Bartkowski R, Köhler H and Kissel T. Chemo-embolization of experimental liver metastases. Part I: distribution of biodegradable microspheres of different sizes in an animal model for the locoregional therapy. *Eur. J. Pharm. Biopharm.* **1998**;46:243-254.
13. Ho S, Lau WY, Leung TWT, Chan M, Ngar YK, Johnson PJ and Li AKC. Clinical evaluation of the partition model for estimating radiation doses from Yttrium-90 microspheres in the treatment of hepatic cancer. *Eur. J. Nucl. Med.* **1997**;24:293-298.
14. Gray BN, Burton MA, Kelleher D, Klemp P and Matz L. Tolerance of the effects of yttrium-90 radiation. *Int. J. Radiation Oncology Biol. Phys.* **1990**;18:619-623.

15. Herba MJ, Illescas FF, Thirlwell MP, Boos GJ, Rosenthal L, Atri M and Bret PM. Hepatic malignancies: improved treatment with intraarterial Y-90. *Radiology* **1988**;169:311-314.
16. Ho S, Lau WY, Leung TWT and Johnson PJ. Internal radiation therapy for patients with primary or metastatic hepatic cancer. *Cancer* **1998**;83:1894-1907.
17. Yorke ED, Jackson A, Fox RA, Wessels BW and Gray N. Can current models explain the lack of liver complications in Y-90 microsphere therapy? *Clin. Cancer Res.* **1999**;5:3024s-3030s.
18. Andrews JC, Walker SC, Ackermann RJ, Cotton LA, Ensminger WD and Shapiro B. Hepatic radioembolization with yttrium-90 containing glass microspheres: Preliminary results and clinical follow-up. *Eur. J. Nucl. Med.* **1994**;35:1637-1644.
19. Mumper RJ, Ryo UY and Jay M. Neutron-activated holmium-166-poly (l-lactic acid) microspheres: A potential agent for the internal radiation therapy of hepatic tumors. *J. Nucl. Med.* **1991**;32:2139-2143.
20. Ackerman NB and Hechmer PA. The blood supply of experimental liver metastases. V. Increased tumour perfusion with epinephrine. *Am. J. Surg.* **1980**;140:625-631.
21. Andrews JC, Walker-Andrews SC, Juni JA, Warber S and Ensminger WD. Modulation of liver tumour blood flow with hepatic epinephrine: a SPECT study. *Radiology* **1989**;173:645-647.
22. Turner JH, Claringbold PG, Klemp PFB, Cameron PJ, Martindale AA, Glancy RJ, Norman PE, Hetherington EL, Najdovski L and Lambrecht RM. <sup>166</sup>Ho-microsphere liver radiotherapy: a preclinical SPECT dosimetry study in the pig. *Nucl. Med. Comm.* **1994**;15:545-553.
23. Lewis DH. Controlled release of bioactive agents from lactide/glycolide polymers. *Biodegradable polymers as drug delivery systems* (ISBN 0-8427-8344-1) **1990**;45.
24. Mumper RJ and Jay M. Poly(L-lactic acid) microspheres containing neutron-activatable holmium-165: A study of the physical characteristics of microspheres before and after irradiation in a nuclear reactor. *Pharm. Res.* **1992**;9:149-154.
25. Nijssen JFW, van het Schip AD and Zonnenberg BA. Apparatus and method for preparing radioactive medicines for administration. European Patent Application, European publication number 0989865. USA Patent Application No. 09/424,624. **1997**.
26. van Es RJJ, Nijssen JFW, Dullens HFJ, Kicken M, van der Bilt A, Hennink WE, Koole R and Slootweg PJ. Establishment of an optimal size of microspheres for embolisation of the rabbit Vx2 head and neck cancer model. *J. Cranio-Maxillofacial Surgery* **in press**.
27. van Es RJJ, Nijssen JFW, van het Schip AD, Dullens HFJ, Slootweg PJ and Koole R. Effect of intra-arterial embolisation of the rabbit Vx2 head and neck cancer model with radioactive holmium-166 poly(L-lactic acid) microspheres. *Int. J. Oral & Maxillofacial Surgery* **in press**.

## Samenvatting

Levermetastasen komen frequent voor bij patiënten met kanker en zijn de oorzaak van 25 tot 50% van alle sterftegevallen gerelateerd aan kanker. Met name bij darmkanker worden regelmatig deze uitzaaiingen gevonden. De gemiddelde levensverwachting van patiënten met levermetastasen is slechts 6 maanden wanneer er sprake is van een uitgebreide metastasering. Zelfs wanneer patiënten met systemische chemotherapie worden behandeld, is de levensverwachting beperkt tot ongeveer 12 maanden. Naast systemische chemotherapie worden locale chemotherapie via de leverarterie of combinatietherapieën gegeven. Deze therapieën verlengen de levensverwachting tot ongeveer 12-24 maanden. Hoewel deze locale therapieën goede palliatieve resultaten laten zien, ondervinden deze patiënten een aantal bijwerkingen zoals misselijkheid, overgeven en diarree. Vaak wordt daarbij ook leverbeschadiging waargenomen. Chirurgie biedt de enige mogelijkheid tot curatief behandelen, maar is slechts bij een minderheid van de patiënten toepasbaar. Nieuwe ontwikkelingen zoals cryo- en radiofrequentie-ablatie resulteren in een verfijning van de chirurgische technieken waardoor meer patiënten kunnen worden behandeld. Desalniettemin zijn de huidige chirurgische therapieën toepasbaar bij slechts 10% van de patiënten.

De toepasbaarheid van uitwendige radiotherapie wordt beperkt door de stralingsgevoeligheid van het normale leverweefsel, dat maximaal 30 Gy kan verdragen. Om deze reden hebben onderzoekers gezocht naar methodes om ter plekke van de metastasen een hoge dosis radioactiviteit te introduceren via de arteriële vascularisatie van de levermetastasen. Zo kwamen aan het eind van de jaren tachtig radioactief yttrium ( $^{90}\text{Y}$ ) gelabelde microsferen die arterieel toegediend kunnen worden, beschikbaar voor de behandeling van maligniteiten in de lever. Patiënten konden met deze therapie worden behandeld met een dosis tot 150 Gy zonder dat er radiatie hepatitis ontstond; een veiligheidslimiet van 80-100 Gy wordt meestal gehanteerd. In een studie met  $^{90}\text{Y}$  microsferen bij 17 patiënten met uitzaaiingen van darmkanker in de lever werd een gemiddelde overlevingsduur van 14 maanden gevonden met daarbij 3 personen die zelfs langer dan 4 jaar overleefden. Naast verlenging van de levensduur geldt de geringe morbiditeit die bij deze therapie wordt gezien als een belangrijk voordeel. Ondanks veelbelovende resultaten met de  $^{90}\text{Y}$  gelabelde microsferen van glas of kunsthars, worden hun hoge dichtheid (3,3 g/ml voor glas en 1,6 g/ml voor kunsthars), niet-degradeerbaarheid en het ontbreken van gammastraling van  $^{90}\text{Y}$  ( $E_{\text{max}}=2,28$  MeV, halfwaardetijd =64,1h), ten behoeve van beeldvorming, als nadelen gezien.

Daarom heeft Mumper polymelkzuur (PLLA) microsferen beladen met radioactief holmium ( $^{166}\text{Ho}$ ) onderzocht als alternatief voor de glas- en kunsthars-systemen. Deze microsferen bezitten een relatieve lage dichtheid (1,4 g/ml) en zijn bovendien biologische afbreekbaar. Een belangrijk extra voordeel is dat  $^{166}\text{Ho}$  wel gammastraling

(81 keV; 6,2%) uitzendt, die gebruikt kan worden voor beeldvorming. Mumper is er echter niet in geslaagd een therapeutische dosis te produceren met voldoende specifieke activiteit. Dit kan waarschijnlijk worden toegeschreven aan de lage holmiumbelading (10% (w/w)) van de microsferen. In Hoofdstuk 2 van dit proefschrift wordt beschreven dat een aanpassing van de bestralingsparameters, die Mumper gebruikte, niet zondermeer leidt tot een toepasbaar systeem met genoeg activiteit. Optimalisatie van de productie-parameters leidde tot PLLA microsferen met een hogere holmiumbelading (16-17% (w/w)). Daarnaast werden de bestralingsparameters bestudeerd en geoptimaliseerd, hetgeen resulteerde in een hogere activiteit met een acceptabele stralings schade aan de microsferen. In dit proefschrift wordt beschreven hoe PLLA microsferen, beladen met therapeutische hoeveelheden radioactief holmium, geproduceerd kunnen worden en tevens weinig lekkage van het holmium vertonen. Het proefschrift eindigt met twee dierstudies waarin de succesvolle “targeting” van de holmium beladen microsferen naar levertumoren in ratten (Hoofdstuk 6), en de haalbaarheid en effectiviteit van deze systemen voor de behandeling van tumoren in de lever van konijnen worden beschreven (Hoofdstuk 7).

**Hoofdstuk 1** geeft een overzicht van de huidige literatuur op het gebied van radioactieve microsferen voor de behandeling van levermetastasen. De eerste klinisch bruikbare microsferen waren  $^{90}\text{Y}$ -glas microsferen. Kunsthars (acrylaat co-polymeren) microsferen met aan de carboxylaat anionen het  $^{90}\text{Y}$ -ion gebonden, worden eveneens klinisch toegepast met vergelijkbare resultaten. Polymelkzuur microsferen beladen  $^{165}\text{Ho}$ -acetylacetaat (HoAcAc), kunnen worden geactiveerd d.m.v. neutronen bestraling (waarbij  $^{165}\text{Ho}$  wordt omgezet in het radioactieve  $^{166}\text{Ho}$ ). Deze microsferen worden beschreven als een nieuwe generatie systemen met superieure eigenschappen ten opzichte van de bekende op glas en kunsthars gebaseerde systemen. De grootte, stabiliteit, toxiciteit, dichtheid, keuze van het gebruikte radio-isotoop en andere vereisten waaraan een optimaal deeltje moet voldoen om bruikbaar te zijn voor radio-embolisatie van levermetastasen worden bediscussieerd.

In **Hoofdstuk 2** wordt de bereiding, via de “solvent evaporation” techniek, van  $^{165}\text{Ho}$  beladen PLLA microsferen beschreven. De optimalisatie van de productieparameters resulteerde in een standaardmethode, waarbij vanuit 10 gram HoAcAc en 6 gram PLLA een opbrengst werd verkregen van ongeveer 4 gram microsferen met een gewenste diameter van 20-50  $\mu\text{m}$  en een holmiumgehalte van 17%. Tevens is de invloed van de bestralingscondities op de integriteit van de microsferen en de holmiumafgifte bestudeerd. Om microsferen te produceren met een therapeutische dosis (ongeveer 20 GBq per 400 mg microsferen) moeten ze watervrij zijn en



gedurende maximaal 1 uur met een relatief lage neutronen flux ( $5 \times 10^{13} \text{ cm}^{-2} \cdot \text{s}^{-1}$ ) worden bestraald. Bij voorkeur kan de bestraling worden uitgevoerd in een bestralingsvat (bijvoorbeeld gemaakt van polyethyleen) dat zelf niet radioactief wordt tijdens de bestraling. Onder deze omstandigheden bleef de integriteit van de microsferen wat betreft de vorm en grootte gewaarborgd. Afgifte-experimenten, waarbij de  $^{166}\text{Ho}$  afgifte werd gemeten tijdens 192 uur incubatie in PBS, plasma, leucocyten suspensie en lever-homogenaat toonden aan dat minder dan 2% holmium uit de microsferen weglekte.

In **Hoofdstuk 3** wordt de kristalstructuur van twee holmium-acetylacetaat ( $\text{HoAcAc}$ ) complexen geïdentificeerd met behulp van röntgendiffractie. De twee structuren,  $[\text{Ho}(\text{C}_5\text{H}_7\text{O}_2)_3(\text{H}_2\text{O})_2] \cdot \text{H}_2\text{O}$  (complex I; bereid bij een pH van 8,5) en  $[\text{Ho}(\text{C}_5\text{H}_7\text{O}_2)_3(\text{H}_2\text{O})_2] \cdot \text{C}_5\text{H}_8\text{O}_2 \cdot 2\text{H}_2\text{O}$  (complex II; bereid bij een pH van 9,0), laten beiden een achtvoudig gecoördineerd holmium(III) ion zien. In beide structuren (I en II) verbinden waterstofbruggen de complexen tot een keten in de [010] richting. In complex I worden deze ketens door de niet-gecoördineerde watermoleculen verbonden tot een twee dimensionaal netwerk. In complex II wordt het netwerk gevormd door twee niet-gecoördineerde watermoleculen tezamen met een vrij 4-hydroxypentaaan-2-on molecuul. Het diaquatrakis(pentaaan-2,4-dionato-O,O')-holmium(III) monohydraat (complex I) is het complex dat in dit proefschrift wordt gebruikt voor de bereiding van holmium beladen microsferen.

In **Hoofdstuk 4** wordt de karakterisering van polymelkzuur microsferen en films beladen met holmium-acetylacetaat ( $\text{HoAcAc}$ ) beschreven. De factoren die verantwoordelijk zijn voor de lage holmiumafgifte, zoals aangetoond in hoofdstuk 2 is beschreven, worden met behulp van gemoduleerde “differential scanning calorimetry” (MDSC), scanning elektronen microscopie (SEM), infrarood spectroscopie (IR) en röntgendiffractie bestudeerd. MDSC analyse van  $\text{HoAcAc}$  kristallen liet twee endothermen zien, die kunnen worden toegeschreven aan de verdamping van het niet-gecoördineerd watermolecuul (eerste endotherm) en de twee gecoördineerde watermoleculen (tweede endotherm). Zowel MDSC als röntgendiffractie toonden aan dat  $\text{HoAcAc}$  moleculair gedispergeerd was in de PLLA matrix bij holmiumbeladingen tot 8% in films en 17% in microsferen. Kristallijn  $\text{HoAcAc}$  werd aangetroffen in films met beladingen van 12% Ho (w/w) of hoger. Door middel van IR metingen werden aanwijzingen gevonden voor interacties tussen de carbonyl groepen van PLLA en het Ho-ion in  $\text{HoAcAc}$ . Deze interacties zijn een mogelijke verklaring voor de geringe afgifte van het holmium uit de microsferen.

**Hoofdstuk 5** beschrijft de invloed van neutronenbestralingen op holmium-acetylacetaat beladen polymelkzuur microsferen. De PLLA matrices met en zonder HoAcAc werden voor en na bestralen geanalyseerd met behulp van MDSC, SEM, gel permeatie chromatografie (GPC), IR-spectroscopie en röntgendiffractie. GPC en MDSC metingen lieten een afname in molecuulgewicht en kristalliniteit zien, welke is toe te schrijven aan ketenbreuk (chain-scission) door bestraling. Bestraling van HoAcAc beladen PLLA matrices resulteerde in verdamping van het niet-gecoördineerde watermolecuul van het HoAcAc complex en werd aangetoond met MDSC en röntgendiffractie. IR spectroscopie gaf aan dat bestraling degradatie van het HoAcAc ion induceerde. Dit hoofdstuk laat zien dat de microsferen hun gunstige eigenschappen (grootte en geringe holmiumafgifte) behouden ondanks de gevonden stralingsschade aan zowel de PLLA matrix als het HoAcAc complex. Dit maakt deze systemen geschikt voor de behandeling van tumoren door middel van radio-embolisatie.

In **Hoofdstuk 6** wordt de biodistributie van de microsferen (20-50  $\mu\text{m}$ ; 17% Ho (w/w), activiteit van 15-20 MBq voor beeldverwerking) onderzocht ná intra-arteriële toediening in de leverarterie van WAG/Rij ratten met geïmplanteerde tumoren. Meer dan 95% van de totale toegediende activiteit werd in de lever met zijn tumor teruggevonden. In de nieren werd slechts een marginale hoeveelheid radioactiviteit teruggevonden, hetgeen duidt op geringe afgifte van  $^{166}\text{Ho}$  uit de microsferen. Histologisch onderzoek gaf aan dat clusters met meer dan 10 microsferen en clusters van gemiddelde grootte (4 tot 9 microsferen) met name werden gevonden in de tumor en zijn directe omgeving. Echter, individuele microsferen waren nagenoeg homogeen verspreid over zowel lever- als tumorweefsel. De gemiddelde tumor-tot-lever ratio op basis van activiteitsmetingen was 6 (bij controle ratten 0,7). Hiermee is aangetoond dat “targeting” naar de tumor met deze microsferen succesvol is.

**Hoofdstuk 7** laat het therapeutisch effect van de  $^{166}\text{Ho}$  beladen PLLA microsferen op levertumoren in het konijn zien. Konijnen (New Zealand White) met geïmplanteerde VX2 (virus geïnduceerd papilloma konijnen carcinoom) tumoren werden behandeld met microsferen met een diagnostische dan wel een therapeutische hoeveelheid activiteit. De referentiegroep bestond uit een groep “sham”-behandelde dieren. Histologie en opnamen met een gammacamera toonden een heterogene activiteitsverdeling en daarmee ook een heterogene verdeling van de microsferen aan. Een “hot spot” was zichtbaar die correspondeerde met de locatie van de geïmplanteerde tumor, waarmee de succesvolle “targeting” naar de tumor werd bewezen. Histologie liet eveneens een ophoping van microsferen zien in en om de tumor. Er werd een tijdelijke stijging van de leverenzymen gemeten ná toediening van

de microsferen, wat wijst op enige levertoxiciteit. In beide controle groepen (“sham”-behandelde en konijnen die diagnostische microsferen kregen ingespoten) werd een normale exponentiële groei van de tumoren gezien. Bij dieren die een therapeutische dosis microsferen kregen toegediend, stopte de tumorgroei en leidde zelfs tot necrose van het tumorweefsel terwijl het gezonde leverweefsel gespaard bleef. Dit is een veelbelovend resultaat voor de verdere ontwikkeling en toepassing van de gebruikte holmium-166 beladen polymelkzuur systemen.

## Dankwoord

Dit veelomvattende proefschrift was niet tot stand gekomen zonder de hulp en expertise van anderen. Het leek er op dat alle  $\beta$ -disciplines van de Universiteit van Utrecht met dit onderzoek te maken kregen. Iedereen die mij heeft geholpen wil ik bedanken voor hun bijdrage aan dit onderzoek. Daarnaast wil ik op deze plek een aantal mensen bedanken, die speciaal betrokken waren bij het holmiumonderzoek.

- Prof. Hennink, beste Wim, ondanks de zeer verschillende inzichten tussen polymeer-chemici, radiochemici en medici bleek het mogelijk om één team te vormen met jouw Biofarmacie en de afdeling Nucleaire Geneeskunde. Je begeleiding was wervelend en “to the point. Je inspirerende aanpak heeft erin geresulteerd dat ik het schrijven van artikelen werkelijk leuk ben gaan vinden. Enorm bedankt voor je enthousiasme.
- Prof. Viergever, beste Max, je werd als laatste toegevoegd aan het rijtje promotoren en co-promotoren. We hebben tot nu toe maar weinig de kans gehad om samen te werken, hopelijk lukt dit in de toekomst bij het aanvragen van nieuwe projecten.
- Dr. van het Schip, beste Fred, onze samenwerking werd getekend door Mac en Windows. Mijn drafts van artikelen werden zelden “geslikt” door jouw Mac. Na een hoop zweetdruppels maakte jij er telkens weer een stuk ware proza van. Je hebt je altijd hard gemaakt om anderen ervan te overtuigen dat het holmiumonderzoek iets anders was dan het verzamelen van gegevens. Beiden hebben we veel geleerd van deze eerste keer.
- Dr. van Rijk, beste Peter, bedankt voor de mogelijkheid om dit onderzoek te mogen doen. Tijdens dit uitgebreide onderzoek hebben we regelmatig gesproken over nieuwe projecten en ideeën. Het is goed te weten dat ik als postdoc de ingezette weg mag voortzetten.
- Don Rook, de laatste jaren raakte je als researchanalist steeds meer betrokken bij het holmiumproject. Jij hebt met name veel geholpen bij de echt biologische kant van dit onderzoek. Turen door de microscoop en tot laat in de avond dierexperimenten verrichten (Zie je hoe leuk biologie is?!). Veel van je werk is terug te vinden in verscheidende gepubliceerde artikelen en abstracts. Hartelijk dank voor al je inspanning en werk.
- Mies van Steenbergen, zoals vaker door anderen geschreven, je bent de smeerolie in die goed lopende machine “Biofarmacie”. Je hebt mij kennis laten maken met een groot aantal technieken en sprong bij wanneer ik in de stress dreigde te raken. Mies, je rol als paranimf zat in ons “pact” wanneer ik Wim zou strikken als promotor. Ik ben blij dat dit gelukt is (p.s. De groeten aan je kids!).
- Dr. Zonnenberg, beste Bernard, het was een groot genoegen om met jou samen te werken. Je hebt de kennis en het charisma van een prof. Je weet de promovendus te motiveren en te belagen met tal van nieuwe ideeën, maar ik had slechts vijf jaar!
- Dr. de Klerk, beste John, het begon allemaal met Jan Puijk en de Boegem<sup>®</sup>-zalf. Het was plezierig om met je samen te werken en mee te rijden op de fiets, maar vooral in de auto. Het eindigt ermee dat jij nu veel meer huisdieren hebt dan ik.

- Studenten zaten niet echt te springen om een stageplek in Nederland aangezien het buitenland immers spannender is. Toch trok het holmiumproject veel goede stagiaires aan. Ir. Patrick van Veenendaal, je was hier op geheel vrijwillige basis, geen studiepunten, geen salaris (hoe herkenbaar). Ook na je vertrek bleef je een vraagbaak. Rogier Lange (10 voor stralingshygiëne, maar minder opruimend op het lab) en Sander Zielhuis (holmiumbepaling op de labtafel, maar de scriptie kwam iets later), jullie waren een team apart en onmisbaar voor de farmaceutische aspecten van het onderzoek. Adrien de Witte, (DSC-films en microspheres) je werk staat in hoofdstuk 4. Was ik echt zo streng? Jan Peter Hoven (bollen tellen), tja dat verslag... Bart Westendorp (nog meer bollen tellen), laat maar gaan dat gaat meestal wel goed (hoe zat het ook alweer; is 60 mg nu 0,006 of 0,06 gram?).
- Dr. Marco van de(r) Weert, bedankt voor alle deskundige hulp en uitleg bij IR.
- Overige collega's Biofarmacie bedankt voor jullie gastvrijheid en gezelligheid (wanneer is er weer taart?). Jullie zijn het bewijs dat hard werken samen kan gaan met een hoop lol. Speciaal dank ik Herre Talsma, Sylvia de Jong, Okke Franssen en Jenny Cadee.
- Overige collega's Nucleaire Geneeskunde. Voor sommigen was ik vreemde eend in de bijt, maar ik werd als bioloog, "bollenman", "konijnenboer" en wetenschapper toch geaccepteerd. Het was leuk veel technieken van de afdeling te kunnen gebruiken. Dank voor alle uitleg en hulp bij mijn onderzoek. Een aantal mensen wil ik in het bijzonder danken: alle analisten waren gezien hun geografische ligging achter de "rode deur" nauw betrokken bij het holmiumproject. Bert & Stephan, bedankt voor jullie technische uitleg en gezelligheid, tweemaal een trap tegen de printplaat en hij doet het weer! Wim, jouw steun aan dit project was voor mij van onschatbare waarde. Maarten Gerrits, bedankt voor al je hulp en steun. John Buijs, die fles wijn staat nog steeds te wachten! Leo, ik ga echt mijn kamer opruimen.
- Beste Huub Kooijman en Loes Kroon-Batenburg jullie röntgendiffractie-metingen in de hoofdstukken 2 t/m 5 waren zeer belangrijk voor de karakterisering van de holmium-microsferen. Loes je had gelijk het was kristallijn!
- Kenmerkend voor dit proefschrift zijn de vele SEM-opnamen. Pim van Maurik hartelijk dank dat je mij deze techniek leerde. In de toekomst zul je me zeker weer tegenkomen.
- Het dierexperimenteel onderzoek werd verricht in het Gemeenschappelijke Dieren Laboratorium te Utrecht. Mijn dank gaat uit naar Kees Brandt, Hans Vosmeer, Nico van Attevelt, Jannico den Breejen, Ate van den Molen, Adrie Versluis en Jeroen van Ark.
- NRG te Petten; Dr. Woittiez, beste Joost, via jou wil ik het NRG hartelijk danken voor alles wat mogelijk was en is. Zonder jouw expertise en inzet was het niet denkbaar om deze therapie zo ver te ontwikkelen. Daarnaast wil ik Piet Snip en alle medewerkers, die geholpen hebben om de bestralingen op tijd en vlekkeloos uit te voeren hartelijk danken.
- Hub Dullens, dank voor het samen uitsnijden van stukjes lever en tumor.
- David Grove jij hebt geholpen met de eerste karakterisering van het holmiumcomplex. (onder TL roze en bij daglicht geel; *it's amazing!*).

- George Voorhout, bedankt voor de eerste echo-opnamen bij de rat. We staan te popelen om de eerste patiënten (honden) te behandelen.
- Rob van der Camp: de “Holmium-man” heeft het geklaard.
- Jeroen van Bokhoven, helaas lukte het tot nu toe niet om een goede Fourier-transformatie te vinden voor de EXAFS-data.
- Zeergeleerde Robert van Es, het was erg prettig om met jou samen te werken. Graag deel ik die bruine boterham met kaas!
- Mallinckrodt BV: Dr. Ensing, beste Geert, veel dank voor je steun en hulp aan dit project. Beste Mark Konijnenberg, bedankt voor je supersnelle dosimetrie-berekeningen.
- Veel dank gaat naar de fotografie en ICT van RRN: Jan, Roy, Karin en Eugène, dank voor alle spoed-glossy’s, -dia’s en het verder opmaken van de omslag van dit proefschrift. Sven, Harm en Karel, bedankt voor jullie assistentie bij mijn computer-vraagstukken.
- Bart van Rijn, met veel enthousiasme heb je meegedacht aan het holmiumproject. Bedankt voor je bemoeienis rond het octrooi en je inzet voor het toedieningsvat.
- Rudy Meijer en Mourat El Ouamari, bedankt voor jullie hulp bij echografie.
- Experimentele cardiologie: Arjan bedankt voor alle uitleg en hulp bij jullie microscoop.
- Vera Baumans, bedankt voor het meedenken bij het opzetten van de dierexperimenten.
- Lidy Weijers, bedankt voor al je hulp bij het catheteriseren.
- Fred de Coo, ik ben blij dat je mijn paranimf wil zijn. Jij maakte me wegwijs in het AZU en gaf me goede raad (*pak die telefoon en bel!, met een grap bereik je meer*). Primus was de uitvalsbasis als ik het even niet meer zag zitten, daar was een “peptalk” van jou genoeg om weer met frisse moed verder te gaan. Het proefschrift is geschreven dus ... bierûh!
- Mijn ouders, jullie hebben me de opleiding meegegeven en belangrijker het doorzettingsvermogen. Zonder deze essentiële aspecten had ik het niet tot hier gebracht. Pa, geen enkel ander moment was goed geweest voor jouw ongeluk. Sorry dat ik niet altijd paraat kon staan. Mamma, jouw “klus” is waarschijnlijk zwaarder dan mijn promotie, maar je doet het goed. Mijn broer Peter, daar waar de druk te hoog werd, sprong jij bij. Bedankt voor al die extra uurtjes die je voor mij “thuis” en in ons winkeltje hebt opgevangen, terwijl ik werkte aan dit proefschrift.
- Lieve Gabriëlle, zoals je al schreef, zouden de rollen omgekeerd zijn: nu bedank ik jou voor al je hulp en geduld gedurende de afronding van dit proefschrift. Het is goed dat jij het allemaal al eens hebt beleefd. Jij hebt gezorgd dat ik volhield en prioriteiten stelde. Onze samenwerking is bruisend en motiverend. Het is geweldig te weten, dat we blijven “samenwerken”. Straks zijn er weer twee Dr<sup>(s)</sup> in ons huisje, zo zijn we ook begonnen!

## **Curriculum vitae**

De schrijver van dit proefschrift is geboren op 22 november 1970 te Hilversum. Na in 1990 het diploma VWO te hebben behaald aan de scholengemeenschap Laar & Berg te Laren, startte hij met de studie Biologie aan de Universiteit van Amsterdam. In 1991 startte hij daarnaast de studie Medische Biologie aan dezelfde universiteit. In 1994 werd in het kader van een wetenschappelijke stage bij de afdeling Nucleaire Geneeskunde van het Academisch Ziekenhuis Utrecht, gedurende een jaar, onderzoek verricht aan het bereiden van holmiumacetylacetaat en polymelkzuur microsferen die in combinatie gebruikt zouden worden als een mogelijke therapie voor de behandeling van levermetastasen. Hij haalde de doctoralen Biologie en Medische Biologie in 1995. Na zijn afstuderen werd hij gevraagd om het eerdere wetenschappelijke werk voort te zetten in de vorm van een promotieonderzoek, op dezelfde afdeling Nucleaire Geneeskunde. Het resultaat van dit onderzoek heeft tot dit proefschrift geleid. Na zijn promotie zal hij zijn werk aan het holmiumproject voortzetten in een postdoc aanstelling bij Nucleaire Geneeskunde.

---

**List of publications***Full paper*

1. Nijsen JFW, Zonnenberg BA, Woittiez JRW, Rook DW, Swildens-van Woudenberg IA, van Rijk PP and van het Schip AD. Holmium-166 poly lactic acid microspheres applicable for intra-arterial radionuclide therapy of hepatic malignancies: effects of preparation and neutron activation techniques. *Eur. J. Nucl. Med.* **1999**;26:699-704.
2. Kooijman H, Nijsen JFW, Spek AL and van het Schip AD. Diaquatrakis(pentane-2,4-dionato-O,O')holmium(III) monohydrate and diaquatrakis(pentane-2,4-dionato-O,O')holmium(III) 4-hydroxypentan-2-one solvate dihydrate. *Acta Cryst.* **2000**;C56:156-158.
3. Nijsen JFW, van Steenberg MJ, Kooijman H, Talsma H, Kroon-Batenburg LMJ, van de Weert M, van Rijk PP, de Witte A, van het Schip AD and Hennink WE. Characterization of poly(L-lactic acid) microspheres loaded with holmium acetylacetonate. *Biomaterials* **in press**.
4. Nijsen F, Rook D, Brandt C, Meijer R, Dullens H, Zonnenberg B, de Klerk J, van Rijk P, Hennink W and van het Schip F. Targeting of liver tumour in rats by selective delivery of holmium-166 loaded microspheres: a biodistribution study. *Eur. J. Nucl. Med.* **in press**.
5. van Es RJJ, Nijsen JFW, Dullens HFJ, Kicken M, van der Bilt A, Hennink WE, Koole R and Slootweg PJ. Establishment of an optimal size of microspheres for embolisation of the rabbit Vx2 head and neck cancer model. *J. Cranio-Maxillofacial Surgery* **in press**.
6. van Es RJJ, Nijsen JFW, van het Schip AD, Dullens HFJ, Slootweg PJ and Koole R. Effect of intra-arterial embolisation of the rabbit Vx2 head and neck cancer model with radioactive holmium-166 poly(L-lactic acid) microspheres. *Int. J. Oral & Maxillofacial Surgery* **in press**.
7. Nijsen JFW, van het Schip AD, Hennink WE, Rook DW, van Rijk PP and de Klerk JMH. Advances in Nuclear Oncology: Microspheres for internal radionuclide therapy of liver tumours. *Current Med. Chem.* **submitted**.
8. Nijsen JFW, van het Schip AD, van Steenberg MJ, Zielhuis SW, Kroon-Batenburg LMJ, van de Weert M, van Rijk PP and Hennink WE. Influence of neutron irradiation on holmium acetylacetonate loaded poly(L-lactic acid) microspheres. *Biomaterials* **submitted**.
9. Nijsen JFW, Rook DW, Westendorp B, Brandt CJWM, Zonnenberg BA, van Rijk PP, Hennink WE and van het Schip AD. Radioactive holmium loaded poly(L-lactic acid) microspheres for treatment of hepatic malignancies: efficacy in rabbits. **in preparation**.



*Patent*

1. Nijsen JFW, van het Schip AD and Zonnenberg BA. Apparatus and method for preparing radioactive medicines for administration. European Patent Application, European publication number 0989865. USA Patent Application No. 09/424,624.

*Award*

1. Mallinckrodt Award **1994**. for the manuscript “Poly lactic acid microspheres containing neutron-activated holmium-166 for therapy of hepatic malignancies”.

*Abstract*

1. Nijsen JFW, van het Schip AD, IJzerman HG, Zonnenberg BA, Rook DW and van Rijk PP. Production of poly lactic acid microspheres (PLA-MS) containing neutron – activated holmium-166 for therapy of hepatic malignancies. *Eur. J. Nucl. Med.* **1995**;22:887.
2. Nijsen JFW, van het Schip AD, IJzerman HG, Linsen MHKJ, Zonnenberg BA, Rook DW, Woittiez JRW, Nieuwendijk BJT and van Rijk PP. Irradiation of holmium-165-poly lactic acid microspheres (Ho-165-PLA-MS) for radiotherapy of hepatic malignancies. *Eur. J. Nucl. Med.* **1996**;23:1249.
3. Nijsen JFW, Woittiez JRW, van Maurik W, van het Schip AD. Conditions during neutron bombardment influencing the integrity of organic holmium-165-poly lactic acid microspheres for radiotherapy of hepatic malignancies. *Eur. J. Nucl. Med.* **1998**;25:895
4. Nijsen JFW, van het Schip AD, IJzerman HG, Linsen MHKJ, Zonnenberg BA, Rook DW, Woittiez JRW, Nieuwendijk BJT and van Rijk PP. Irradiation of holmium-165-poly lactic acid microspheres (Ho-165-PLA-MS) for radiotherapy of hepatic malignancies. *Tijdschr. Nucl. Geneesk.* **1999**;21:109.
5. Nijsen JFW, Brandt CJWM, Rook DW, Zonnenberg BA, de Klerk JMH, and van het Schip AD. A rat model for the biodistribution of radioactive holmium-loaded poly lactic acid microspheres for the treatment of liver tumours. *Tijdschr. Nucl. Geneesk.* **1999**;21:114.
6. Van Es RJJ, Nijsen JFW, van der Meijs BB, Cadee J, Slootweg PJ and Koole R. Biodistribution of dextran hydrogel and holmium-166 PLLA microspheres, following intra-arterial embolization of the rabbit VX2 head-and-neck cancer model. (a nuclear and histologic pilot study) *J. Cranio-Maxillofacial Surgery* **2000**;28:131.
7. Rook DW, Nijsen JFW, Brandt CJWM, van Rijk PP, Zonnenberg BA, de Klerk JMH, Hennink WE and van het Schip AD. A rat model studying the biodistribution of holmium loaded microspheres in liver tumours. *Eur. J. Nucl. Med.* **2000**;27:1178.
8. Nijsen JFW. Holmium-166 geladen microsferen als therapie voor de behandeling van levermetastasen. *Nederlandse Vereniging Stralingshygiëne Nieuws* **in press**.

9. Rook DW, Westendorp B, van het Schip AD and Nijsen JFW. Efficacy of holmium-166 loaded microspheres in the treatment of liver tumours in rabbits. *J. Nucl. Med.* ***in press***

*What's good?  
Life's good—  
But not fair at all.*

Lou Reed,  
Magic and Loss